

7

Amide Hydrolysis by Catalytic Antibodies

by

Oguz Ersoy

B.S. Biology and Chemistry
Bates College 1990

Submitted to the Department of Chemistry
in Partial Fulfillment of the Requirements
for the Degree of

Doctor of Science
in Chemistry

at the

Massachusetts Institute of Technology
June, 1996

© Massachusetts Institute of Technology
All rights reserved

Signature of the Author

Department of Chemistry, May 22, 1996

Certified by

Professor Satoru Masamune, Thesis Advisor

Accepted by

Dietmar Seyferth, Chairman
Departmental Committee on Graduate Students
Science

MASSACHUSETTS INSTITUTE
OF TECHNOLOGY

JUN 12 1996

This doctoral thesis has been examined by a Committee of the Department of Chemistry as follows:

Professor Frederick D. Greene

_____ Chairman _____

Professor Satoru Masamune

_____ Thesis Advisor _____

Professor William H. Orme-Johnson

Amide Hydrolysis by Catalytic Antibodies

by

Oguz Ersoy

Submitted to the Department of Chemistry on May 24, 1996
in partial fulfillment of the requirements for the
Degree of Doctor of Science

Abstract

A novel approach that has generated amide bond cleaving catalytic antibodies is described. In this approach, the use of phenol as an auxiliary nucleophile was coupled with the heterologous immunization protocol for potential generation of bi-functional antibody binding sites. Three haptens were designed and synthesized; two of these were used as an immunogen-pair in heterologous immunization, and also individually in homologous immunizations. One antibody from each immunization protocol was found to effect the cleavage of *p*-nitroaniline propionate **87** in the presence of phenol. Detailed kinetic studies of these antibody catalysts are presented. Significantly, all three antibodies required the participation of phenol for catalytic activity while the addition of phenol had no effect on the rate of the background reaction. These results point to the power of nucleophilic catalysis that had previously not been harvested for antibody catalysis. Possible future applications of this approach to reactions other than amide hydrolysis are discussed at the end of this account.

Thesis Supervisor: Professor Satoru Masamune

Title: Arthur C. Cope Professor of Chemistry

We live, as we dream - alone.

- Joseph Conrad,

The Heart of Darkness

Everything is miraculous. It is miraculous that one
does not melt in one's bath.

- Pablo Picasso

"Every act of creation
is preceded by a period of confusion."

This thesis is dedicated to my cat **Hanno**
the most perfect creature I have known in my life,
who has been with me through the hardest
and the happiest moments of these six years,
and who has always known when:

'to bite me, when I wanted to be bit,
and lick me, when I wanted to be licked.'

very few people will ever realize the subtlety...

Acknowledgements

First and foremost, I would like to express my gratitude to my thesis advisor, Professor Satoru Masamune, for the extraordinarily high standards of research he has maintained in his research group that has made me grow as a scientist, and also for his kind persona. I take an enormous pride in being a "Masamune-student".

I am also grateful to Professor Anthony J. Sinskey, in whose labs the biological portions of this project were realized, and who always had a fresh perspective to offer on research in science.

Thanking can not be sufficient to display my appreciation of the efforts of Mr. Roman Fleck; in addition to performing a significant portion of the work that is summarized in Chapter 3, he was often the bearer of the brunt of my frustrations, adding a level of sanity and continuity to this project. I wish him the best of luck for the rest of his tenure at MIT.

Two colleagues stand out as my early sources of encouragement in the Masamune Labs. Dr. Simon F. Williams supplied with me with indispensable lift when my scientific wings were still too wet to open, and Dr. Hiro Suga served an extraordinary course of intellectual nourishment, as well as well-timed motivation. I shudder to think where I would be without their help.

A number of colleagues also added to my experience in Masamune Labs, chiefly Dr.'s Thomas Jaetsch, Sandra Filla, Lian-Yong Chen, Emma Parmee and Takeshi Tsumuraya. I send them my heartfelt thanks.

I would also like to extend my appreciation and thanks to the staff of the Chemistry Headquarters, especially M.T. Kuo, Susan Brighton, Kitty Valleli and Marian Curley, for their competence, friendliness and helpfulness. I thank Dr. Kristin Rosner for her critical reading of this thesis, and of course, Janet McLaughlin for her excellent job in keeping the Masamune group in working-order.

These six years would have not passed without the wonderful companionship of Mr. Peter H. Lorenz, my dearest friend, co-reign in Boston, and a candidate for Ph.D. degree in International Relations at Boston University. Thank you, my "Manda"! The Kuemmerle family; Amy, Lou-Beth, Fred, Jill, Patty and of course, "Gramms", has been my home away from home for nearly all of my ten years in the United States. The warmth of your love I will carry with me no matter how far I travel.

Finally, a word of thanks to the city of Boston for all the cultural stimulation it has offered me to develop my personality, intellect and general awareness; of others, as well as myself. I will surely miss my days and nights in this city. Some thanks are also due to the city of New York for helping me keep in mind that there is always something better. As Rimbaud said; "Life is Elsewhere"...

Table of Contents

Chapter 1: Introduction	10
Chapter 2: Background	17
2.1 Phosphate, Phosphonate and Phosphinate based Haptens	17
2.1.1 Regioselective Ester Hydrolysis by Catalytic Antibodies 18	
2.1.2. Enantioselective Ester Hydrolysis by Catalytic Antibodies	19
2.1.3 Cocaine Degradation by Catalytic Antibodies	22
2.1.4 Pro-drug Activation by Catalytic Antibodies	23
2.1.5 Investigations of Amide Hydrolysis by Catalytic Antibodies Raised to Phosphonate Haptens	25
2.2 Second Generation Haptens Based on Antigen-Antibody Charge Complementarity or Metal co-factors	29
2.2.1 Pyridinium Alcohol Haptens for the Antibody Catalyzed Hydrolysis of Benzoate Esters	30
2.2.2 Esterolytic Antibodies Induced to Haptens with a 1,2-Amino Alcohol Functionality	31
2.2.3 Metal Based Haptens to Generate Amidase Antibodies .	33
2.3 Third Generation Hapten Design: Heterologous Immunization ..	35
2.3.1 Original Antigenic Sin	36
2.3.2 Esterolytic Antibodies Generated by Heterologous Immunization	38
2.4 Fourth Generation of Haptens: Combination of Heterologous Immunization with Nucleophilic Catalysis	40
2.4.1 A Brief Synopsis of Proteolytic Enzymes	41
2.4.2 Mechanistic and Structural Studies of Acyl Hydrolyzing Antibodies	42
2.4.3 Remarks	47
Chapter 3: Catalytic Antibodies for Amide Hydrolysis	49
3.1 Introduction	49

3.2 Hapten Design	49
3.3 Synthesis of Haptens, Inhibitors and Substrates	52
3.4 Homologous and Heterologous Immunizations	55
3.5 Fusions and Generation of Hybridomas	56
3.5.1 Homologous Immunizations	56
3.5.2 Heterologous Immunizations	57
3.6 Antibody Production and Purification.....	57
3.7 Amide Hydrolysis Assay with Unimolecular Substrate 75	59
3.8 pH-optimum Studies	61
3.9 Cleavage of Propionyl p-Nitroanilide with Phenol	64
3.10 Conclusion	71
3.11 Perspectives.....	71
Chapter 4: Experimental	73
4.1 Synthesis of Haptens and Substrates	73
4.1.1 General Methods	73
4.1.2 Synthesis of Hapten 72	74
4.1.2 Synthesis of Hapten 74	82
4.1.3 Synthesis of the Substrate 75	88
4.2 Biological Methods	89
4.2.1 Preparation of Carrier Protein-Hapten Conjugates	89
4.2.1.1 Carrier Protein- 72 and - 74 Conjugates	90
4.2.1.2 Carrier Protein- 73 Conjugate	90
4.2.2 Immunizations	90
4.2.3 Enzyme Linked ImmunoSorbent Assay (ELISA)	91
4.2.4 Preperation of media	93
4.2.5 Preperation of Myeloma cells	94
4.2.6 Determination of Cell Viability	95
4.2.7 Fusion	95
4.2.8 Limiting Dilution (Subcloning)	97
4.2.9 Cryogenic Storage of Cell Lines	98

4.2.10 Ascites Production From Monoclonal Hybridomas	98
4.2.11 Purification of Monoclonal Antibodies	99
4.2.12 Assays for Catalysis.....	100
Biographical Note	102
References	103

Chapter 1

Introduction

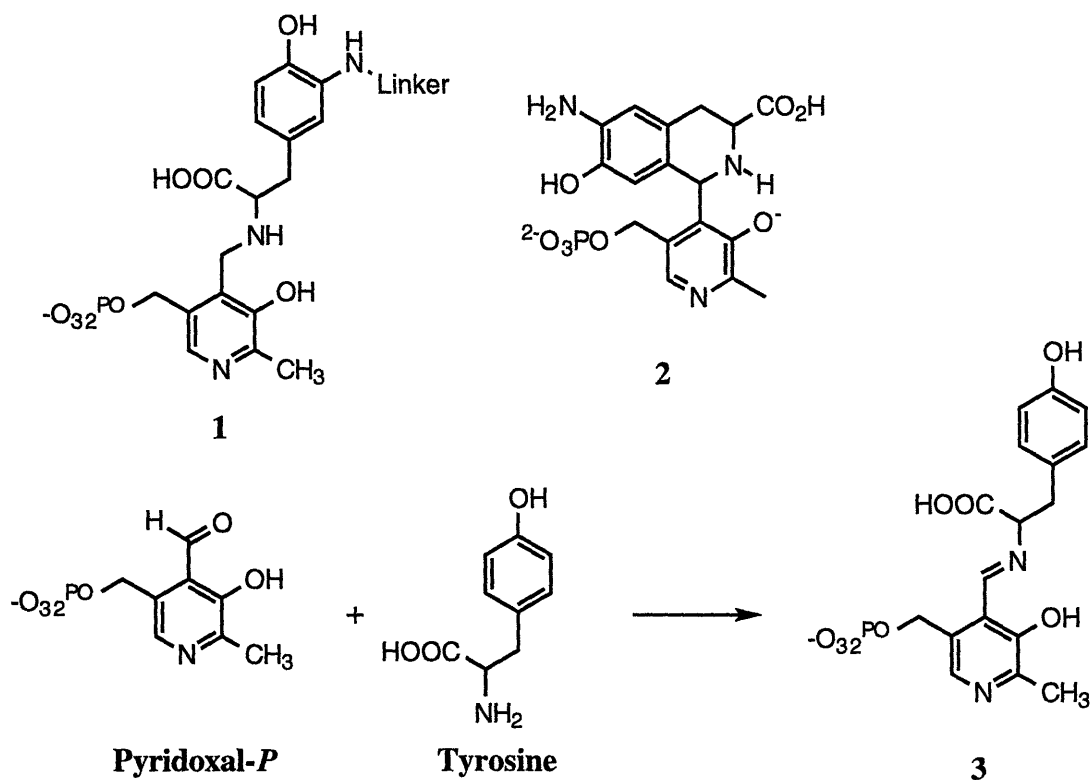
Catalysis of biological, chemical and industrial processes is a thriving area of research due to its scientific as well as economical importance. Thus, in 1989 more than \$1 trillion worth of goods was produced in the U.S. that made use of a catalytic process. This is equivalent to roughly 30% of the U.S. Gross National Product for that year¹. The demand for rationally-designed and highly selective catalysts is greater than ever with a growing emphasis on the stereo-selective synthesis of therapeutics. The late 1970's and early 1980's saw the development of organo-metallic catalysts that accomplished some very important organic transformations with high enantio- and diastereo-selectivities. In a monumental report in 1983, Masamune and Sharpless reported the high-yield stereospecific synthesis of all of the eight isomers of L-hexoses starting from an achiral building block and using a simple reiterative two-carbon extension protocol coupled with a chiral catalyst². In the following years to date, the field of asymmetric organic synthesis has been expanding with continuous development of catalysts and ligands for a variety of reactions ranging from Diels-Alder reaction to Michael Addition³.

With growing environmental concerns in the 1990's, there is an increasing demand to use biological or bio-compatible catalysts. Enzymes offer themselves to such use with their superb catalytic efficiencies, which in some cases reach the ceiling that is dictated by the rate of diffusion in solution. On the other hand, the high substrate specificity of enzymes have limited their use as applied catalysts, and only in a few cases it has been possible to manipulate this specificity to derive economic benefits; for example in the production of high-fructose corn syrup.

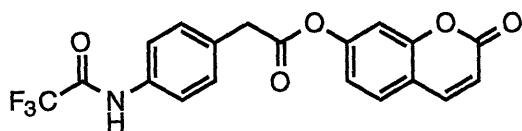
Another set of biomolecules that rival enzymes in their binding specificity are antibodies. Using an elaborate mechanism of genetic recombination followed by somatic mutation and affinity maturation, antibodies can be made in mammalian systems that bind almost any given molecule with high specificity and affinity.

The harvesting of this tremendous potential toward catalysis was first hinted at by Pauling⁴ who proposed fifty years ago that both enzymes and antibodies use similar binding interactions, but enzymes selectively bind the transition state of a reaction thus lowering its free energy of activation while antibodies bind ground state structures. Thus, he concluded that catalysis is only accomplished by the former species. In 1969, W.P. Jencks suggested that if an antibody were induced to a transition state analog, it could serve as a catalyst for the corresponding reaction⁵.

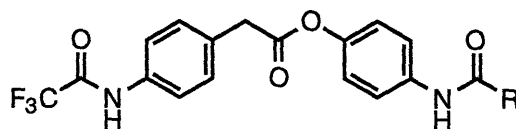
This proposal inspired a number of research groups to work on synthesizing transition state analogs and generate antibodies. Before the eventual success in 1986, the most significant of these early studies is that of Raso and Stollar⁶ between 1973 and 1975. They aimed to prepare polyclonal antibodies that could catalyze the formation of Schiff base **3** by condensation of pyridoxal phosphate and tyrosine, and hopefully, also catalyze the reactions that proceed via intermediate **3**, such as transamination. Polyclonal antibodies were prepared to two different haptens, **1** and **2** that were designed to mimic the Schiff base **3**. (In subsequent work, these haptens were shown to cause inhibition of tyrosine transaminase and tyrosine decarboxylase). Although a five-fold rate acceleration of the transamination of tyrosine to the corresponding α -keto carboxylic acid was observed with the polyclonal antibodies to **1**, neither the individual accelerated step of this reaction nor the kinetic characteristics of the catalysis could be determined due to the heterogeneous nature of the polyclonal antibodies. The authors drew a rather pessimistic conclusion and abandoned any further investigation.



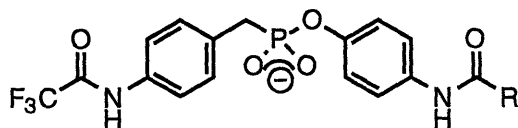
The introduction of monoclonal antibody technology by Kohler and Milstein⁷ in the following year rekindled interest in generating catalytic antibodies, particularly that of Tramontano and Lerner⁸. They were intrigued by earlier studies that phosphate, phosphonate and phosphoramidate structures serve as effective transition state based inhibitors of acyl transfer enzymes⁹. In 1984, they launched a program to synthesize the phosphonate hapten **6**, in order to raise antibodies that would catalyze the hydrolysis of the coumarin ester **4**. Three of the 18 monoclonal antibodies they subsequently screened appeared to have esterase activity, hydrolyzing coumarin ester **4**. However, when one of these antibodies, 6D4, was studied in more detail, it was apparent that the reaction was stoichiometric and not catalytic¹⁰.



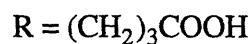
4



5

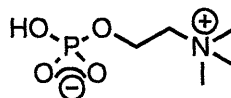
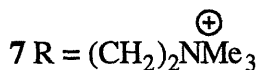
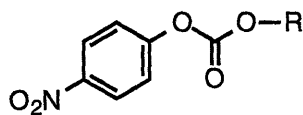


6



Antibody 6D4 was subsequently examined with an alternative ester substrate **5** and catalysis was observed¹¹. The antibody was reported to obey classical Michaelis-Menten kinetics ($k_{\text{cat}} = 1.62 \text{ min}^{-1}$; $K_{\text{m}} = 1.9 \text{ }\mu\text{M}$), and bound the transition state analog **6** with greater affinity ($K_{\text{i}} = 0.16 \text{ }\mu\text{M}$) than the ester substrate (**5**).

Simultaneously, Schultz¹² reported a monoclonal antibody that catalyzed the hydrolysis of carbonate **7**. In his more efficient approach, he realized that one of the numerous antibodies to phosphocholine esters (**8**) that had been previously raised and characterized by others could act as a catalyst if the corresponding carbonate **7** was synthesized and screened. This approach indeed provided him with two catalytic antibodies, MOPC167 and TEPC-15, that hydrolyzed the p-nitrophenyl carbonate **7** with Michaelis-Menten kinetics. Antibody MOPC167 was then characterized to have $k_{\text{cat}} = 0.4 \text{ min}^{-1}$; $K_{\text{m}} = 208 \text{ }\mu\text{M}$; and $K_{\text{i}} = 5.0 \text{ }\mu\text{M}$.

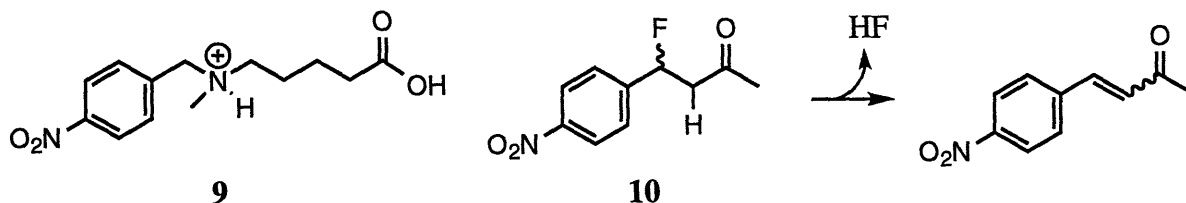


8 Phosphorylcholine

These two initial accounts were quickly followed by a number of other reports where haptens were designed to mimic the transition state of reactions based on simple charge and steric complementarity. Thus, phosphonate haptens were used

to induce the catalysis of acyl transfer reactions of various types¹³, and the six membered transition state of a Claisen rearrangement¹⁴ was mimicked by a stable six-membered hapten. This initial design concept of charge and shape complementarity can be thought of as a first generation of hapten design.

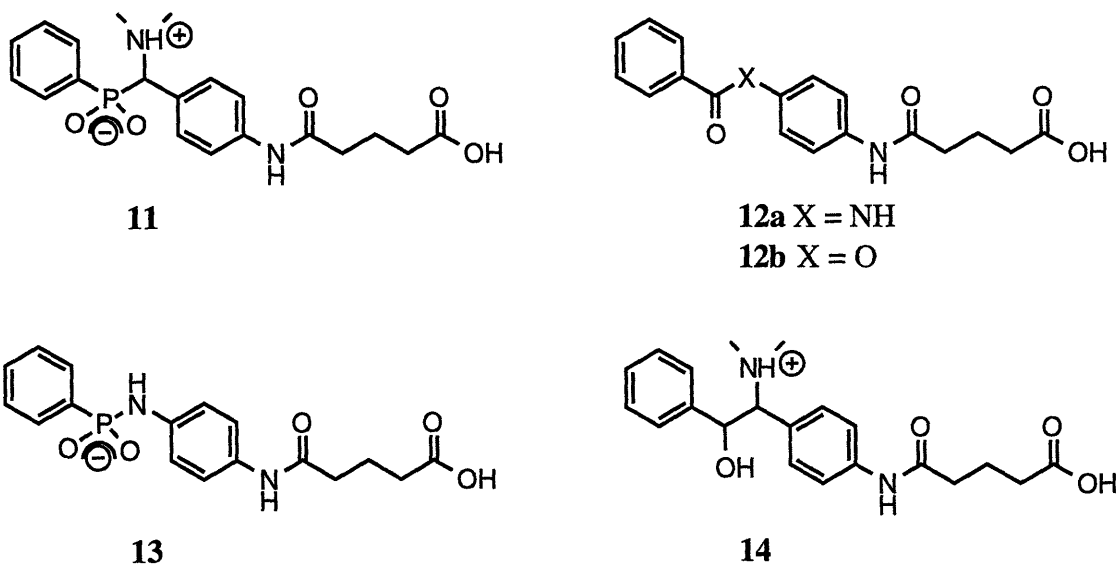
The second generation of hapten design was first reported by Schultz.¹⁵ His approach was to generate a basic residue in the antibody-binding sites via charge complementarity to a positively-charged hapten. Such charge complementary salt-bridge interactions between antibody-antigen pairs had previously been shown by X-ray crystallography studies¹⁶. Hence ammonium hapten **9** was synthesized and was subsequently shown to effect the β -elimination of the 2-fluoroketone **10**. (Janda and Lerner also arrived at this concept, naming it "Bait and Switch" catalysis¹⁷ and applied it to ester hydrolysis - *vide infra*.)



The reader can easily imagine that a third generation hapten design would comprise the combination of the two principles in the form of a zwitterionic ammonium-phosphonate hapten. This concept was indeed investigated in 1990 in the Masamune laboratories¹⁸. The zwitterionic 1,2-amino-phosphinate hapten **11** was designed with the aim of generating ester and amide hydrolyzing antibodies that incorporated a catalytic diad of acidic and basic residues in their active sites. These residues were expected to aid in the hydrolysis of the substrates **12a** and **b** in a similar way to the mechanism of aspartic protease enzymes. However, during the synthesis of hapten **11**, we realized the synthetic challenge involved with such zwitterionic structures, and decided to seek alternative approaches.

Based on our knowledge of the concept of "original antigenic sin" (explained in detail in chapter 2) we imagined to separate the charged portions of hapten **11**

into two structurally similar haptens **13** and **14**, and immunize in succession with both haptens. This process was termed "heterologous immunization" and indeed provided more efficient esterolytic antibodies than the immunization with only one of these haptens (homologous immunization)⁴⁹. Unfortunately, this protocol, by itself, remained unsatisfactory for the ultimate goal of amide hydrolysis.



The hydrolysis of amide bonds is an important target for antibody catalysis. As these bonds constitute the backbone of proteins, selective and efficient cleavage of amide bonds will undoubtedly create important therapeutic and industrial applications for antibody catalysts. In light of the apparent failure of heterologous immunization to generate amidase antibodies, we decided to supplement the heterologous immunization protocol with the incorporation of an auxiliary nucleophile into our hapten design. We envisioned using phenol as an auxiliary nucleophile to effect the cleavage of the amide bond, similar to the use of co-factors by enzymes. Additionally, heterologous immunization was employed to generate bi-functional catalytic residues in the antibody binding sites. This approach has indeed afforded amide hydrolyzing antibodies of superior catalytic efficiency.

A short review of previous efforts to generate catalytic antibodies with acyl-transfer capabilities, including heterologous immunization, will be presented in

chapter 2. Subsequently, chapter 3 will disclose our fruitful attempt in the generation of amidase antibodies via auxiliary nucleophile catalysis. Finally, the experimental details of the work will be presented in chapter 4.

Chapter 2

Background: A Brief History of Catalytic Antibodies for Acyl Transfer Reactions

In this chapter, the progressive sophistication of hapten designs for acyl transfer reactions will be reviewed. The ultimate goal of these efforts has been to establish a reliable method to cleave amide bonds by antibodies. The progress made will be presented in four steps: 1) pentavalent phosphorus haptens based on steric complementarity; 2) haptens that emphasize charge complementarity; 3) bi-functional haptens presented in a heterologous immunization protocol; 4) combination of heterologous immunization with nucleophilic catalysis. Significantly, the last two approaches have been conceived in the Masamune laboratories and involved the efforts of the author. The successful outcome of the final design which has finally afforded effective amidase antibodies will be described in Chapter 3.

2.1 Phosphate, Phosphonate and Phosphinate based Haptens

After the initial reports by the Lerner and Schultz groups, a wealth of research on antibody catalysis followed to exploit the suitability of the oxy-anionic phosphorus center to mimic the tetrahedral transition state of acyl transfer reactions. The suitability of phosphorus haptens stems from a number of factors: 1) the tetrahedral orientation of ligands around the pentavalent phosphorus center; 2) the partial negative charge that is present on the phosphorus oxygens; 3) the effective mimicking of the scissile C-O bond by P-O bonds that are 15% longer than a ground state C-O bond.

Many of the early reports have concerned the catalysis of ester and carbonate hydrolysis/formation reactions because of their relatively low energy of activation.

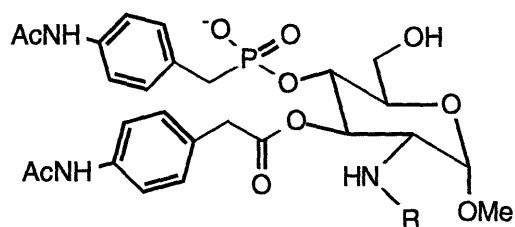
While the importance of catalyzing the hydrolysis of amide bonds has also been realized early on, reported attempts toward this end have been few. This probably also reflects the fact that many failed attempts were not reported.

The early studies established that antibodies raised to pentavalent phosphorus haptens could bring about ester and carbonate hydrolysis with rate accelerations typically 10^3 over the uncatalyzed reactions. As comprehensive reviews of these early efforts already exist in the literature¹⁹, this section will discuss only those examples where ester or carbonate hydrolysis by an antibody has been coupled to other important criteria such as regio- or enantio- selectivity, degradation of a narcotic, or the activation of a pro-drug. These should also illustrate some of the inherent power of using antibodies as catalysts. While apparently sufficient in ester and carbonate hydrolysis; the simple phosphonate hapten design has been generally unsuccessful in generating amide hydrolyzing antibodies. However, a handful of exceptional cases will be discussed at the end of this section.

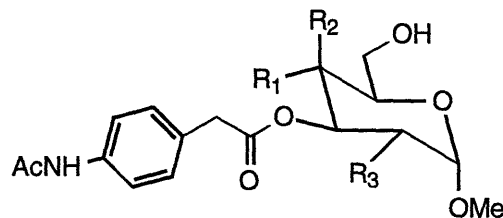
2.1.1 Regioselective Ester Hydrolysis by Catalytic Antibodies

Antibodies have unique three dimensional binding sites that can be programmed by the appropriate hapten to achieve site-selective catalysis of a substrate. This obviates the need for the protection or chemical differentiation of similarly reactive sites in the molecule.

Fujii and co-workers raised antibodies to the phosphonate hapten **18** to selectively hydrolyze the 4'-phenylacetate moiety of the 3',4' protected carbohydrate **19**²⁰. The phosphonate of the hapten was positioned to correspond to the 4'-phenylacetate of the substrate. Furthermore, by using a rather large sized hapten it was hoped that the antibodies would tolerate substrate variability at the 1' and 2' positions of the carbohydrate, thus generating catalysts with wide substrate applicability.



18



19a: R₁=AcNH-Phe-CH₂-CO₂ R₂=H R₃=AcNH

19b: R₁=H R₂=AcNH-Phe-CH₂-CO₂ R₃=AcNH

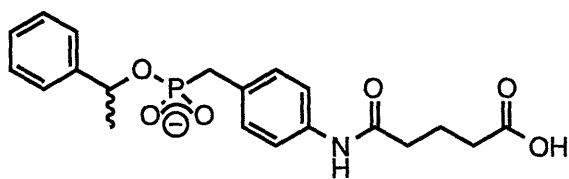
19c: R₁=AcNH-Phe-CH₂-CO₂ R₂=H

R₃=AcNH-Phe-CH₂-CO₂

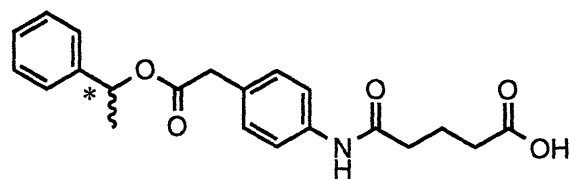
12 monoclonals were generated to **18**, two of which were found to selectively hydrolyze at the 4' position of the substrate **19a**. One of these, 17E11 was characterized in further detail. It displayed a $k_{\text{cat}} = 0.182 \text{ min}^{-1}$ which corresponded to 2740 fold rate acceleration, and was competitively inhibited by hapten **18**. Almost perfect regio-selectivity was observed when a large amount of the antibody catalyst was used. Furthermore, this antibody was shown to be stereo-selective, the 4'-axial enantiomer, **19b** was not accepted as a substrate. Finally, using the tri-ester substrate **19c** the authors showed that the antibody could selectively enhance the hydrolysis of 4'-ester 91 fold over the other two positions of the carbohydrate. This study is especially important given the ubiquitous presence of carbohydrates in antitumor and antibacterial agents.

2.1.2. Enantioselective Ester Hydrolysis by Catalytic Antibodies

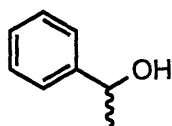
The tight binding specificity of antibodies to their substrates dictates that only one enantiomer is selectively bound and accepted as a substrate. This implies that the use of an enantiomerically-pure hapten will generate antibodies that should only catalyze the corresponding enantiomeric transition state. On the other hand, if the requirement is the enantioselective catalysis of the *either* enantiomer without specification, then catalytic antibodies offer even a bigger advantage. A racemic hapten can be used as each monoclonal antibody will be raised to only one



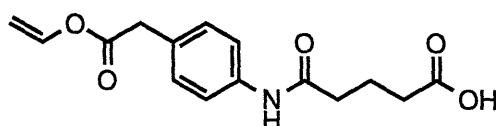
23



(R)- or (S)-24



(R)- or (S)-25



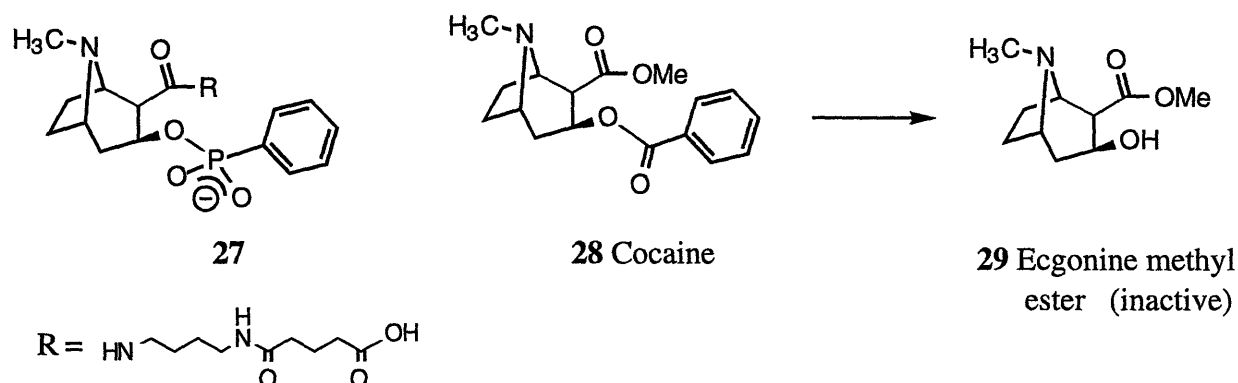
26

Subsequently, it was shown that antibody 21H3 could also catalyze the reverse reaction, namely the trans-esterification of vinyl ester **26** with (*S*)-**25** to give (*S*)-**24**²⁶. A ping-pong mechanism with a covalent intermediate was proposed. 21H3 was able to accept a variety of aromatic alcohols similar to **25**, and therefore it was claimed that these alcohols bound antibody with an induced fit mechanism - an unequivocal proof of which is only possible by determining x-ray crystal structures.

2.1.3 Cocaine Degradation by Catalytic Antibodies

Cocaine addiction is a serious current problem that afflicts most western cultures. There are no known antagonists of cocaine receptor, and it has been shown that antibodies that simply bind the receptors of narcotics such as heroin, are easily overwhelmed by repetitive high doses. Cocaine (**28**) involves two ester moieties that are perfectly poised for antibody catalysis. Upon cleavage of the benzoate, the non-neuroreactive ecgonine methyl ester **29** is produced. The research group of D. W. Landry raised antibodies to the hapten **27** which was designed to mimic the transition state for the hydrolysis of the benzoate of cocaine (**28**)²⁷. Two out of the 29 antibodies tested catalyzed this hydrolysis reaction, and 3B9 was shown to offer 540 fold rate enhancement compared to the background

reaction. The authors concluded by citing that roughly 1000 fold more efficient catalysts would be needed for use in animal clinical studies.

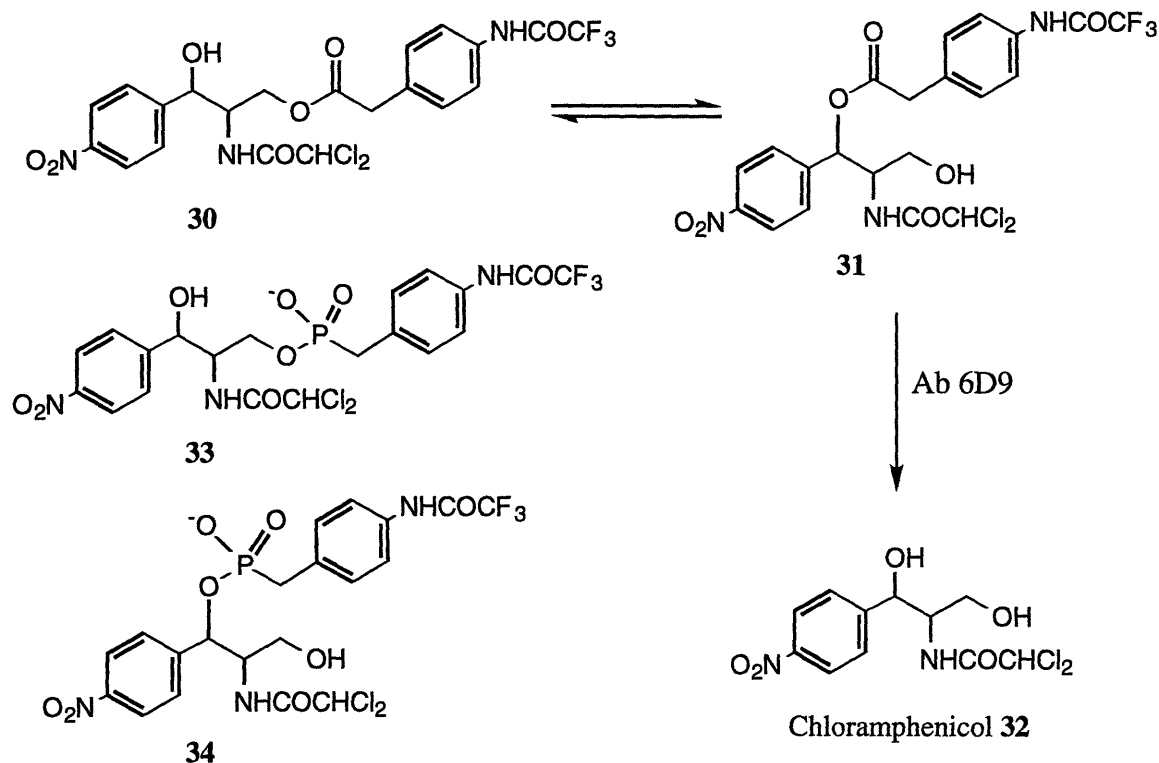


2.1.4. Pro-drug Activation by Catalytic Antibodies

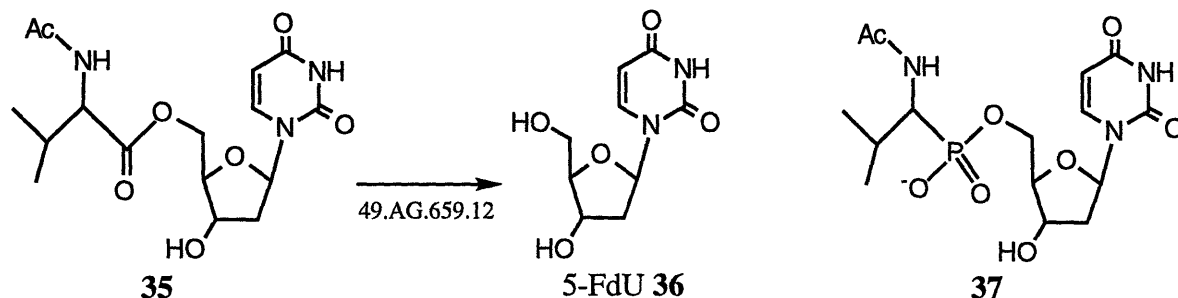
The use of pro-drugs is an interesting approach for the site-specific delivery of drugs to avoid unwanted side effects. This approach often relies on the presence of an enzyme or some other conditions that is specific for the pro-drug and localized to the target area so that the liberation of the drug occurs solely at this locale. With their programmable specificities, antibodies have a tremendous potential in this area with the choice of a reaction that has a negligible background reaction by non-specific endogenous enzymes. Furthermore, chimeric bi-functional antibody technology offers to take this utility one step further by generating antibodies that recognize a target (e.g. tumor) cell with one binding site and catalyze the activation of the pro-drug with the other binding site²⁸.

The first group to realize the pro-drug activation potential of catalytic antibodies has been that of Fujii where they raised antibodies to the phosphonate **33** to cleave a phenyl acetate **30** and liberate the antibiotic chloramphenicol **32**²⁹. As the phenyl acetate exists as a mixture of two isomers **30** and **31**, antibodies were also raised to the C-1 analog hapten **33**. None of the 23 antibodies raised to this hapten were found to be catalytic, while 6 out of the 12 to hapten **34** were. One antibody, 6D9 was characterized further and was found to accelerate the hydrolysis of **2** 2000 fold over the background rate. It displayed multiple turnovers, as well as growth

inhibition in a bacterial assay. In a paper-disc agar diffusion assay, the combination of the pro-drug and antibody 6D9 inhibited the growth of bacteria in a circular zone of 12 mm. The authors commented that this protocol could be used as a selection tool during the phagemid expression of antibodies in bacteria.



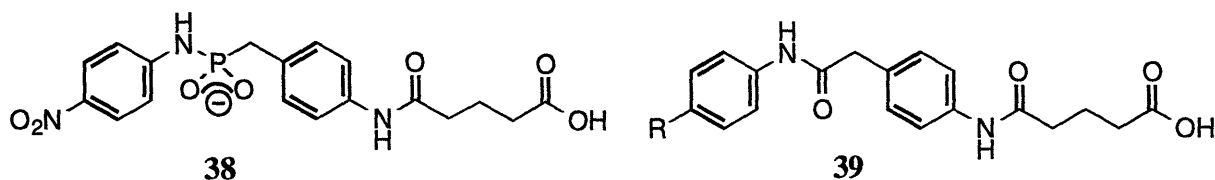
Another pro-drug activation study came from the laboratories of Peter Schultz, where antibodies were raised to catalyze the hydrolysis of the 5'-D-Val ester **35** of the antitumor agent 5-FdU **36**³⁰. They used a phosphonate analog hapten **37** and achieved a rate acceleration of 10^3 with antibody 49.AG.659.12. The non-natural D-isomer of valine was used as most endogenous esterases can not hydrolyze D-amino acid esters.



The activity of 49.AG.659.12 was tested *in vitro* where it inhibited the growth of *E. Coli* in the presence of the prodrug, while the prodrug alone showed no growth inhibition.

2.1.5. Investigations of Amide Hydrolysis by Catalytic Antibodies Raised to Phosphonate Haptens

Ironically, the most encouraging report of antibody catalyzed amide hydrolysis was the first one. Janda *et al.* raised 44 monoclonal antibodies to the phosphonamide hapten **38**, one of which was found to accelerate the hydrolysis of the *p*-nitroanilide substrate **39**³¹. Antibody NPN43C9 displayed Michaelis-Menten kinetics ($k_{cat} = 0.05 \text{ min}^{-1}$, $K_m = 562 \text{ }\mu\text{M}$) and was competitively inhibited by hapten **38** ($K_i = 10 \text{ }\mu\text{M}$). Unfortunately, this catalyst also displayed strong inhibition by the products of the reaction as well as high salt concentration. Thus, it is likely that this antibody did not achieve many turnovers. The catalytic activity was shown to be very substrate-specific, *m*-nitroanilide or other para-substituted anilides were not accepted as substrates. Interestingly *m*-nitroanilide was a competitive inhibitor of the reaction. This suggests that a specific binding pocket for the aromatic nitro group had been formed and that the lack of catalysis is probably due to the incorrect orientation of this substrate in the binding pocket. This is in accord with the known strong immunogenicity of aromatic nitro compounds.

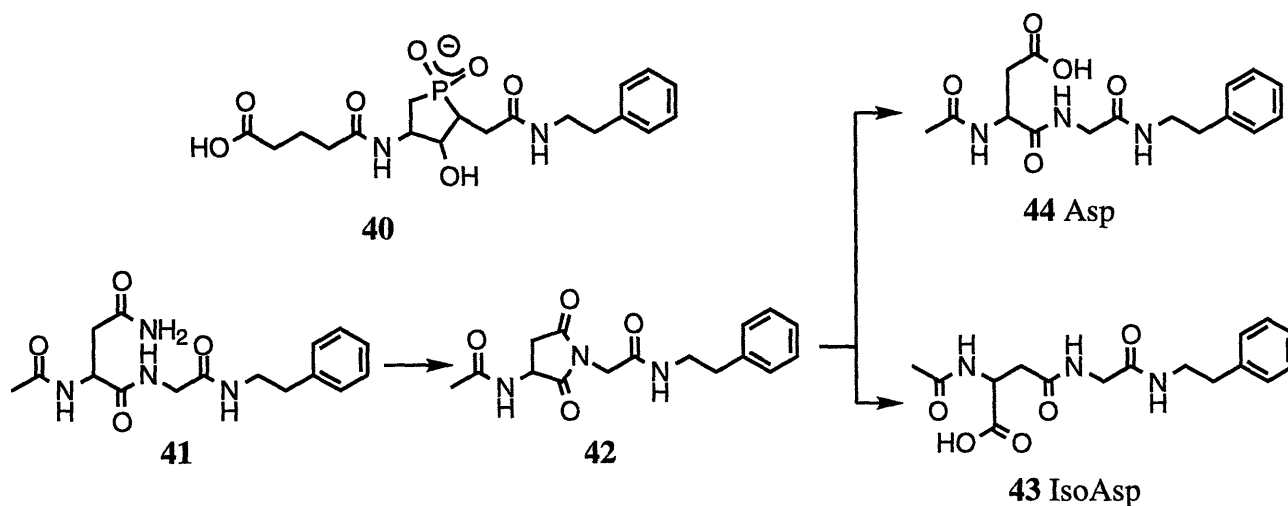


Since this initial report, a number of mechanistic studies of antibody NPN43C9 has shown that catalysis takes place by the formation of an acylimidazole intermediate with a histidine residue in the antibody binding pocket. Details of this

seemingly fortuitous mechanism, as well as its implications on the importance of nucleophilic catalysis to antibody catalyzed amide hydrolysis will be discussed in section 2.4.

Subsequently, Janda *et al.* tried to improve on this catalyst by using a combinatorial library approach to raise antibodies to phosphoramidate **38**³². This technique isolates the genes that code for different antibodies directly from the immunized animal and expresses different antibody binding sites by cloning the genes into bacterial hosts. Of all of the different **38**-binding antibodies that were screened, none catalyzed the hydrolysis of **39** although one, 1D, did catalyze the hydrolysis of the corresponding ester with modest rate acceleration. This result underscores the difficulty and improbability of generating an amide-hydrolyzing antibody by simple phosphonate haptens.

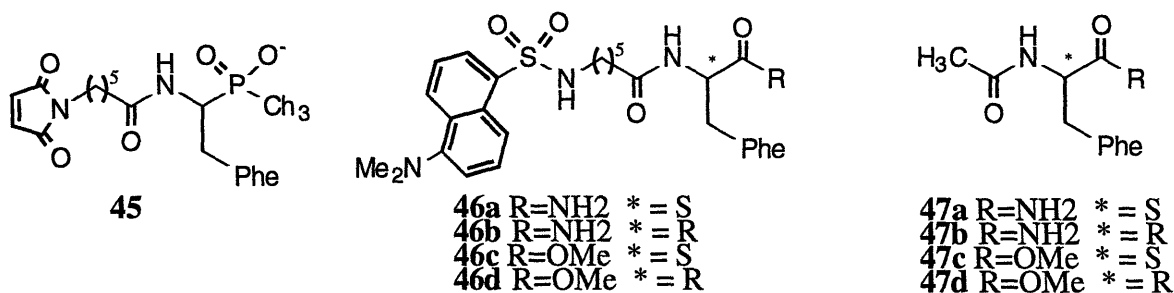
An interesting approach to cleaving peptide bonds has been reported by Benkovic where the target reaction was the well-documented β -aspartyl shift, a natural mechanism of the aging of proteins³³. This report described antibodies raised to the bi-functional hapten **40**, which catalyzed the conversion of asparaginyl-glycyl(*N*-phenethyl)amide **41** first to succinimide **42**, and subsequently to the hydrolysis products **43** and **44**.



These conversions can potentially provide an alternative means (to direct amide bond cleavage) for the deactivation of protein functions *in vivo*. Hapten **40** was designed so that its two tetrahedral transition state analogs (phosphonate and secondary alcohol) could mimic all of the transition states on the pathways leading from substrate **41** to the β -aspartyl shift product **43**, or, to the aspartate deamination product **44**. In the initial report, two monoclonal antibodies (2E4 and 24C3) were found to accelerate the cyclization of **41** to **42** and 2E4 was characterized kinetically to have $k_{\text{cat}} = 0.0072 \text{ min}^{-1}$ at pH 9.0 which corresponds to a rate acceleration of only about 70 when compared to the water catalyzed reaction.

A later comprehensive analysis found that two classes of catalytic antibodies had been generated³⁴: those that only catalyze the hydrolysis of the succinimide **42**, and those that catalyze both the cyclization of **41** to succinimide **42**, as well as the subsequent hydrolysis of **42**. Antibody 23C7 from the first group and 23E4 from the second group were characterized for their substrate specificities and product ratios. Whereas the uncatalyzed reaction gave products **43** and **44** in a ratio of 3.7:1, antibody 2E4 produced these products in a lower ratio (~1) when the substrate was the L-isomer, and in a higher ratio (7:1) when the substrate was the D-isomer. This selectivity was reversed with antibody 23C7 giving 1:1 ratio of the products with the D- isomer and 1:30 with the L- isomer. As a racemic hapten was used, the authors rationalized these results by proposing: 1) 23C7 had been generated by the D-isomer of the hapten while 2E4 had been raised to the L- hapten; 2) the antibody binding site complementary to the phosphinate moiety of the hapten is four-fold more reactive than the site raised to the secondary alcohol; and 3) both isomers of the substrate can be bound as the N-acetyl group of the succinimide **42** corresponding to the linker group of the hapten does not make significant binding interactions with these antibodies.

Again targeting a primary amide, M. T. Martin *et al.* raised 68 monoclonal antibodies to the phosphonate **45** and found that one of these accelerated the hydrolysis of the dansylated phenylalanine primary amide **46** 132 times over the background reaction³⁵. An interesting aspect of this work is the early screening method that was utilized. Antibodies from the cell supernatants of the 68 monoclonals that initially bound to the hapten were immobilized on a gel matrix. These were directly screened for catalysis in the presence of 4 primary amide substrates (**46a,b** ; **47a,b**) and 4 methyl ester substrates (**46c,d** ; **47c,d**) at three different pH values. After each reaction, the antibody in the solid phase was recycled by simple filtration. The immobilized antibodies were shown to be stable after 24 such reaction cycles. Furthermore, incorporation of a dansyl chromophore in the linker portion of the substrates enabled these workers to perform a rough fast screen for catalysis via thin layer chromatography. The most efficient catalyst 13D11 was shown to be specific for the (*R*)-**46b** and did not catalyze the hydrolysis of the corresponding methyl ester **46d**.



Maximum activity was observed at pH 9.5 and was completely inhibited upon the addition of one equivalent of hapten. Surprisingly, this antibody required the presence of the dansyl group in the substrate although this group was absent in the inducing hapten. Thus, acetyl substrate **47b** was not accepted for catalysis.

The above three studies show that although amide hydrolyzing antibodies have been obtained with simple phosphorus based haptens, the catalytic efficiency, as well as the probability of finding a catalyst have been quite poor. This is

probably due to the fact that these haptens only emphasize the formation of an acid residue in the antibody binding sites that facilitates the transition state for the formation of the tetrahedral intermediate. On the other hand, mechanistic studies of amide hydrolysis have shown that the rate determining transition state is that of the breakdown of the tetrahedral intermediate with the departure of the amino group⁵. As it is known that the relatively facile amidase antibody NPN43C9 acts by a fortuitously-induced nucleophilic catalyst, it can be speculated that the latter two inefficient amidase antibodies may be acting by a mechanism where the induced acidic residue is in the proximity to shuttle its proton to the departing amine, albeit inefficiently. What is needed then, is a paradigm to generate a more effective proton donor to the departing amine, in addition to the stabilization of the tetrahedral intermediate.

2.2 Second Generation Haptens Based on Antigen-Antibody Charge Complementarity or Metal co-factors

After the seminal report of Schultz that a charged ammonium hapten (**9**) could generate antibodies that catalyzed a β -elimination reaction¹⁵, ostensibly through the generation of a charge-complementary basic antibody residue, two research groups independently envisioned that a similar basic residue could be utilized in ester and amide hydrolysis. This basic residue would be used to deprotonate an incoming water molecule, and also shuttle the removed proton to the departing amine or alcohol to increase its leaving group ability.

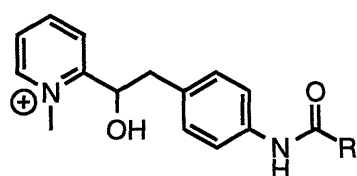
The research group of Janda was the first to report the application of this design to ester hydrolysis, with the use of a pyridinium secondary alcohol (*vide infra*)³⁶. Although this design was successful in generating esterolytic antibodies, it carries an inherent limitation. The ester substrate must be a benzoate due to the incorporation of the positive charge into an adjacent aromatic ring. On the other

hand, our own design which was subsequently-reported is free of this limitation and is more generally applicable due to the employment of an alkyl ammonium alcohol for the same purpose (*vide infra*)³⁹.

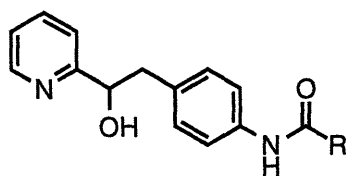
Finally, Iverson *et al.* used a metal trien complex to generate antibodies that would hydrolyze amide bonds via the activation of the amide bond with metal coordination (*vide infra*)⁴¹. Although seemingly successful, the discrepancy between the accepted substrate and the inducing metal-trien hapten hints at the fortuitous nature of this finding; especially after a similar, if not more sophisticated approach, was found to be unsuccessful by Blackburn *et al.*⁴²

2.2.1 Pyridinium Alcohol Haptens for the Antibody Catalyzed Hydrolysis of Benzoate Esters

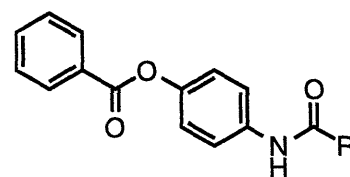
Janda *et al.* raised antibodies to the pyridine-derived haptens *N*-methyl pyridinium **48** and uncharged **49**³⁶. Approximately twenty antibodies raised to each hapten were screened against benzoate **50**. None of the antibodies raised to hapten **49** were able to catalyze the hydrolysis of ester **50**, while seven of the antibodies raised to the *N*-methyl-pyridinium hapten **48** were found to be catalytic.



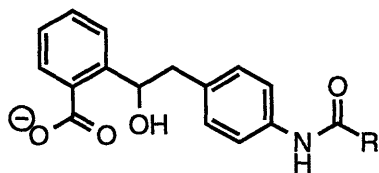
48 R = (CH₂)₃COOH



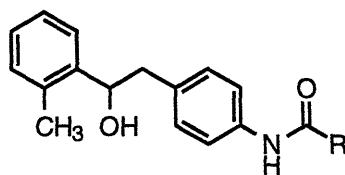
49 R = (CH₂)₃COOH



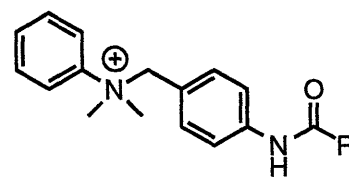
50 R = (CH₂)₃COOH



51 R = (CH₂)₃COOH



52 R = (CH₂)₃COOH



53 R = (CH₂)₃COOH

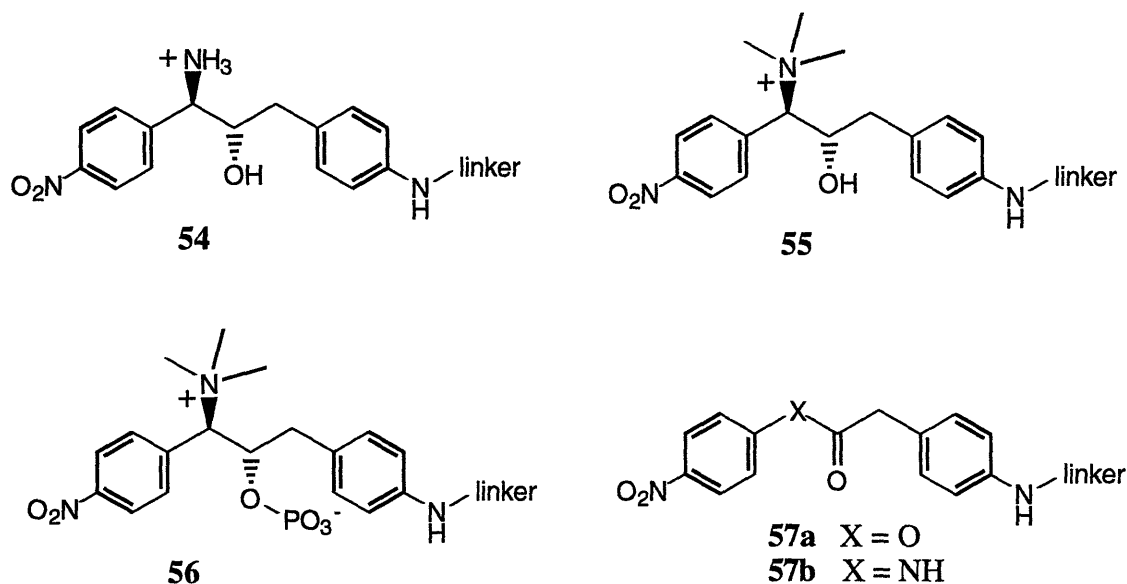
These antibody catalyzed reactions could all be inhibited in a competitive manner with their corresponding haptens. Antibody 30C6, displayed Michaelis-Menten kinetics where: $k_{\text{cat}}/k_{\text{uncat}} \sim 100$; $K_{\text{m}} = 1.12 \text{ mM}$; and $K_{\text{i}} = 83 \text{ }\mu\text{M}$. The pH-rate studies pointed to the involvement of a basic residue in the antibody binding site with an apparent $\text{p}K_{\text{a}}$ of 6.3 thus confirming the success of the charge-complementarity approach to the generation of esterolytic antibodies.

Subsequently, Janda *et al.* prepared three more haptens **51**, **52** and **53** to determine the importance of charge and the ability of a secondary alcohol to function as an effective mimic of the acyl transfer transition state³⁷. After screening twenty-two antibodies specific for hapten **53**, no significant catalysis was observed in the hydrolysis of benzoate **50**. Substituting the secondary alcohol for a quaternary ammonium group (hapten **52**) also failed to provide catalytic antibodies. On the other hand, three out of eighteen antibodies raised to hapten **51** catalyzed the hydrolysis of benzoate **50** and could be competitively inhibited. One antibody 27A6 was characterized further and showed increasing catalytic activity as the pH of the reaction medium was increased, but no ionizable antibody residues. This suggests that this antibody relied on general base catalysis from the solvent for its catalytic activity. These results prompted the authors to conclude that a combination of both charge and transition state complementarity is critical in obtaining antibody acyl transfer catalysts.

2.2.2 Esterolytic Antibodies Induced to Haptens with a 1,2-Amino Alcohol Functionality³⁸

We have designed and synthesized three haptens **54**, **55**, **56** based on an amino alcohol framework to test the correlation between hapten structure and catalytic efficiency³⁹. Another goal of the study was to establish how the binding affinity to haptens, substrates or products relates to the observation of catalysis.

All three haptens incorporated a positively charged ammonium moiety next to a secondary alcohol and the size difference between the hapten and the substrate was varied. Hapten **54** contained a primary ammonium next to a secondary alcohol while hapten **55** reproduced the same structure but with a quaternary ammonium. When the hapten is replaced with the substrate, the position of this amine was expected to provide a convenient binding site for the water nucleophile. Finally, hapten **56** carried an additional negatively charged phosphate to induce an acidic residue that would stabilize the oxy-anion transition state, albeit with some structural mismatch. Thirty-four, 48 and 20 monoclonal antibodies were generated to these haptens, respectively, and each antibody was tested for catalyzing the hydrolysis of the *p*-nitrophenyl ester **57a**.



Interestingly, all of the three haptens were able to generate esterolytic antibodies with roughly similar rate accelerations ($k_{cat}/k_{uncat} = 1-3 \times 10^3$). In a study first of its kind, the dissociation constants (K_d 's) were measured to substrates, respective haptens and products. No major differences in binding affinities were observed between catalytic and non-catalytic antibodies from each of the three haptens. This confirmed our belief that antibody catalysis relies on the generation

of appropriately placed catalytic residues in antibody binding sites and not on a general paradigm of binding affinity.

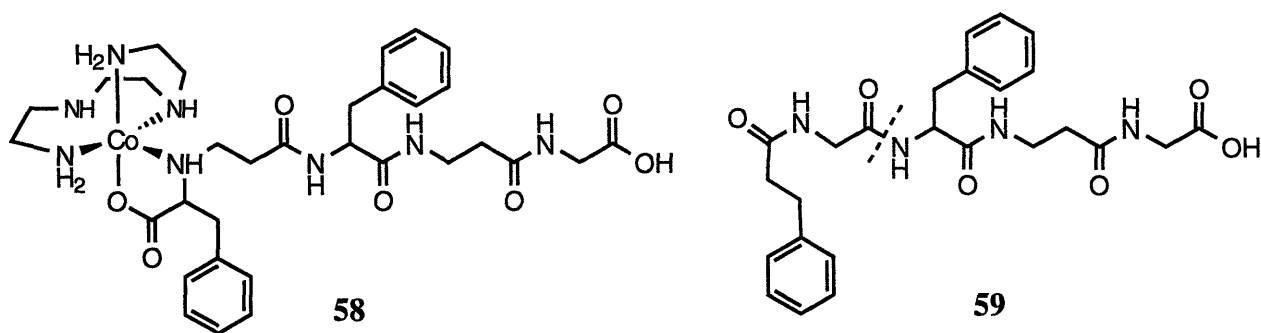
Another significant finding of the study was that hapten **54** gave the highest probability of generating catalytic activity with 16 out of the 34 antibodies induced to this hapten being catalytic. Whereas 7 out of 48, and 4 out of 20 haptens were found to be catalytic with haptens **55** and **56**, respectively. It was deduced that the quaternary ammonium of the latter haptens were ineffective presenters of the haptenic positive charge to the antibody repertoire probably due to the steric interference of the methyl groups. Additionally, the phosphate group of hapten **56** was deemed too large to generate a useful acidic residue in proximity to the reaction site. None of the antibodies generated to the three haptens were seen to accelerate the hydrolysis of the amide substrate **57b**⁴⁰.

The most important conclusion that can be derived from the above two studies is that hapten-designs based on charge-complementarity could generate esterolytic antibodies with similar catalytic efficiencies ($k_{\text{cat}}/k_{\text{uncat}} = 1000$) to antibodies generated to phosphonate haptens, while this new design principle still proved inadequate to provide amidase antibodies. We proposed that the use of zwitterionic haptens were essential for the generation of the amidase catalysts. Unfortunately, the synthesis of such zwitterionic haptens presents considerable synthetic challenge. This problem was circumvented by our development of a unique immunization protocol, named heterologous immunization⁴⁹ which will be described in section 2.3.

2.2.3 Metal Based Haptens to Generate Amidase Antibodies

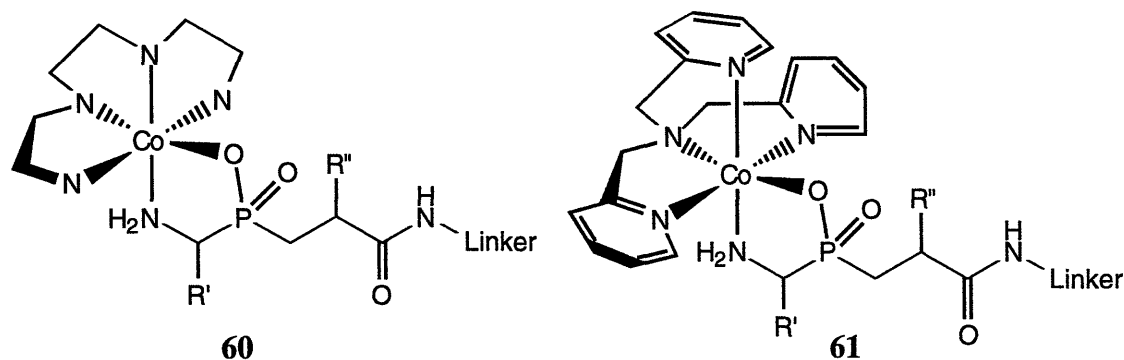
Metal ions are known to catalyze the cleavage of amide bonds and certain metallopeptidases, such as carboxypeptidase, use divalent metal cations as cofactors in catalysis. Two mechanisms are available by which metal ions can facilitate

amide bond hydrolysis. Either the metal ion can polarize the carbonyl group by coordination with the carbonyl oxygen, a process which assists nucleophilic attack at the carbonyl carbon, or alternatively, the metal ion can directly deliver bound hydroxide to the carbonyl carbon. By synthesizing a stable Co(III)trien complexed to a tetrapeptide **58**, Iverson and Lerner hoped to induce an antibody binding site that would place the scissile bond of the substrate in close proximity to a bound metal trien complex so that the amide bond hydrolysis could be catalyzed by one of the two mechanisms described above⁴¹.



Thirteen monoclonal antibodies specific for the hapten **58** were screened for hydrolytic activity against six peptide substrates with several different trien metal complexes. One antibody, 28F11, catalyzed the hydrolysis of substrate **59** in the presence of trien ligand and several different metals including Zn(II), Fe(III), Ga(III), Cu(II) and Ni(II). The most efficient metal cofactor complex compatible with antibody 28F11 was reported to be a Zn(II)trien with optimum activity between pH 6.0 and 8.0, although detailed kinetic studies were not undertaken. Several issues call for a certain amount of skepticism when reviewing these results: 1) substrate cleavage occurred specifically at the Gly-Phe bond, a position somewhat displaced from the anticipated metal binding site, 2) rate of background hydrolysis in the presence of metal-trien complexes were not determined, 3) inhibition constant with the inducing hapten was not reported.

No doubt inspired by the above results of Iverson and Lerner, Blackburn sought to improve on this design by incorporating a phosphinate moiety at the haptenic site corresponding to the scissile amide bond, ensuring a more correct orientation of the metal ligand⁴². Initially, hapten **60** was synthesized involving the original trien ligand. However, this compound was found to be poorly immunogenic and the design was modified to the tris-pyridyl hapten **61**. Unfortunately, no further reports appeared on the immunization or catalysts generated with hapten **61**. Thus, it is compelling to assume that the outcome of the immunological or kinetic studies has been negative. Nonetheless, that of Blackburn represents one of the most elaborate hapten designs that has been reported to generate acyl hydrolyzing antibodies.



2.3 Third Generation Hapten Design: Heterologous Immunization

As mentioned above, one of the conclusions of our studies with 1,2-amino alcohol haptens was that zwitterionic haptens are probably essential to generate amidase antibodies. We were inspired by the earlier immunological studies of antibody cross reactivity to two distinct but structurally similar antigens that was termed "original antigenic sin". We envisioned that the phosphinate and ammonium groups of a zwitterionic hapten could be bisected into two haptens. These could then be used to immunize in succession and generate antibodies that would be cross reactive to both of the haptens, and display enhanced catalytic

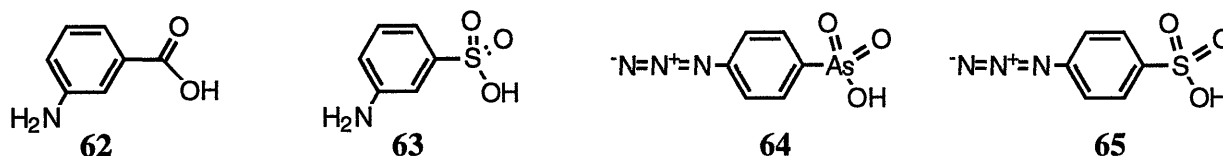
efficiency. This section will first present a brief outline of the studies on original antigenic sin, and then discuss the successful outcome of the devised immunization regimen that we termed "heterologous immunization"

2.3.1 Original Antigenic Sin

The humoral arm of the Immune system consists of up to 10^{10} different B-cells each of which has a unique genetic formula to produce a unique antibody⁴³. Upon encounter with an antigen, the B-cells that produce antigen-binding antibodies are proliferated. In the primary immune response, IgM class of antibodies are produced which have low affinity to the antigen. If the antigen presence persists, starting with the second week, the class of antibodies produced is changed from IgM to IgG (the so-called "class-switch") which have longer lifetimes in the blood-serum. Concurrently, the induced B-cells undergo a process called "somatic mutation" where their antibody-specific genes are subjected to mutation followed by continuous selection to give tighter-binding antibodies. After the antigen threat is overcome, most of these B-cells are cleared from the body, but a small subset is retained to serve as memory B-cells. When the same antigen is encountered a second time, a secondary immune response occurs where the specific memory B-cells are directly induced to proliferate, producing tight binding IgG class antibodies.

In 1953, during the studies of immune response to different strains of influenza virus, a phenomenon was observed which was later termed "original antigenic sin"⁴⁴. When animals that were already immune to a primary antigen (viral coat protein) were stimulated with a different but related antigen it was seen that the resulting polyclonal antibodies reacted stronger with the original antigen than the secondary antigen. A number of studies ensued to investigate the issue but these were more speculative in nature than conclusive⁴⁵.

Finally, Bussard *et al.* studied this phenomenon in more quantitative terms⁴⁶. Two structurally similar haptens, *m*-aminobenzoic acid **62** and *m*-sulfanilic acid **63** were used as haptens and the number of specific B-cells generated were used to quantitate the strength of each immune response. The use of molecularly defined haptens assured the uniformity of the immunization procedures. In animals immunized with only one of the haptens, no cross-reactivity to the other hapten was observed. In contrast, when animals were immunized with **62** followed by **63** they displayed a similar-strength response to both haptens, and with the reverse regimen, a stronger response to the primary (**63**) hapten. Clearly in both cases, the secondary antigen was triggering the production of antibodies from memory B-cells that had already been generated toward the primary hapten.



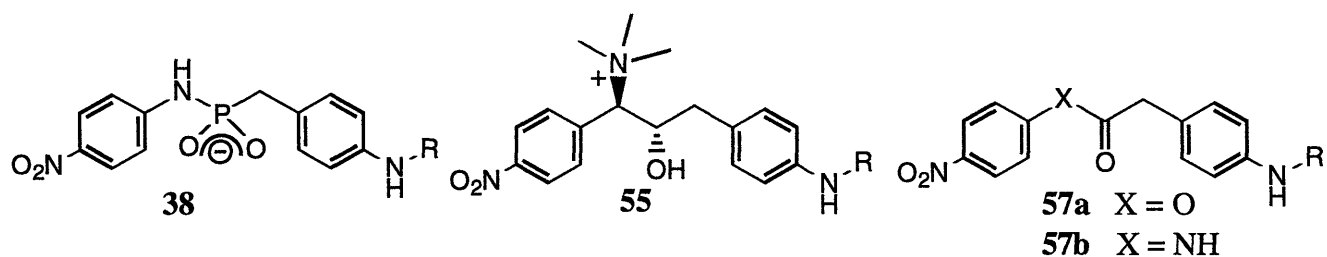
This hypothesis was subsequently proven at the molecular level by Manser *et al.*⁴⁷ after the development of hybridoma and DNA manipulation technologies in the early 80's. From their earlier studies, these researchers had already determined the genetic make up of the immune response to a *p*-azidophenylarsonate (**64**) hapten⁴⁸. By immunizing animals already immune to **64** with a structurally similar *p*-azidophenylsulfonate (**65**) hapten and determining the genetic make up of antibody response, they could show that the same gene family was used to bind both the primary (**64**) and the secondary (**65**) haptens. Furthermore, they could show that the development of the cross-reactivity was achieved by the **65**-induced somatic mutation of variable region genes in **64**-specific memory B-cells .

As encouraging as these landmark studies were, it should be noted that the structural variation between the primary and secondary antigens was quite small. Thus, it was not clear whether the same "original antigenic sin" mechanism could

be recruited to cross-reactively respond to two haptens that would incorporate two opposing point charges in their nonetheless-similar structures. Fortunately, this was a risk we were willing to take.

2.3.2 Esterolytic Antibodies Generated by Heterologous Immunization

With the aim of generating amidase antibodies that catalyze the hydrolysis of amide **57b**, we raised antibodies to haptens **55** and **38** using the heterologous immunization protocol⁴⁹. Thus, mice were immunized twice with **55** and a final boost was delivered with the phosphoramidate hapten **38** before the production of hybridomas. As a control, antibodies were also raised to hapten **55** and **38** alone (homologous immunization). It was found that 19 out of the 50 antibodies generated by the heterologous immunization catalyzed the hydrolysis of ester substrate **57a**, while only 7 of the 48 antibodies raised to **55** alone displayed catalysis. Furthermore, 9 of the 19 *heterologous* catalytic antibodies displayed greater than 10^4 acceleration, while the seven *homologous* catalytic antibodies to hapten **55** all had similar rate accelerations of about 10^3 .



Homologous immunization with **38** also generated catalytic antibodies with high probability (17 out of 48), however 12 of the 17 catalysts displayed strong product inhibition with *p*-nitrophenol. The most efficient catalyst from this group, antibody H2-23, displayed a rate acceleration of 11,000 and burst kinetics. However, this initial burst was due to strong product inhibition by *p*-nitrophenol which diminished catalytic activity by 30% after 5-6 turnovers.

The best catalyst obtained from heterologous immunization, H5H2-42, accelerated the ester hydrolysis 10^5 fold over the background reaction at pH 6.6 and displayed more than 500 turnovers. It was shown to be competitively inhibited by both **55** and **38**, while no product inhibition was seen with either *p*-nitrophenol or the acid. The pH dependence studies pointed to the existence of two ionizable antibody residues that participated in catalysis with apparent pK_a 's of 5.6 and 8.7; thus confirming the generation of bi-functional antibody residues with the heterologous immunization strategy.

Interestingly, the reverse order of heterologous immunization, namely two injections with **38** followed by a boost with **55** failed to give cross reactive antibodies. Antibodies generated in this fashion were shown to have a weak affinity to **55** and no affinity to **38**. These were also shown to belong to the IgM subclass. All of this evidence pointed to the fact that this immunization order simply led to a primary immune response to hapten **55** rather than recruiting the memory B-cells that were previously generated to **38**. This was tentatively explained to be a phenomenon of sterics where the bigger hapten **55** fails to bind and stimulate epitopes that were originally generated to **38**. However, it should be pointed out that a similar phenomenon has also been observed with our subsequent studies in heterologous immunization (see Ch. 3), and in that case sterics failed to offer an explanation.

Dissociation constants (K_d 's) of all (catalytic, non-catalytic, homologous and heterologous) antibodies were measured to the amide substrate **57b**, both of the haptens and both of the products. No general differences were observed in the binding affinity to the substrate showing that this is not a criteria for catalytic efficiency. Catalysis by all of the *homologous* antibodies were specifically inhibited by their inducing haptens but not with the opposite hapten. This pattern was also reflected in the binding affinity (K_i 's) of the *homologous* antibodies where minimal

binding to the opposite hapten was observed. Finally, all of the catalytic antibodies were assayed for catalyzing the hydrolysis of amide **57b** and none of them displayed catalysis.

As a summary, this seminal work on heterologous immunization has shown that zwitterionic haptens can be dissected into two structurally-similar haptens and used to generate antibodies that bind both haptens. Furthermore, it was shown that heterologous antibodies are up to two orders of magnitude more efficient catalysts than their homologous counterparts. On the other hand, this rate improvement was not sufficient to achieve the catalysis of the corresponding amide **57b**. A thorough re-evaluation of the mechanistic studies of serine proteases and previous acyl-transfer antibodies pointed to nucleophilic catalysis as an effective way to augment the rate accelerations achieved by heterologous immunization.

2.4 Fourth Generation of Haptens: Combination of Heterologous Immunization with Nucleophilic Catalysis

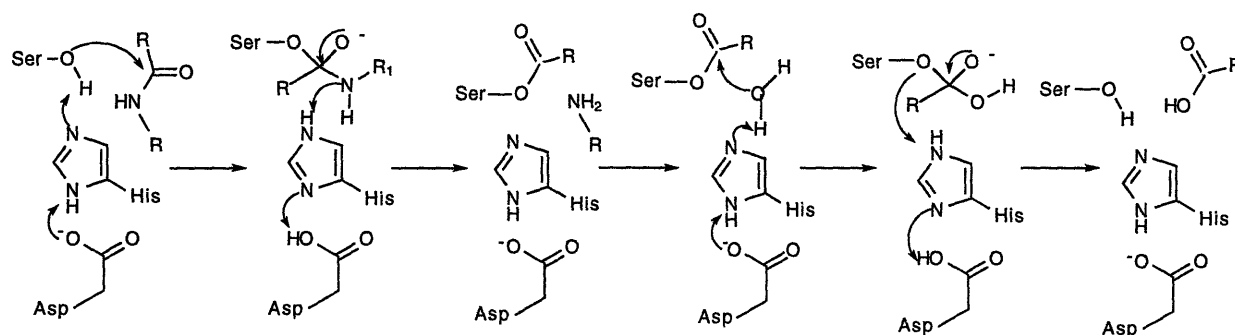
The rate determining step of most amide hydrolysis reactions is the breakdown of the tetrahedral intermediate to expel the amine⁵. Heterologous immunization with oppositely charged haptens tries to facilitate this process by generating residues to donate a proton to the departing amine. To find an extra source of catalysis, we reasoned that the use of a more effective nucleophile than water should lead to an increase in the population of the tetrahedral intermediate. This could in turn lead to an increase in the rate of break-down of the tetrahedral intermediate to an acid and amine. Similar nucleophilic catalysis is commonly employed by enzymes, and it is significant that three out of the four classes of proteases and all of the acyl hydrolyzing antibodies characterized so far display the use of a fixed internal nucleophile.

2.4.1 A Brief Synopsis of Proteolytic Enzymes

Proteolytic enzymes are commonly divided into four classes according to their mechanism of action. With the exception of aspartic proteases, all of the other three classes of proteases function by positioning the initial nucleophile that attacks the amide bond at an optimal location. Hence, in the case of metalloproteases this nucleophile is a hydroxide bound to a metal in the active site, and in serine and cysteine proteases it is an active site alcohol or thiol residue, respectively⁵⁰.

Of all the types of proteases, the mechanism of serine proteases has been the most extensively studied. It involves a so-called "catalytic triad" of three active site residues (scheme 2.1). The nucleophilic attack by an active site serine residue is aided by general base catalysis by a histidine which is in turn activated by an aspartate, leading to the formation of the acyl-enzyme tetrahedral intermediate. The subsequent expulsion of the amine is aided by its protonation by histidine generating the acyl-enzyme species. Then the process is repeated in reverse for the hydrolysis of the acyl intermediate liberating the acid portion of the substrate.

Scheme 2.1



In addition to the catalytic triad, another feature of serine proteases that is essential for catalytic activity is the so-called oxy-anion hole. This is formed by two active site hydrogen-donor residues that stabilize the oxy-anionic tetrahedral intermediates in the acylation and hydrolysis steps of the reaction.

As the phosphonate haptens are expected to generate the antibody equivalent of this oxy-anion hole, and the complementary ammonium-alcohol haptens should

generate the equivalent of the general-base histidine residue (probably in the form of a carboxylate); it became apparent to us that the remaining factor to simulate the mechanism of serine-proteases was to incorporate a nucleophilic residue into our antibody binding sites. This nucleophile should ideally be nucleophilic enough to attack an amide bond, and also its formed ester should be facily hydrolyzed in water. Further support on the importance of nucleophilic catalysis to acyl hydrolyzing antibodies was drawn from the mechanistic and structural studies of esterase and amidase antibodies where researchers proposed similar acyl-antibody intermediates.

2.4.2 Mechanistic and Structural Studies of Acyl Hydrolyzing Antibodies

The amidase antibody NPN43C9 that was described in section 2.1.5 has been the antibody whose mechanism has been investigated most extensively. Initially, Benkovic *et al.* analyzed the steady state parameters, k_{cat}/K_m and k_{cat} as a function of pH, and discovered that an apparent pKa of 9.0 was displayed for an ionizable residue⁵¹. This could be interpreted as either a reaction mechanism involving an active site residue whose deprotonation promotes hydrolysis, or a mechanism featuring a change in the rate-determining step around an intermediate antibody-bound species, occurring as a function of pH. No isotope effect was observed for the anilide **39** when the pH- k_{cat} rate profile was measured in D₂O which tends to rule out the possibility of a general acid/base catalysis involving an active site residue in the rate determining step.

Mechanism of NPN43C9 was also studied with the *p*-nitrophenol ester analog of **39**. Initially, no direct evidence for the formation of an antibody acyl covalent intermediate could be found: no rapid formation of *p*-nitrophenol was observed; and no exchange of ¹⁸O from H₂¹⁸O into the substrate was observed⁵². The former observation does not, however, rule out the possibility of an intermediate at steady

state levels, and the latter does not eliminate the possibility of an asymmetrical intermediate or again, steady state acyl species. Two mechanisms were considered to account for the observations, one involving an active site nucleophile whose reactivity was dependent on its pK_a , and a second mechanism, where the pK_a of the active site nucleophile was outside of the observable pH range. The pH-rate profile was explained by a change in the rate-determining step from *p*-nitrophenol release at low pH to hydroxide mediated hydrolysis at high pH.

A second study on the same antibody NPN43C9 sought further evidence for an acyl-antibody intermediate, by examining the antibody catalyzed hydrolysis of a series of *p*-substituted phenyl ester substrate analogs⁵³. Hammett structure-reactivity correlation studies indicated a mechanism involving nucleophilic attack by a neutral nitrogen such as imidazole. On the basis of molecular modeling studies which showed that one of two histidines in the antibody combining site might be in the correct orientation for nucleophilic attack on the substrate, and chemical modification studies with diethylpyrocarbonate which inactivated the catalyst, the authors suggested that the substrate might be acylated by an antibody active site histidine.

To further prove the existence of a imidazole-acyl intermediate in the antibody binding site, a three dimensional computer simulation model of the antibody 43C9 was constructed based on the previously-solved X-ray structures of antibody heavy and light chains that displayed sequence homology to 43C9⁵⁴. Histidines L91 and H35 were identified as likely candidates for the imidazole nucleophile, while arginine L96 was found to be situated ideally to stabilize the oxyanion tetrahedral intermediate. A phagemid expression system was developed for the production of single-chain Fv of 43C9 in *E. Coli*.

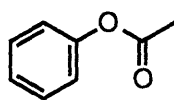
Site-directed mutagenesis experiments using the above expression system showed HisL91 and ArgL96 to be the active site residues responsible for catalysis.

Mutation of these residues resulted in the loss of catalytic activity without concomitant loss in substrate binding. On the other hand, a second histidine, HisH35 was found to be structurally important for this antibody, as any mutation of this residue resulted in the loss of both catalytic activity and binding ability. Finally tyrosines L32 and H95 were mutated separately into histidines as the modeling studies had indicated that these residues were in appropriate location to act as general acid catalysts. Surprisingly, both mutations caused a decrease in the catalytic activity, ostensibly pointing to the limitations of the molecular modeling experiment. Furthermore, mutation of HisL91 to a more nucleophilic serine or cysteine also decreased the catalytic activity.

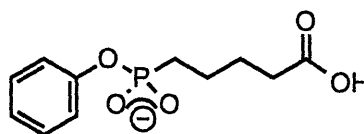
The final proof for the antibody-acyl intermediate came from electrospray mass spectroscopy studies where a covalently bound species of mass weight equal to an acylated antibody was detected at pH 5.9 which represented 10% of the total antibody⁵⁵. In the presence of the hapten, this species was not detected. Based on the kinetics and mutation experiments, the authors concluded that at pH values less than 9, the rate limiting step is the hydroxide ion mediated hydrolysis of the acyl intermediate, while above this pH, the rate determining step becomes either product release (*p*-nitrophenyl ester) or the formation of the acyl intermediate (other esters and *p*-nitroanilide). Hence, the mechanism of 43C9 with ester substrates can be summarized as follows: the attack of HisL91 on the substrate carbonyl forms the acyl-histidine complex, while ArgL95 stabilizes the forming oxy-anion tetrahedral intermediate. The liberated phenol remains bound to the antibody. This intermediate is then hydrolyzed by hydroxide ion to give a ternary complex of antibody, phenol and the acid. The two ligands are then released sequentially to complete the catalytic cycle. The authors expressed their belief that the nucleophilic catalysis displayed by antibody 43C9 had been generated

fortuitously and that further acid-base catalysts could be introduced by site-directed mutagenesis.

The mechanism for the hydrolysis of phenyl acetate **66** by antibody 20G9 raised to hapten **67** was investigated by Martin *et al.*⁵⁶. In contrast to the above esterolytic activity by NPN43C9, the hydrolysis of phenyl acetate by antibody 20G9 was characterized by a pre-steady state burst producing phenol. The latter was an inhibitor of the antibody, where $K_i^{\text{app}} = 2.5 \mu\text{M}$. At pH 8.8, the initial kinetic constants were $k_{\text{cat}} = 4.9 \text{ min}^{-1}$ and $K_m = 300 \mu\text{M}$, and at steady state $k_{\text{cat}} = 0.54 \text{ min}^{-1}$ and $K_m = 36 \mu\text{M}$. Examination of the pH rate profile indicated an active site residue with a $\text{pK}_a = 9.6$, and a constant value of K_m over the pH range 7.0 - 11.0. Phenol and phenolate were shown to inhibit the reaction equally which indicates that the pH-rate profile depends on k_{cat} (rather than any pH dependence for the dissociation of the antibody-phenol complex). Finally, chemical modification studies with tetranitromethane and affinity labeling reagents specific to phenols caused a loss of activity. This led the authors to suggest that the mechanism of 20G9 involved an acyl-tyrosine intermediate in the binding site.



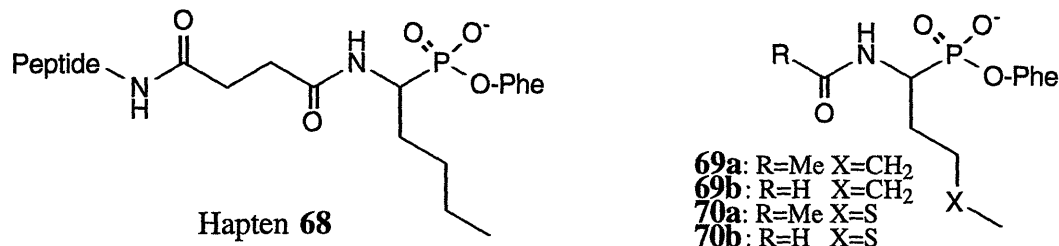
66



67

Another valuable inquiry into the mechanism of action of esterolytic antibodies came from the laboratory of Thomas Scanlan⁵⁷. Phosphonate hapten **68** was used to generate an antibody 17E8 that catalyzed the hydrolysis of the phenyl esters of norleucine (**69a,b**) and methionine (**70a,b**) 2.2×10^4 fold over the background reaction at pH 7.2. In fact, at pH 9.5 where the antibody catalyzed reaction is 20 fold faster, the comparative rate acceleration approaches 10^6 over the water catalyzed reaction, which is one of the fastest ever reported. Greater than 1000 turnovers were also observed. This antibody was found to be selective for the

(*S*) enantiomers of the substrates matching the conformation of the inducing hapten, and displayed a bell-shaped pH optimum which indicated the participation of two catalytic residues with pKa's 8.9 and 10.1.



It was found that this antibody displayed six fold selectivity for formylated over acetylated substrates as well as a eight fold selectivity for norleucine over methionine esters. The mode of catalysis was seen to involve the formation of a covalent acyl intermediate with a binding site residue whose rate of formation was the rate determining step. Thus when hydroxylamine was added to the reaction mixture, a hydroxyamic acid product was also formed from the partitioning of the acyl intermediate, while the overall rate of catalysis was not affected. It was commented that the covalent intermediate might also be an oxazolone that is formed by the intramolecular cyclization of the substrate. This would explain the preference for the formylated over the acetylated substrates.

In a following paper the authors determined the X-ray structure of the Fab fragment of this antibody bound to its hapten⁵⁸. A protonated lysine (H97) was found to form a salt bridge with the phosphonate pro-*S* oxygen. This lysine is then a very likely candidate for the catalytic residue with a pKa of 10.1 which stabilizes the oxy-anion of the transition state. Both the phenyl ring and the norleucine side chains were found to be buried in hydrophobic pockets explaining the substrate selectivity for norleucine over methionine esters. This finding supports the notion that a phosphonate hapten can faithfully generate antibody residues to stabilize the oxy-anion transition state of acyl hydrolysis. The identity of the pKa 8.9 residue was more dubious, however. This pKa is in the right range for a tyrosine residue

and Tyr^{H101} was proposed to be a participant in catalysis. This residue acts as a hydrogen bond donor to Ser^{H99}. Above pH 8.9, this tyrosine is deprotonated which frees the serine to rotate 180 degrees and be in the correct position to attack the acyl group of the substrate and form the observed acyl-intermediate. Furthermore, it was speculated that this serine is also in the vicinity to form a hydrogen bond to His^{H35} similar to the catalytic triad of serine proteases.

Further indirect evidence for Ser^{H99} as a nucleophile came from a subsequent paper, where the four catalytic antibodies out of the total 20 that were generated by hapten **68** were sequenced, including antibody 17E8⁵⁹. The second most active antibody, 29G11 which is four-fold less active, displayed high structural homology to 17E8 based on computer modeling. Interestingly, in this antibody, Ser^{H99} was found to be replaced by Gly^{H99} and the formation of a covalent intermediate was not observed by hydroxylamine partitioning studies. As 29G11 also displays a bell shaped pH optimum curve, the authors proposed that this antibody functions by a general acid-base catalysis and His^{H35} acts as the base to deprotonate an incoming water molecule.

2.4.3 Remarks

The above information shows that nucleophilic catalysis is a powerful mode of catalysis that previously had only been generated in catalytic antibodies by chance. We considered the different possible methods of inducing a nucleophilic residue in antibody binding sites, and it became apparent that a nucleophilic side chain residue could not be generated via immunization. The only reliable method to install such residues in antibody binding sites is via post-immunization mutagenesis. Furthermore, in the few cases that this approach was taken, it was seen to be labor - intensive as well as ineffective, since the engineered antibodies did not have enhanced reactivity compared to the original clones⁶⁰.

Thus, we decided that the only reliable method to incorporate nucleophilic catalysis into antibody binding sites was to use an auxiliary catalyst. This is possible either by the incorporation of such a residue into the substrate design, i.e. intramolecular catalysis, or by bringing it in externally, similar to the use of co-factors by enzymes. The following chapter is an account of a successful effort wherein we have designed a reaction system and haptens that were flexible enough to permit both methods of the use of an auxiliary nucleophile.

Chapter 3

Catalytic Antibodies for Amide Hydrolysis with an Auxiliary Nucleophile

3.1 Introduction⁶¹

Three haptens were designed and synthesized to incorporate three design concepts that were conceived to be crucial for amide hydrolysis by antibody catalysts: 1) the generation of bi-functional binding sites with the use of zwitterionic charges; 2) the division of the zwitterionic charges into two haptens and the employment of the previously shown heterologous immunization protocol; and 3) incorporation of an auxiliary nucleophile to perform the initial nucleophilic attack on the amide bond. An additional goal was to employ homologous immunizations with each of the two haptens and compare the results with the heterologous immunization regimen.

3.2 Hapten Design

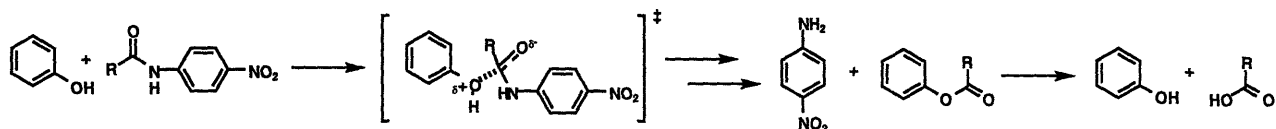
Previous attempts at amide hydrolysis has relied on a water molecule to diffuse into the antibody binding site and effect the nucleophilic addition to the amide carbonyl. However, it is obviously difficult to program an antibody binding site to selectively bind and orient a water molecule, and at the same time keep this binding site accessible to an aqueous environment. Our approach was to replace the water nucleophile with one that can be selectively recognized in aqueous solutions. Hydrophobic interaction is a convenient recognition element, as these interactions have been shown in X-ray crystallography studies of antibody-antigen complexes. On the other hand, the low catalytic efficiencies of catalytic antibodies dictate that this nucleophile should also be readily water-soluble. The combination of these two criteria pointed to the selection of an aromatic nucleophile.

A second point of consideration is that once this initial nucleophile has cleaved the amide, the hydrolysis of this intermediate should also be facile, completing the formal hydrolysis of the amide bond, and insuring against product inhibition. In effect, we desired this auxiliary nucleophile to behave in a similar fashion to enzymatic co-factors.

Phenol was chosen to be the auxiliary nucleophile as it fits all of the above criteria well: 1) the phenyl ring can be bound tightly in a hydrophobic antibody binding pocket; 2) the low pKa of phenol facilitates the removal of its proton by a basic antibody residue; 3) it is readily soluble in water; and finally 4) phenyl esters are easily cleaved in water.

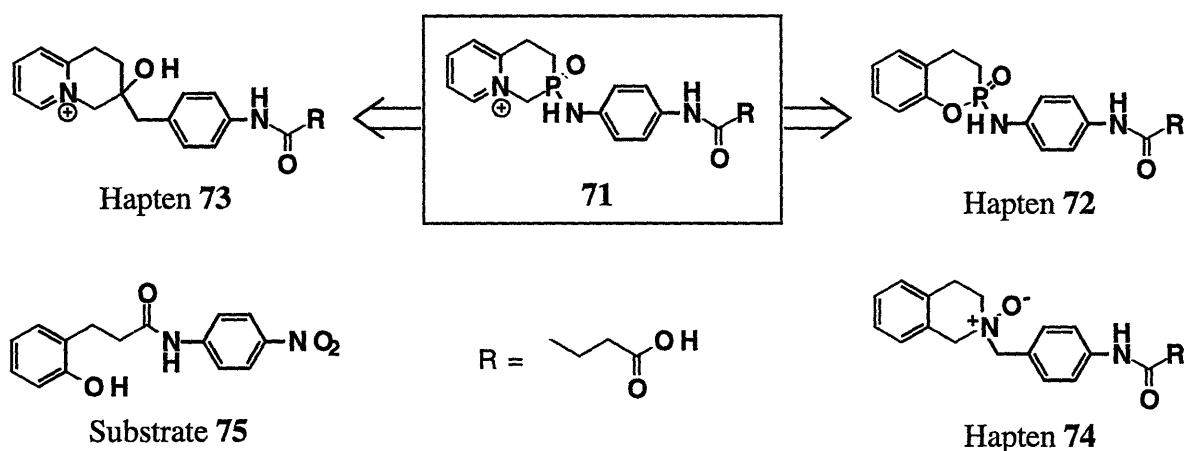
A *p*-nitroanilide was chosen to be the substrate as the *p*-nitroaniline leaving group is a good chromophore which ensures enhanced detection sensitivity for this inherently slow reaction. This reaction mechanism is shown in Scheme 3.1.

Scheme 3.1



With the selection of phenol and *p*-nitroanilide as the auxiliary nucleophile and amide substrate, respectively, and also consideration of our previous experience with esterolytic antibodies^{39,49}, the four essential features for a successful hapten emerged: 1) an aromatic ring to generate the hydrophobic antibody binding pocket, 2) a positively charged residue placed in proximity of the location of the phenolic hydroxyl. This should induce a basic residue in the antibody binding site to deprotonate the phenol and subsequently protonate the departing amine. 3) a negatively charged tetrahedral species such as a phosphonate or *N*-oxide to represent the oxy-anionic tetrahedral intermediate, and finally, 4) the appropriate disposition of the aromatic ring in relation to the amide by incorporation in a six membered structure.

A pyridinium phosphonamidate hapten **71** then appears as the ideal (hypothetical) hapten which can be bisected into haptens **72** and **73** according to our heterologous immunization protocol⁴⁹. An *N*-oxide hapten **74** was also designed as a replacement for **72**, should the synthesis of the latter have posed a problem. Initially, it was planned to also synthesize hapten **71** and compare the results of immunization with this hapten with the heterologous immunization of **72** plus **73**. However, preliminary synthetic studies indicated that **71** would be an unstable compound in aqueous solutions that are employed for immunizations⁶².

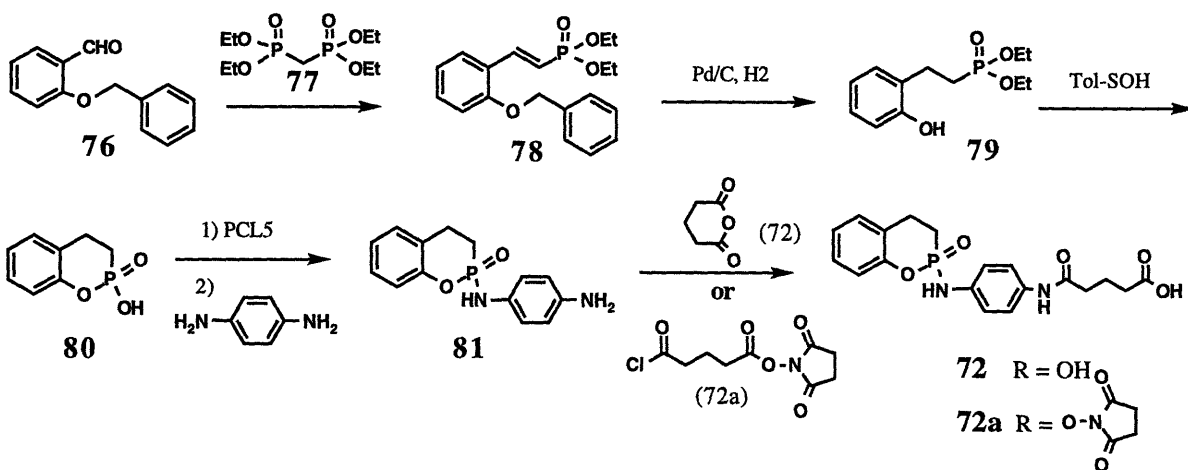


These six membered hapten structures also offered a hidden benefit. Preliminary screens for catalysis could be performed with substrate **75** in an unimolecular fashion. This avoids the difficulty of testing more than a hundred potential antibody catalyst candidates in an initial bi-molecular screen, as each antibody will have a different binding constant (or K_m) to the two components of the reaction. Thus conditions for each molecule, the phenol and the amide would need to be optimized with each catalytic antibody candidate or an effective catalyst could easily be overlooked. Clearly, this is a very laborious procedure. Substrate **75** provided an easy initial screen for catalysis. Once effective catalysts are identified with **75**, these can then be screened under the bimolecular conditions, with phenol and propionic *p*-nitroanilide.

3.3 Synthesis of Haptens, Inhibitors and Substrates

The synthesis of the phosphonamidate hapten **72** is shown in Scheme 3.2. Horner-Wittig olefination of benzyl protected salicylaldehyde **76** with the methylene biphosphonate⁶³ **77** under biphasic conditions gave the styrylphosphonate **78** as the pure (*E*)-isomer in good yield. Reduction of the olefin and removal of the benzyl protecting group is then carried out in one step by catalytic hydrogenation to give the saturated diethylphosphonate **79**. At this point it was decided to cyclize **79** first and subsequently install the labile phosphonamidate bond. One of the ethoxy groups of the phosphonate **79** could easily be exchanged for chloride via reaction with PCl₅, but various reaction conditions failed to give the cyclized product. Generating the monophosphonate and reacting with various acyl-coupling reagents such as BOP or carbodiimides also failed to effect cyclization. The cyclization was finally realized under acid catalyzed conditions with toluene-sulfonic acid. The optimization of reaction conditions and the use of anhydrous toluene-sulfonic acid quickly achieved two transformations in one pot giving the cyclized phosphonic acid **80** in 90% yield.

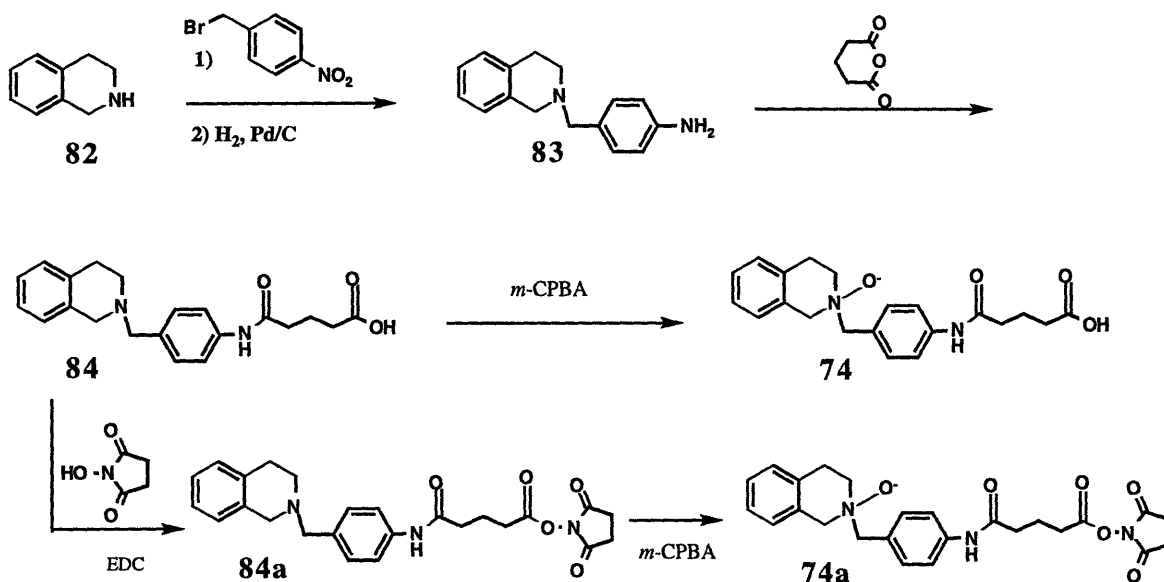
Scheme 3.2



The formation of the phosphonamidate bond presented the greatest challenge in this synthetic scheme. The phosphonyl chloride of **80** was found to be very unreactive and failed to react with *p*-nitroaniline, aniline or even with a carbamate

protected phenylenediamine under various reaction conditions. Only an excess unprotected phenylenediamine showed the requisite nucleophilicity to add to this unreactive phosphonyl chloride. The difficulty of handling excess phenylenediamine was solved by a three step purification scheme that involved removal of the excess phenylenediamine via sublimation, followed by two column chromatography steps to yield the desired phenylenediamino-phosphonamidate **81**. Coupling with glutaryl anhydride afforded hapten **72**.

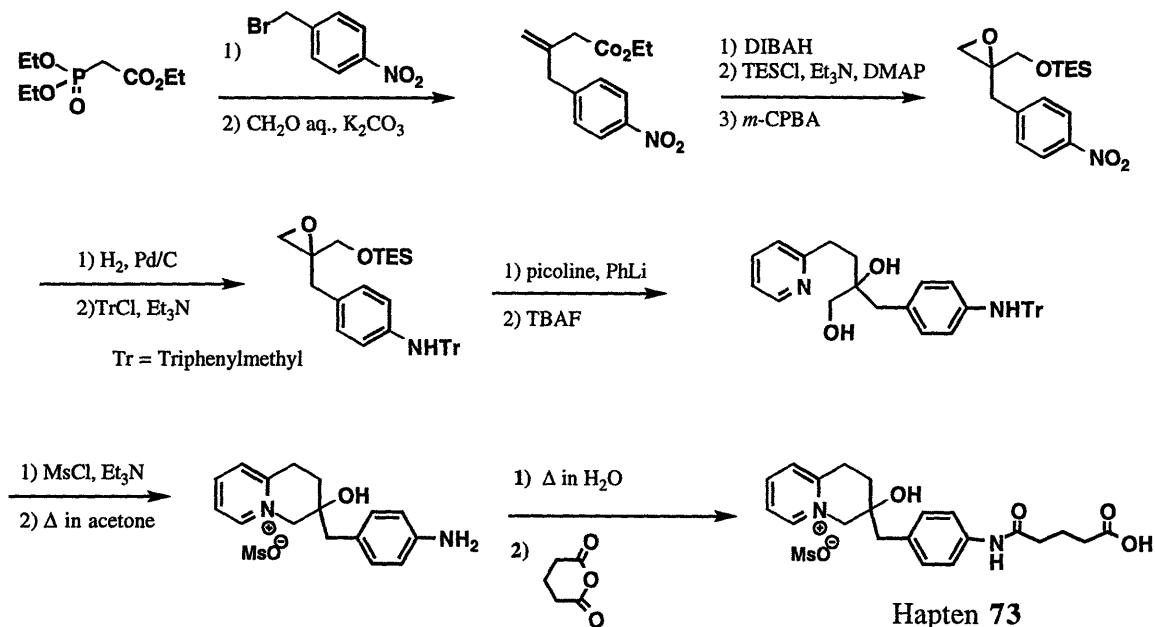
Scheme 3.3



The *N*-oxide hapten **74** was conceived as an alternative to the phosphonamidate hapten **72**, since the *N*-oxide moiety also represents a tetrahedral orientation with an oxy-anionic negative charge. However, the bond angles as well as lengths are less suitable than phosphonate-type haptens in mimicking the tetrahedral transition state of acyl transfer reactions. The synthesis of hapten **74** was straight-forward as shown in Scheme 3.3 with no problematic steps. Thus, dihydroisoquinoline **82** was alkylated with *p*-nitrobenzyl bromide followed by the reduction of the nitro group to give **83**. Coupling with glutaryl anhydride then afforded compound **84**. The tertiary amine of **84** was relatively unreactive towards

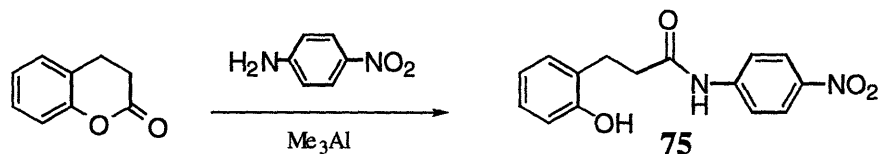
oxidation to the *N*-oxide, and after testing various reagents and conditions including different peroxides and dioxirane; *m*-CPBA was found to be the most effective reagent giving hapten **74** in 57% percent overall yield.

Scheme 3.4



The synthesis of hapten **73** (Scheme 3.4) was carried out in 13 steps and 10.9% overall yield by Mr. Roman Fleck⁶¹. Substrate **75** was synthesized in one step by the opening of dihydrocoumarin **85** with *p*-nitroaniline and trimethylaluminium (Scheme 3.5). All three haptens were individually coupled to carrier proteins Keyhole Limpet Hemocyanine (KLH) and Bovine Serum Albumin (BSA) via the reaction of their activated *N*-hydroxysuccinimide esters (**72a**, **73a**, **74a**) with the surface lysine residues of these proteins. Successful conjugation was confirmed with UV spectrophotometry. The KLH conjugates were used in the immunizations as this protein is known to induce strong immune responses, BSA conjugates were used in the subsequent Enzyme Linked Immuno Sorbent Assays (ELISA's) of the generated hybridomas.

Scheme 3.5



3.4 Homologous and Heterologous Immunizations

With each hapten-KLH conjugate, eight Balb/C mice each received a subcutaneous injection of 100 µg of the hapten-KLH conjugate. The protein suspensions of KLH- **72** and KLH-**74** were injected as an emulsion in an Alum adjuvant, while KLH-**73** remained in solution and was injected as an emulsion in RIBI adjuvant (MPL and TDM emulsion). Two weeks later, the same injections were repeated. Seven days after the second injection, blood serum from each animal was analyzed by ELISA for the strength of the immune response to their inducing haptens.

All of the animals injected with KLH-**72** and KLH-**73** displayed strong immune responses to their respective hapten-BSA conjugates (titers = 1 : 25,600), weaker immune responses to KLH alone (titers = 1 : 12,800) and no response to BSA alone. These results indicated that antibodies had successfully been generated to **72** and **73**. On the other hand, animals injected with KLH-**74** showed no response to BSA-**74** or BSA; while displaying adequate response to KLH (titers = 1 : 6400). This result indicated that either **74** was a poorly immunogenic substance or this hapten was degraded once it was injected into mice. These mice were discarded and all subsequent investigations were continued with mice injected with KLH-**72** or KLH-**73**.

For the homologous immunization protocol, four out of the eight mice from each group (KLH-**72** or KLH-**73**) received a final booster injection with the KLH conjugate (100 µg) of the same hapten two weeks after the second injections. These injections were delivered intravenously in the absence of adjuvants in sterile phosphate buffered saline (PBS) solutions and proved to be quite stressful to the animals. In half of the cases, immediate death ensued due to a severe seizure from immunological shock. However, this is not an uncommon occurrence especially when a strongly immunogenic antigen is used. The surviving animals were

sacrificed 3 days after the final boost in order to isolate B-cells from their spleens and generate hybridomas.

For the heterologous immunizations, the remaining four animals from each group were immunized with the KLH conjugate (100 µg) of the opposite hapten using the same procedure and time schedule. It should be noted that the fatality rate was lower in these cases of heterologous immunization. The reasons for this remain unclear. After 3 days, 2 animals from each immunization regimen (**72**, **72**, **73** and **73**, **73**, **72**) were sacrificed to generate hybridomas.

3.5 Fusions and Generation of Hybridomas

Three days after the final boost, the animals were sacrificed, and their spleens were harvested for B-cells. The single cell suspensions from each spleen were fused with 5×10^7 653/HGPRT⁻ myeloma cell with the aid of polyethylene glycol (PEG), a cell membrane denaturant. Upon the removal of PEG, cells were suspended in HAT selection media, plated into ten 96-well plates, and incubated in a 37° C sterile incubator. Two weeks after the fusion, each well was checked by ELISA for the presence of antibodies that bound either their respective hapten (*homologous* immunization) or both of the haptens (*heterologous* immunization).

3.5.1 Homologous Immunizations

Seventy-one clones combined from two fusions were found to respond positive to BSA-**72** by ELISA. These were also checked for binding to BSA-**73** and only 4 showed very weak cross-reactivity. These were each grown to 1 mL scale and put into limiting dilution wherein they were diluted serially and the positive binders from the most dilute sample were re-grown. This process insures that each cell line originates from a single parent and is genetically homogeneous. Hence, each selected cell line produces a single type of antibody, a so-called monoclonal antibody.

Fifty-nine cell lines were found to grow and secrete BSA-72 binders after the first round of limiting dilutions. These were put into a second round of limiting dilution to ascertain monoclonality, and 55 monoclonal cell lines remained after the second limiting dilution.

Eighty-two clones from two fusions were found to be positive to BSA-73 by ELISA. None of these were found to bind to BSA-72. After two rounds of limiting dilutions 54 monoclonal cell lines were isolated.

3.5.2 Heterologous Immunizations

In the heterologous immunization with 72, 72, 73 a total of about 200 cell lines from two fusions were found to bind BSA-72. Of these 78 clones also responded to BSA-73. These 78 clones were selected and put through two rounds of limiting dilutions to assure monoclonality. 40 cell lines that were cross-reactive to both haptens remained after the limiting dilution processes.

In the heterologous immunization with 73, 73, 72 no cell lines were found to respond to BSA-73 from 2 combined fusions. 40 cell lines did respond weakly to BSA-72. All of these were later found to be of the sub-type IgM, representing a primary immune response to 72. As this is not suitable for the purposes of heterologous immunization, these cell lines were discarded. The reasons for this interesting phenomenon remain unclear but most probably reside in the requirements for the cross-reactive stimulation of memory B-cells. A similar observation has also been made in our previous study of heterologous immunization³¹.

3.6 Antibody Production and Purification

The cell lines that remained at the end of two rounds of limiting dilutions were each grown to 10 mL scale and to >95% viability (percentage number of viable

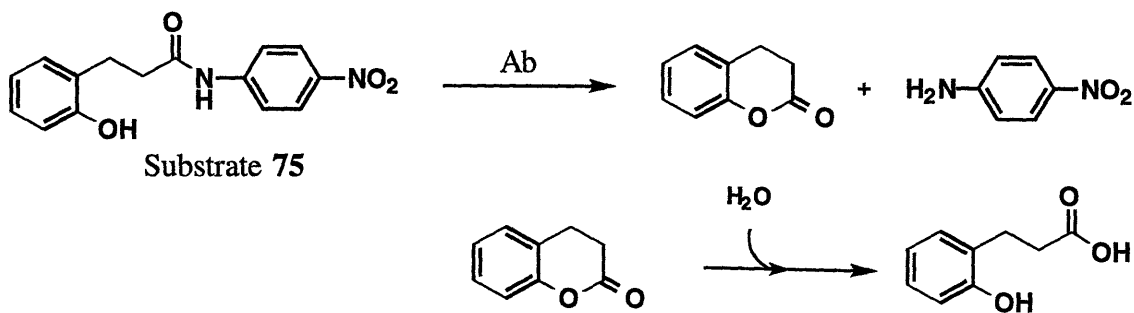
cells). At this point 5×10^6 cells from each were transferred to 1 mL of 8% DMSO in Fetal Bovine Serum (FBS) solution and stored initially at $-80\text{ }^\circ\text{C}$ for four months after which they were transferred to $-180\text{ }^\circ\text{C}$. These frozen stocks are then stable indefinitely and can be re-grown upon proper thawing.

Another 1.5×10^6 cells were injected in PBS into the intraperitoneal cavity of Balb/C mice which had been primed with pristane. The pristane priming induces plasmocyte formation of the injected hybridomas. An ascitic fluid is produced which is enriched (up to 10 mg/mL) in antibodies. This was isolated from the intraperitoneal cavity via three taps with a hypodermic needle.

A three step protocol was used to purify each monoclonal antibody. Precipitation with ammonium sulfate (at 45% final concentration of saturated solution) was followed by DEAE anion exchange chromatography. The fractions containing the antibody were pooled and re-purified via protein G affinity column chromatography. Protein G is a bacterial protein that binds to the constant region of most subtypes of mouse antibodies with high specificity.

Collected antibody fractions were quantified via the constant UV absorption of their tryptophan residues at 280 nm. Each antibody solution was then exchanged into 10 mM PIPES buffer at pH 6.8 with 0.1% sodium azide to inhibit bacterial growth. These were concentrated to 6 mg/mL concentration and were stored at $4\text{ }^\circ\text{C}$ until they were assayed in the appropriate reaction buffer (at 50 mM assay buffer concentration at the final pH)

3.7 Amide Hydrolysis Assay with Unimolecular Substrate 75



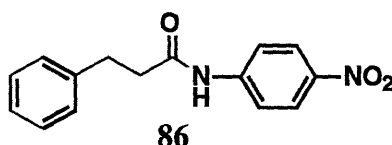
Initial assays were performed at two different pH's (50 mM PIPES, 80 μ M NaCl, pH 6.8; 50 mM CHES, 80 μ M NaCl, pH 9.0). High Performance Liquid Chromatography (HPLC) was used to separate Substrate **75** from products dihydrocoumarin and *p*-nitroaniline with 45% acetonitrile (AcN), 0.1% trifluoroacetic acid in H₂O as the isocratic eluent. The reactions were followed by monitoring the appearance of *p*-nitroaniline at 382 nm (absorption maximum). 50 μ M 4-Phenylazophenol was used as the internal standard to calibrate against variance in injection volumes.

Of the 55 hybridoma clones raised to **72**, only 39 yielded sufficient quantities of antibody to screen for catalysis. After the initial screens, 2 out of the 39 were found to be catalytic. The more efficient catalyst 6-17 was characterized further. It was found to obey Michaelis-Menten kinetics with a $k_{\text{cat}} = 1.8 \times 10^{-3} \text{ min}^{-1}$ and $K_m = 0.86 \text{ mM}$ at pH 6.8. It was inhibited competitively by hapten **72** with a $K_i = 36 \mu\text{M}$. As expected, no inhibition was seen with hapten **73**. This antibody displayed a pH optimum at 8.0 (*vide infra*) where $k_{\text{cat}} = 2.7 \times 10^{-3} \text{ min}^{-1}$ and $K_m = 0.98 \text{ mM}$. The K_i at pH 8.0 could not be determined due to the instability of hapten **72** at this pH, although competitive inhibition was seen.

Twenty out of the 54 monoclonal clones generated to hapten **73** yielded sufficient quantities of antibody to screen, and one, 3-49, was found to be a catalyst. The catalytic efficiency of this antibody increased with increasing hydroxide concentration (*vide infra*) and its Michaelis-Menten parameters were determined at

pH 9.0 ($k_{\text{cat}} = 4.2 \times 10^{-3} \text{ min}^{-1}$, $K_{\text{m}} = 0.77 \text{ mM}$). It was also shown to be competitively inhibited by its respective hapten **73** ($K_{\text{i}} = 380 \text{ }\mu\text{M}$), while no inhibition was seen with hapten **72**.

Fifteen out of the 40 monoclonal antibodies generated by the heterologous immunization (**72**, **72**, **73**) were of screenable quantity and 3 were found to be catalytic. The most efficient catalyst 14-10 was characterized by Michaelis Menten kinetics. At pH 6.8 $k_{\text{cat}} = 0.0093 \text{ min}^{-1}$ and $K_{\text{m}} = 1.40 \text{ mM}$. In accord with its binding affinity to both haptens, the catalytic activity of this hapten was competitively inhibited by both **72** ($K_{\text{i}} = 51 \text{ }\mu\text{M}$) and **73** ($K_{\text{i}} = 790 \text{ }\mu\text{M}$). This antibody displayed a bell shaped pH optimum curve hinting at two ionizable binding site residues that participate in catalysis and displayed a pH optimum at pH 8.0 (*vide infra*). At this pH, $k_{\text{cat}} = 0.015 \text{ min}^{-1}$ and $K_{\text{m}} = 1.27 \text{ mM}$. As in our previous studies with esterolytic antibodies, antibody 14-10 generated by heterologous immunization is an almost ten-fold more efficient catalyst than its homologously generated counterparts.



The background rate of hydrolysis of amide **75** at pH 6.8 was measured to be $4.7 \times 10^{-7} \text{ min}^{-1}$.⁶⁴ Interestingly, the background hydrolysis reaction of the phenyl substrate **86** was found to be almost identical ($4.8 \times 10^{-7} \text{ min}^{-1}$) showing that under aqueous conditions the phenol group does not participate in an intramolecular catalysis. This is to be expected as substrate **75** should preferentially exist in an extended conformation leaving its phenolic group at a severe entropic disadvantage to compete with the solvent water molecules, either as an intra-molecular proton-donor or a nucleophile.

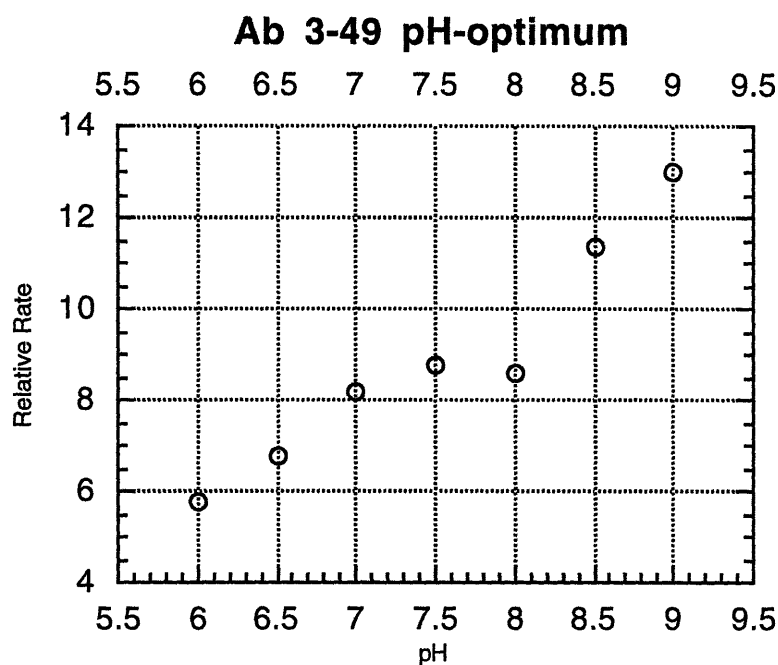
The evidence for the intramolecular participation of the phenol of **75** in the antibody catalyzed reaction came from the studies with substrate **86**. None of the

three antibody catalysts accelerated the observed hydrolysis of **86**. This shows that the phenol moiety is required for antibody catalysis. Based on the design of the inducing haptens, it seems likely that this phenol acts as a nucleophile generating dihydrocoumarin and releasing *p*-nitroaniline. Dihydrocoumarin was observed to be a weak competitive inhibitor for all three catalysts although inhibition constants could not be determined due to the relatively facile rate of hydrolysis of dihydrocoumarin at pH 8.0 - 9.0.

The kinetics of the antibody-catalyzed hydrolysis of dihydrocoumarin was not investigated, as more direct evidence for the intramolecular participation of phenol was obtained from the studies of the targeted inter-molecular reaction. All three of the catalytic antibodies were found to catalyze the cleavage of propionyl *p*-nitroanilide **87** with phenol.

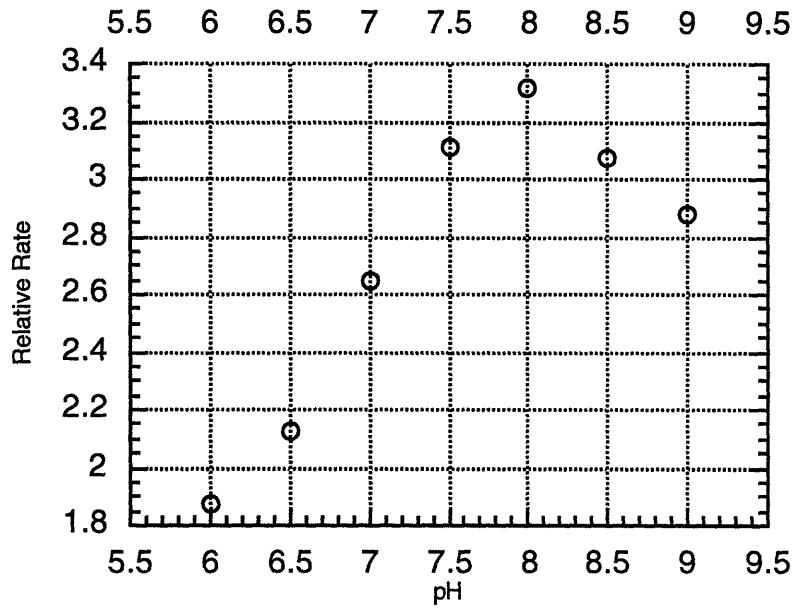
3.8 pH-optimum Studies

The pH-optimum of the three catalytic antibodies were investigated at pH 6.0, 6.5, 7.0, 7.5, 8.0, 8.5, 9.0 with the three component buffer MHD (12.5 mM MES, 12.5 mM HEPES, 25.0 mM Diethanolamine). Due to limited quantity of the antibodies, k_{cat} and K_m 's were not be determined at every pH value. Two types of pH dependency were observed. Antibody 3-49 displayed an almost-linear dependency on pH with a steep slope which hints that hydroxide ion concentration is a major component of the rate equation for the antibody catalyzed reaction.

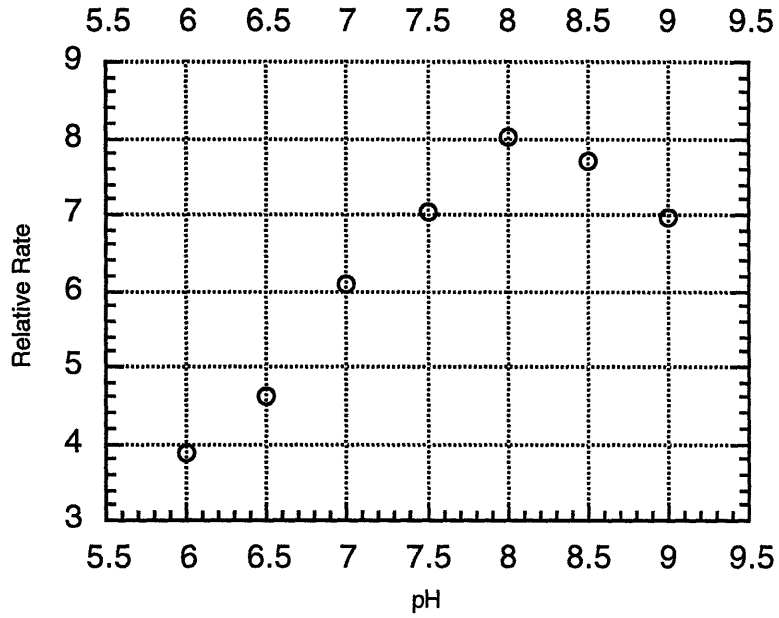


Both 6-17 and 14-10 displayed bell shaped reaction-rate vs. pH curves with an optimum pH of action at 8.0. It is tempting to speculate that these plots reflect the presence of two ionizable residues of each antibody that participate in the catalysis. However, such claims should only be made after careful plots of k_{cat} vs. pH or k_{cat}/K_m vs. pH. These two plots are nonetheless encouraging as our initial aim was to generate bi-functional binding site residues in the antibody catalysts. Further studies with bi-molecular amide hydrolysis were performed at pH 8.0 as this appeared to be the optimal pH for at least two of the catalytic antibodies.

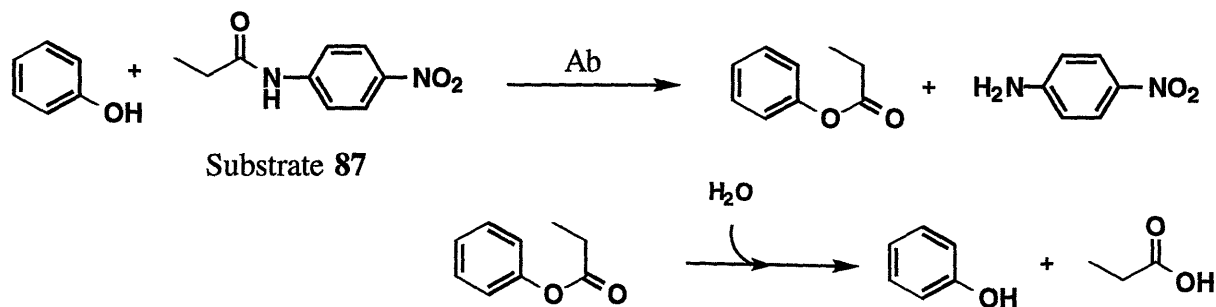
Ab 14-10 pH-optimum



Ab 6-17 pH-optimum



3.9 Cleavage of Propionyl *p*-Nitroanilide with Phenol



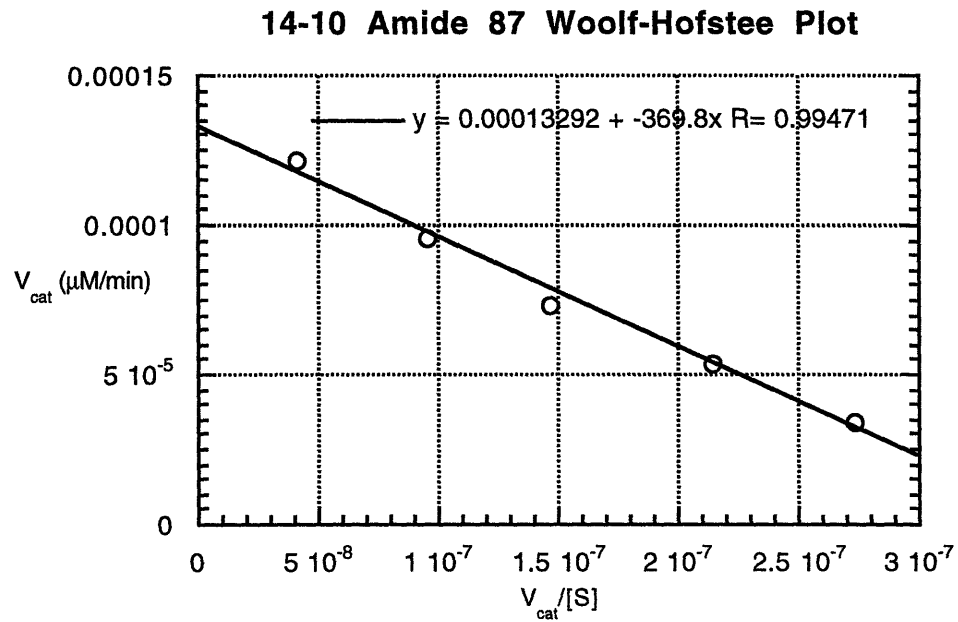
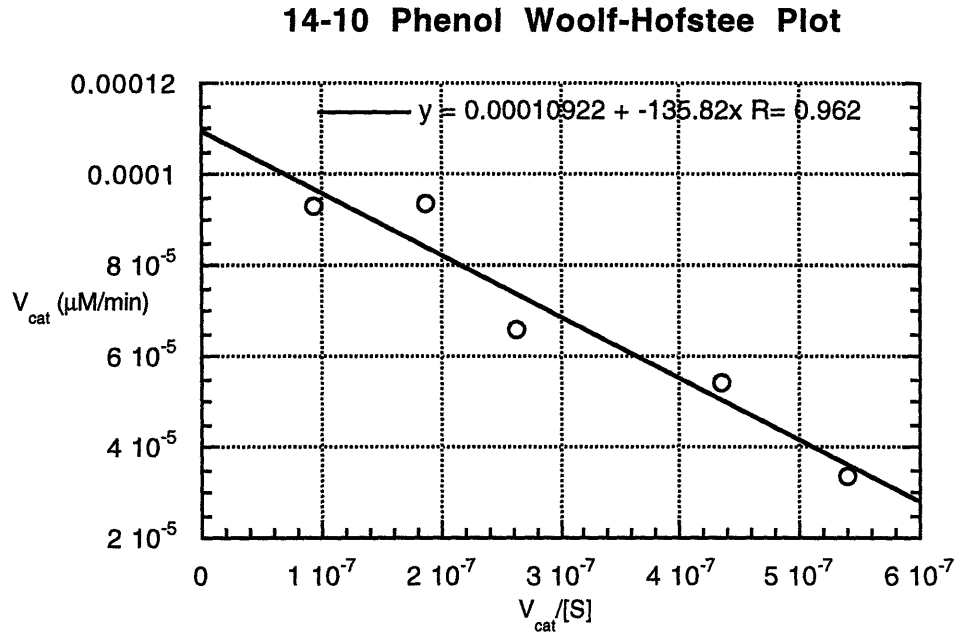
Assays were carried out at pH 8.0 using the three component buffer MHD. HPLC was used to follow the appearance of *p*-nitroaniline (35% AcN, 0.1% trifluoroacetic acid in H₂O as the isocratic eluent). The reactions were followed at 382 nm, and 50 μM 4-phenylazophenol was used as the internal standard.

Antibodies 3-49, 6-17 and 14-10 were assayed for the acceleration of the cleavage of propionyl *p*-nitroanilide in the presence of 10 fold excess of phenol at pH 8.0. All three antibodies were found to accelerate this reaction and their Michaelis-Menten parameters were determined. The heterologously generated antibody 14-10 was again the most efficient catalyst with $k_{\text{cat}} = 1.33 \times 10^{-4} \text{ min}^{-1}$ at pH 8.0. For phenol $K_{\text{m}} = 136 \mu\text{M}$ and for **87** $K_{\text{m}} = 370 \mu\text{M}$. Both haptens were shown to effectively inhibit the reaction.

6-17 was the next most efficient catalyst with $k_{\text{cat}} = 2.1 \times 10^{-5} \text{ min}^{-1}$. The Michaelis constants $K_{\text{m}}^{\text{Phenol}} = 78 \mu\text{M}$ and $K_{\text{m}}^{\text{87}} = 310 \mu\text{M}$ were observed. This antibody was competitively inhibited by its respective hapten, **72** while no inhibition was seen with **73**.

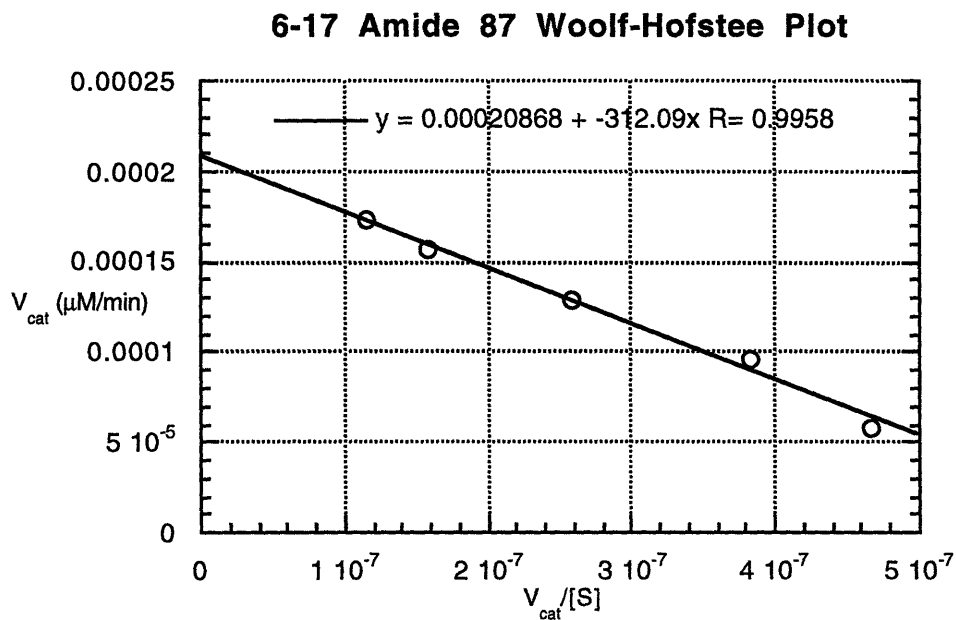
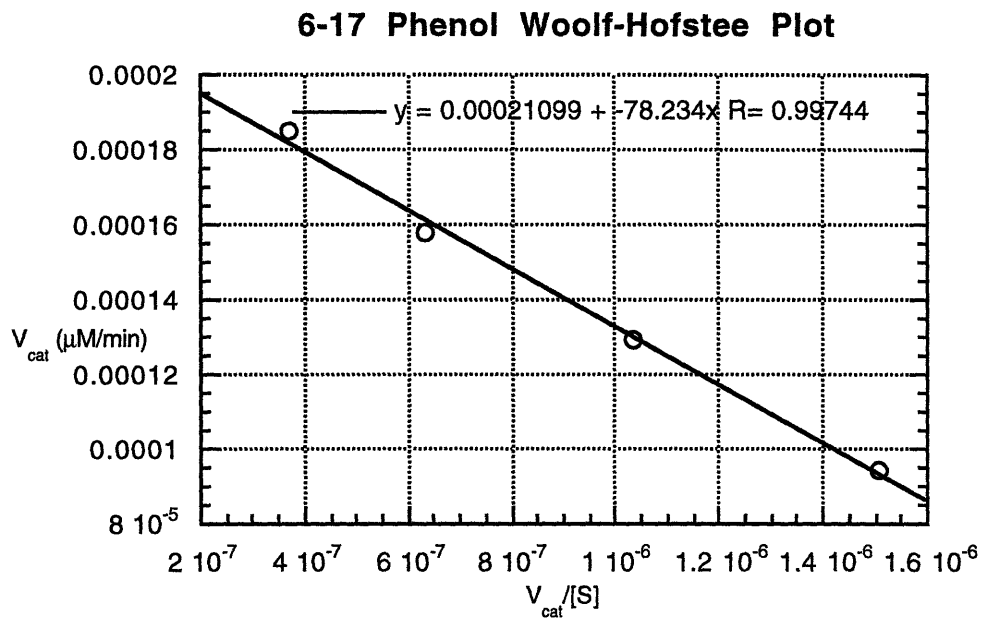
3-49 was the slowest catalyst with $k_{\text{cat}} = 1.28 \times 10^{-5} \text{ min}^{-1}$. Interestingly, it also displayed the smallest Michaelis constants, $K_{\text{m}}^{\text{Phenol}} = 14 \mu\text{M}$ and $K_{\text{m}}^{\text{87}} = 77 \mu\text{M}$. Hapten **73** effectively inhibited the observed catalysis with 3-49 while no inhibition with hapten **72** was observed.

Figure 3.1 Woolf-Hofstee Plots of 14-10 for Phenol and Amide 87



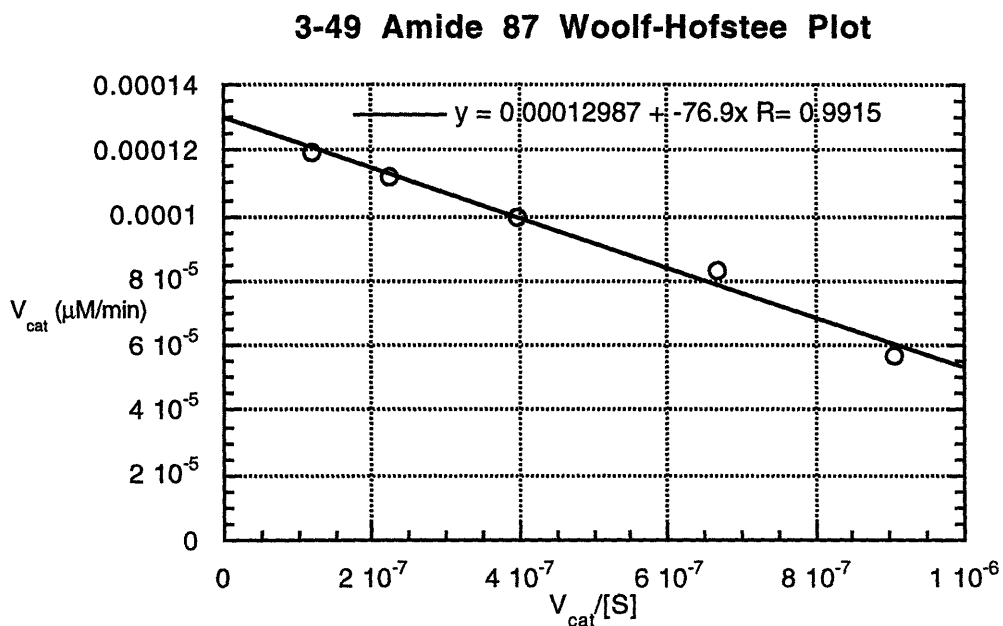
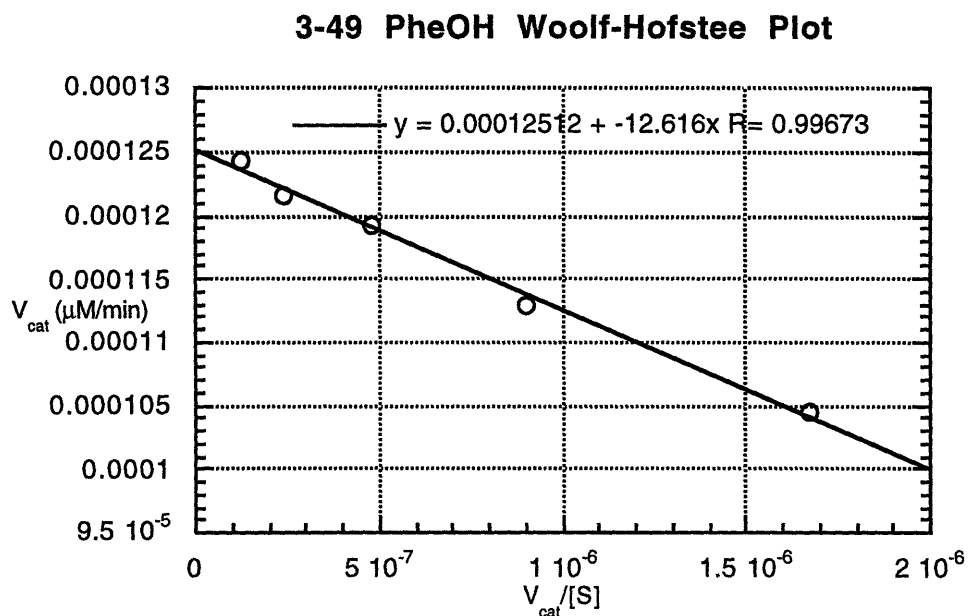
Assay Conditions: 1 μM Antibody; 62.5, 125, 250, 500, 1000 μM phenol; 125, 250, 500, 1000, 3000 μM 87; pH 8.0; MHD buffer. ($y = V_{max} - K_m * x$).

Figure 3.1 Woolf-Hofstee Plots of 6-17 for Phenol and Amide 87



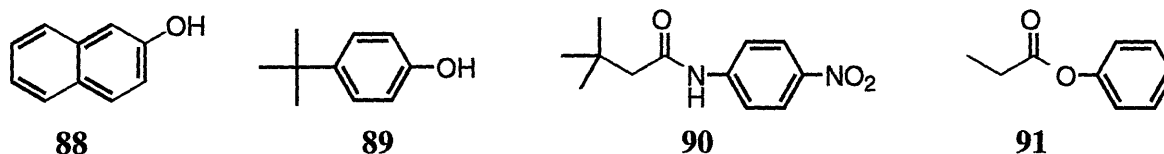
Assay Conditions: 10 μM Antibody; 62.5, 125, 250, 500 μM phenol; 125, 250, 500, 1000, 1500 μM 87; pH 8.0; MHD buffer. ($y = V_{max} - K_m * x$).

Figure 3.1 Woolf-Hofstee Plots of 3-49 for Phenol and Amide 87



Assay Conditions: 10 μM Antibody; 62.5, 125, 250, 500, 1000 μM phenol; 62.5, 125, 250, 500, 1000 μM 87; pH 8.0; MHD buffer. ($y = V_{max} - K_m * x$).

The participation of phenol in antibody catalysis was proven beyond doubt with a simple control experiment. In the absence of phenol, all three antibodies showed no acceleration of the cleavage of amide **87**. Furthermore, neither 2-naphthol (**88**) nor 4-*tert*-butyl phenol (**89**) were accepted for catalysis by any of the three catalysts. These results indicate the existence of a dedicated binding pocket for the phenol auxiliary nucleophile. Similarly, these catalysts were also shown to be specific for propionyl anilide. *t*-butyl-acetyl *p*-nitroanilide (**90**) was not accepted as a substrate, indicating that a dedicated and specific binding pocket also exists for the amide **87**. Together with the observation that phenyl propionic amide **86** was not subject to antibody catalysis, these results confirm that the participation of phenol is essential for the antibody catalyzed cleavage of amide **87**.



Finally, the product phenyl propionate (**91**) did not inhibit the antibody catalyzed cleavage of **87** even at relatively high concentrations (5 mM **91** and 0.5 mM **87**) indicating that the product **91** efficiently diffuses out of the antibody binding site upon formation. Furthermore, none of the three antibodies displayed significant acceleration of the hydrolysis of **91**.

The background rate for the hydrolysis of amide **87** was found to be $2.1 \times 10^{-7} \text{ min}^{-1}$ at pH 8.0. However, this rate can not be directly compared with the k_{cat} 's above as the antibody catalyzed reaction requires the participation of phenol, while the uncatalyzed rate of cleavage of amide **87** is not accelerated by the addition of phenol.

It is important to note that the order of catalytic efficiency among the three catalysts reflects the pattern seen with the unimolecular substrate **75**, despite the fact that the Michaelis constants are varied for the three antibodies. This supports

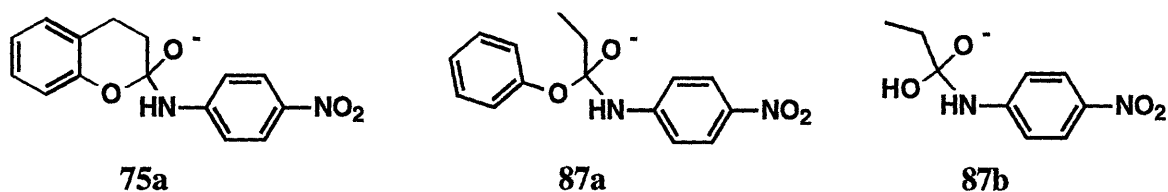
the notion that catalytic efficiency by antibodies is independent of the efficiency of substrate binding but rather depends on transition state binding and the participation of optimally placed catalytic residues.

All of the K_m 's for the bi-molecular reaction were smaller than the K_m 's for the unimolecular substrate **75**. This can be explained by the mismatch between the expected conformation of **75** and the conformation of the inducing haptens. In aqueous solutions, the carbonyl and the phenol of **75** should be far removed in an extended conformation, whereas in the haptens these two moieties are in close proximity. Therefore, it is likely that the binding of **75** by these antibodies proceeds in two steps with either the phenol or the carbonyl being bound first, followed by the second portion of the substrate as it motions into the correct orientation in the antibody binding cavity.

Another point of consideration is that the K_m 's for phenol were smaller than the K_m 's for **87**. This can be rationalized by the placement of the phenol away from the glutaric acid linker portion in the hapten designs. Therefore, it is likely that the phenol is bound in a deep pocket in the antibody binding sites while the binding pocket for **87** is more solvent accessible. The observation of small K_m 's for phenol by the three antibodies is also a subtle vindication of our choice of phenol as the external nucleophile. Interestingly, at high concentrations (> 10 mM) phenol was seen to inhibit the bi-molecular reaction. This can be a result of phenol starting to compete with **87** for its binding pocket at such high concentrations. This could also be a point of improvement for the future designs of auxiliary nucleophiles in antibody catalysis, i.e. the effective differentiation of auxiliary binding from substrate amide binding.

The lower k_{cat} 's displayed by the three antibodies towards amide **87** as compared with **75** could be stemming from three reasons: The six membered structure of **75** might be bestowing a more optimal attack angle for phenol to the

carbonyl than can be provided by antibody binding alone as in the case of **87** and phenol. Alternatively, the formed tetrahedral intermediate **75a** could be forced by antibody binding to expel the amide more preferentially than **87a** where there is more rotational freedom available. A similar argument is that in **87a** the amine is less optimally placed in the binding site for its protonation by a hydrogen donor. Finally, the ortho hydrogen of phenol could be experiencing a steric repulsion from the β -hydrogens of the propionate as the hapten structures represent this interaction with a carbon-carbon bond.



Perhaps the most important aspect of the antibody catalyzed cleavage of **87** is that the background rate of hydrolysis ($2.1 \times 10^{-7} \text{ min}^{-1}$) of **87** decreases with an increasing amount of phenol that is present in the medium. This is in accord with the expected mechanism of the uncatalyzed reaction with water where the expulsion of the *p*-nitroaniline from the tetrahedral intermediate **87b** is the rate determining step. Given that the phenoxide is a better leaving group than hydroxide ion, it is expected that the rate of amide expulsion from **87b** is greater than that from **87a**. Increasing the amount of phenol in the uncatalyzed reaction results in an increase in the formation of **87a** compared to **87b** and accordingly, a decrease in the observed rate of hydrolysis of **87**.

Given that the rate of hydrolysis of **91** ($1.1 \times 10^{-4} \text{ min}^{-1}$) is three orders of magnitude faster than the rate of hydrolysis of amide **87**, and that **91** appears to freely diffuse out of antibody binding site (i.e. no product inhibition is seen with **91**), it can be said that all three antibodies have, in-effect, achieved the hydrolysis of the amide bond of **87**, with the rate determining step of the overall transformation being the formation of **91** from **87**.

3.10 Conclusion

We have shown here a novel approach to the hydrolysis of amide bonds with antibody catalysts. Phenol was used as an external nucleophile to aid in the cleavage of an amide bond. Furthermore, our heterologous immunization method has been shown to generate a more efficient catalyst (14-10) than either of the two homologous immunizations. This is in accord with our previous report with esterolytic antibodies where heterologous immunization was seen to result in a 100 fold more efficient antibody catalysis⁴⁹. Although the achieved rate acceleration of the bi-molecular reaction is low, the significance of the catalysis rests on the high energy of activation that is inherent in cleaving amide bonds, as well as the lack of phenol participation in the reaction in the absence of the antibody catalysis.

Two paths can be taken to improve the rate acceleration with this present approach: First, different nucleophiles can be examined instead of phenol, such as imidazole or pyridine. Second, the protonation of leaving amine of the tetrahedral intermediate can be further stressed by appropriate hapten designs. Finally, this design concept, catalysis by external nucleophiles, can also be applied to other hydrolysis reactions, such as glycolysis or phosphodiester hydrolysis. A similar mechanism with the use of the 2' hydroxyl is already known to be used in the cleavage of RNA by RNase's.

3.11 Perspectives

As accumulating evidence indicates that efficient antibody catalysis requires more than simple preferential binding to the transition state (and thus, to the transition state analog hapten), it is desirable to incorporate a screen for catalysis as early in the search for catalytic antibodies as possible. It is rather expensive in

time, money and effort to generate 150 monoclonal antibodies that initially displayed affinity to a hapten only to isolate 3 catalysts! An alternative approach termed catELISA has been reported⁶⁵ that screens directly for catalysis in the first ELISA screen after the fusion. Instead of detecting antibodies bound to an immobilized hapten, the catELISA method screens for the presence of a reaction product, after antibodies have been incubated in the presence of immobilized substrates.

Research in the Masamune group will incorporate catELISA techniques to the presently demonstrated auxiliary nucleophilic catalysis method to isolate antibody catalysts that achieve novel transformations of therapeutic and theoretical importance.

Chapter 4

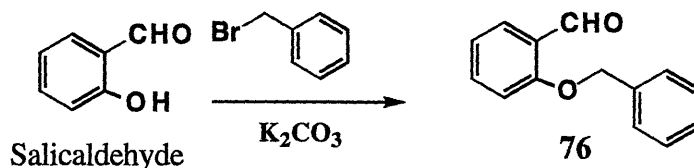
Experimental

4.1 Synthesis of Haptens and Substrates

4.1.1 General Methods

All reactions were carried out in oven-dried glassware under an argon atmosphere unless otherwise noted. Aqueous reactions were run under ambient atmosphere. Column chromatography was performed using 230-400 mesh silica gel (Merck). Proton (^1H NMR) magnetic resonance spectra were recorded at 300 MHz on a Varian XL-300 instrument. The chemical shifts of ^1H NMR spectra were referenced to CDCl_3 (7.24 ppm), DMSO (2.49 ppm), CD_2Cl_2 (5.32 ppm), or CD_3OD (3.30 ppm). ^1H NMR peak multiplicities are reported as follows: s (singlet), d (doublet), t (triplet), q (quartet), quint (quintuplet), m (multiplet), br (broad). Coupling constants (J) are reported in Hz. Proton-decoupled-carbon (^{13}C NMR) and phosphorus (^{31}P NMR) magnetic resonance spectra were recorded at 75.44 MHz and 121.44 MHz on a Varian XL-300 instrument. The chemical shifts of ^{13}C NMR spectra were referenced to CDCl_3 (77.0 ppm), DMSO (39.5 ppm), CD_2Cl_2 (53.8 ppm), or CD_3OD (49.0 ppm). ^{31}P NMR spectra were referenced to 85% H_3PO_2 as an external standard (capillary tube within NMR tube). Infrared (IR) spectra were recorded on a Perkin-Elmer 283B spectrometer. Melting points were not corrected. High-resolution mass spectra (HRMS) were recorded on a Finnigan MAT 8200 spectrometer. Reagents were used as supplied by the vendors, except in moisture sensitive reactions where reagents were dried CH_2Cl_2 (over Na), THF (over Na) and Pyridine (over CaH_2). The following abbreviations are used: DMSO (dimethylsulfoxide), AcN (acetonitrile), MeOH (methanol), THF (tetrahydrofuran), EtOAc (ethylacetate), DMAP (dimethylamino pyridine), EDC (1-(3-Dimethylaminopropyl)-3-ethylcarbodiimide), rpm (rounds per minute).

4.1.2 Synthesis of Hapten 72

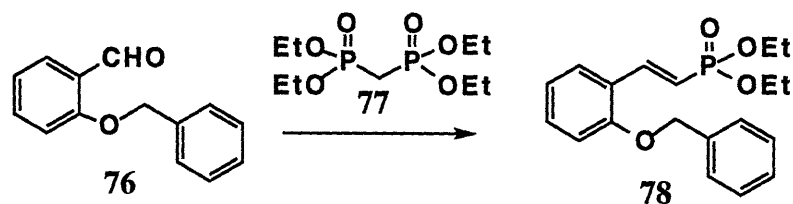


Benzyl protection of salicylaldehyde⁶⁶:

A mixture of 300 mL of MeOH, 600 mL of CHCl₃, and anhydrous K₂CO₃ (29.9 g, 216 mmol) was refluxed for 15 min under a stream of argon before salicylaldehyde (5.25 mL, 49.1 mmol) and benzyl bromide (6.45 mL, 54 mmol) were added, and the mixture was refluxed for 1 day. After filtration, the filtrate was evaporated, and the residue was dissolved in CH₂Cl₂, washed with 1N HCl, dried over MgSO₄ and concentrated in vacuo to give **76** (10.3 g, 98.8 %) as a slightly yellow oil. ¹H NMR of the crude showed it to be sufficiently pure and it was used in the next step without any further purification.

Physical Data:

¹H NMR (300 MHz, CDCl₃): δ 10.57 (s, 1 H), 7.86 (d, *J* = 8.0 Hz, 1 H), 7.57-7.49 (m, 1 H), 7.47-7.32 (m, 5 H), 7.08-7.00 (m, 2 H), 5.19 (s, 2 H)
IR (film): 3053, 3020, 2751, 1687, 1598, 1480, 1462, 1374, 1284, 1236, 1187, 1155, 1100, 1014, 911, 851, 829, 753, 693, 655.



Horner-Wittig coupling of 76 with tetraethylmethylenephosphonate:

To benzyl-salicylaldehyde ether **76** (0.74 g, 3.48 mmol) and bisphosphonate **77** (0.86 mL, 3.48 mmol) in 6 mL of CH₂Cl₂ was added 6 mL of 50% NaOH, and the biphasic reaction was stirred vigorously open to ambient atmosphere for 4 hours. The reaction mixture was diluted with 20 mL of water and extracted twice with 20 mL of CH₂Cl₂. The organic layers were combined, dried over MgSO₄, and concentrated in vacuo to afford styrylphosphonate **78** as a colorless oil (1.1 g, 92%)

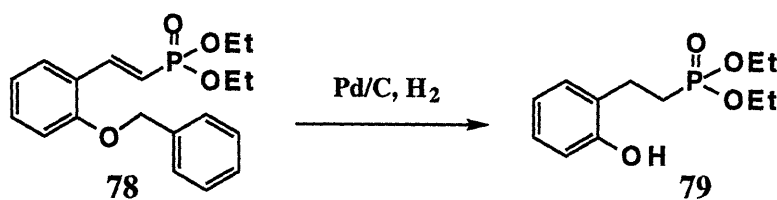
Physical Data:

¹H NMR (300 MHz, CDCl₃): δ 7.88 (dd, $J^{P-H} = 23.4$ Hz, $J^{H-H} = 17.7$ Hz, 1 H), 7.46 (dd, $J = 4.8, 1.5$ Hz, 1 H), 7.41-7.21 (m, 6 H), 6.92 (t, $J = 9.0$ Hz, 2 H), 6.32 (dd, $J^{P-H} = 19.5$ Hz, $J^{H-H} = 17.7$ Hz, 1 H), 5.19 (s, 2 H), 4.07 (quin, $J = 7.2$ Hz, 4 H), 1.28 (t, $J = 7.2$ Hz, 6 H)

¹³C NMR (75.44 MHz, CDCl₃): δ 154.26, 143.85 (d, $J^{C-P} = 117.2$ Hz), 141.16 (d, $J^{C-P} = 11.1$ Hz), 133.46, 131.65, 128.67, 128.45, 128.29, 127.64, 126.97, 126.63, 122.82, 63.27, 62.10 (d, $J^{C-P} = 4.9$ Hz), 31.78

IR (film): 3209, 2977, 2745, 2612, 1594, 1500, 1456, 1378, 1224, 1041, 970, 865, 754.

HRMS (M⁺): Calcd 346.3630 Found 346.3629



Reduction and deprotection of styrylphosphonate 79 via catalytic hydrogenation:

To styrylphosphonate **78** (1.99 g, 5.72 mmol) in 30 mL of EtOH was added a catalytic amount of 10% Pd/C. The mixture was shook under 50 psi of H₂ for three days, filtered through celite and concentrated in vacuo to yield the phenol diethylphosphonate **79** (1.45 g, 98%) as a colorless oil. This was used in the next step without further purification.

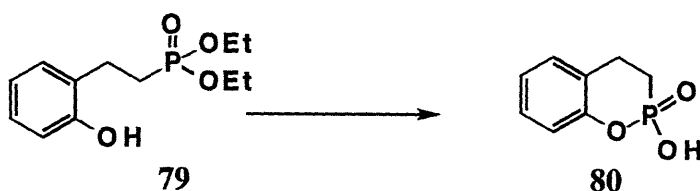
Physical Data:

¹H NMR (300 MHz, CDCl₃): δ 8.45-8.10 (br, 1 H), 7.10-7.02 (m, 2 H), 6.88 (d, *J* = 8.2 Hz, 2 H), 6.78 (t, *J* = 7.8 Hz, 2 H), 3.99 (quin, *J* = 7.2 Hz, 4 H), 2.89 (dt, *J*^{P-H} = 22.8 Hz, *J*^{H-H} = 7.2 Hz, 1 H), 2.12 (dt, *J*^{P-H} = 17.1 Hz, *J*^{H-H} = 7.2 Hz, 1 H), 1.33 (t, *J* = 7.2 Hz, 6 H)

¹³C NMR (75.44 MHz, CDCl₃): δ 131.67, 130.84, 128.59, 128.19, 126.63, 121.52, 62.10 (d, *J*^{C-P} = 4.8 Hz), 31.78, 25.56 (d, *J*^{C-P} = 11.5 Hz), 20.45 (d, *J*^{C-P} = 125.6 Hz)

³¹P NMR (121.44 MHz, CDCl₃): δ 45.58

HRMS (M⁺): Calcd 258.2542 Found 258.2537



De-esterification and cyclization of the phenol diethylphosphonate **79** to cyclic phosphonic acid **80**:

Phenol diethylphosphonate **79** (1.8 g, 6.97 mmol) and anhydrous toluenesulfonic acid (1.57 g, 9.07mmol) in 40 ml of xylene were refluxed under ambient atmosphere for 24 hours. The reaction mixture was cooled to room temperature, concentrated in vacuo to a volume of 3-4 mL and cooled to 5 °C overnight. Cyclic phosphonic acid **80** (1.15 g, 90%) was collected as a white solid precipitate. This was found to be pure by ¹H NMR and used without further purifications. It can be recrystallized from acetone for analytical purposes.

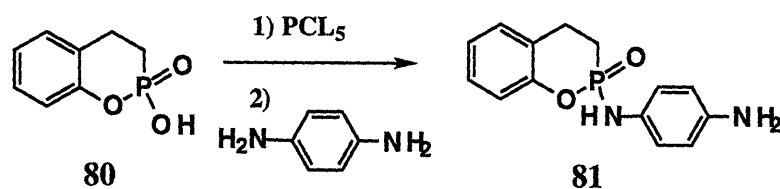
Physical Data:

¹H NMR (300 MHz, DMSO): δ 7.29-7.16 (m, 2 H), 7.12-6.98 (m, 2 H), 3.04 (dt, $J^{P-H} = 23.6$ Hz, $J^{H-H} = 7.4$ Hz, 2 H), 2.12 (dt, $J^{P-H} = 17.9$ Hz, $J^{H-H} = 7.4$ Hz, 2 H)

¹³C NMR (75.44 MHz, DMSO): δ 129.77, 129.46, 128.70, 127.69, 124.94, 119.28 (d, $J^{C-P} = 7.5$ Hz), 32.47 (d, $J^{C-P} = 9.8$ Hz), 28.02 (d, $J^{C-P} = 107.9$ Hz)

³¹P NMR (121.44 MHz, DMSO) δ 25.76

HRMS (M⁺): Calcd 184.1314 Found 184.1311



Coupling of phenylene diamine to the cyclic phosphonic acid **80** via its phosphoryl chloride to yield **81**:

Cyclic phosphonic acid **81** (1.150 g, 6.3 mmol) and PCl_5 (2.0 g, 9.6 mmol) were suspended in 10 mL of dry CH_2Cl_2 and refluxed overnight. Xylene was added and the mixture was concentrated in vacuo. Azeotropic removal of xylene was repeated a number of times to remove the POCl_3 by-product of the reaction.

The phosphoryl chloride (0.77 g, 3.8 mmol) was redissolved in 10 mL of dry CH_2Cl_2 and added dropwise over 1 hour via an addition-funnel to a solution of freshly-sublimed phenylene diamine (0.87 g, 8.0 mmol), dry pyridine (0.67 mL, 8.0 mmol) and DMAP (cat.) in 2 mL of dry DMF. The reaction was stirred for another 6 hours at room temperature. After the addition of 40 mL of CH_2Cl_2 , the precipitated pyridinium chloride was removed by filtration, and the filtrate was concentrated in vacuo. Excess unreacted phenylene diamine was removed by sublimation in vacuo (1mm Hg, 120 °C) and the remaining residue was dissolved in MeOH, coated onto silica gel and purified via column chromatography (2-5% gradient methanol in CH_2Cl_2). The fractions containing the product **81** with the contaminating phenylene diamine were then pooled, concentrated in vacuo, re-dissolved in methylene chloride, coated onto silica gel and purified again by column chromatography (75-100% EtOAc gradient in Hexane with 0.1% NH_4OH) to yield product **81** (0.364 g, 35%) as an off-white solid. This compound is stable indefinitely in ambient atmosphere.

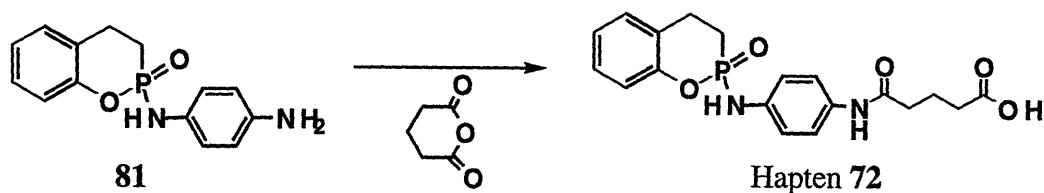
Physical Data:

^1H NMR (300 MHz, CD_3OD): δ 7.26-7.12 (m, 2 H), 7.08-6.94 (m, 4 H), 6.80 (d, $J = 8.4$ Hz), 3.18-3.02 (m, 2 H), 2.27-2.11 (m, 2 H)

^{13}C NMR (75.44 MHz, DMSO): δ 150.89 (d, $J^{\text{C-P}} = 6.6$ Hz), 136.53, 132.62, 128.64, 127.70, 124.15 (d, $J^{\text{C-P}} = 10.4$ Hz), 123.32, 120.96 (d, $J^{\text{C-P}} = 5.5$ Hz), 118.30 (d, $J^{\text{C-P}} = 6.9$ Hz), 118.15, 23.93 (d, $J^{\text{C-P}} = 9.3$ Hz), 20.52 (d, $J^{\text{C-P}} = 115.9$ Hz).

^{31}P NMR (121.44 MHz, DMSO): δ 27.16

HRMS (M^+): Calcd 274.2591 Found 274.2592



Preparation of Hapten 72:

A mixture of phosphonamidate **81** (0.215 g, 0.785 mmol) and glutaryl anhydride (0.99 g, 0.86 mmol) in 20 mL of dry CH₂Cl₂ were stirred at room temperature for 3 hours. The product **72** (0.275 g, 91%) precipitated as a white solid and was isolated via filtration. It was shown to be pure by ¹H NMR and HPLC analysis and can be stored indefinitely under ambient atmosphere. It was found to be acid-labile in organic solvents and both acid- and base-labile in aqueous solutions. It was shown to be stable for at least two weeks in pH 7.0 phosphate buffer.

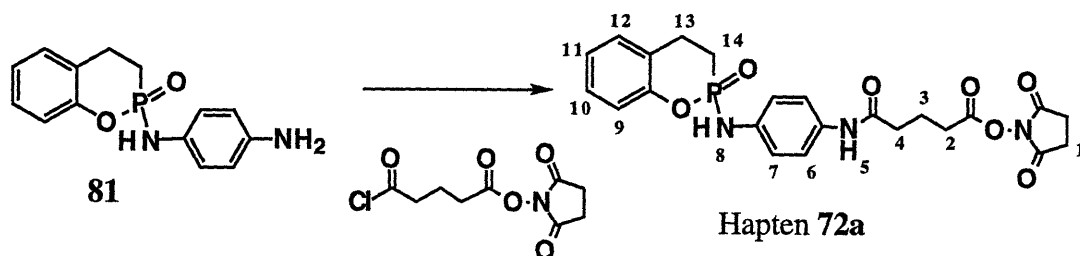
Physical Data:

¹H NMR (300 MHz, CD₃OD): δ 7.36 (d, *J* = 9.6 Hz, 2 H), 7.21-7.13 (m, 2 H), 7.04-6.95 (m, 4 H), 3.20-3.02 (m, 2 H), 2.35 (t, *J* = 7.5 Hz, 2 H), 2.34 (t, *J* = 7.5 Hz, 2 H), 2.24-2.11 (m, 2 H), 1.94 (quin, *J* = 7.2 Hz, 2 H)

¹³C NMR (75.44 MHz, CD₃OD): δ 176.39, 172.76, 152.08 (d, *J*^{C-P} = 8.0 Hz), 136.13, 134.02, 129.91, 129.00, 125.31 (d, *J*^{C-P} = 12.7 Hz), 124.62, 122.08, 120.26 (d, *J*^{C-P} = 5.7 Hz), 119.68 (d, *J*^{C-P} = 6.9 Hz), 36.45, 33.77, 25.18 (d, *J*^{C-P} = 8.1 Hz), 21.80 (d, *J*^{C-P} = 114.3 Hz), 21.58

³¹P NMR (121.44 MHz, CD₃OD): δ 27.49

HRMS (M⁺): Calcd 388.3600 Found 388.3598



Preparation of *N*-hydroxysuccinimide activated **72a**:

A mixture of phosphonamidate **81** (0.05g, 0.182 mmol), *N*-hydroxysuccinamide glutary chloride (0.07g, 2.01mmol) and pyridine (25 μ L, 0.3 mmol) in 5 mL THF were stirred for 1 hour. The pyridinium chloride precipitate was removed by filtration. The filtrate was concentrated in vacuo, and purified by column chromatography (2-5% MeOH in CH₂Cl₂) to afford **72a** (0.05 g, 47%) as a white solid.

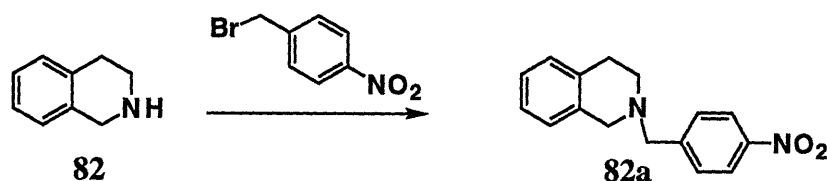
Physical Data:

¹H NMR (300 MHz, CD₂Cl₂): δ 8.21 (s, 1 H, H₅), 7.36 (d, J = 8.8 Hz, 2 H, H₆), 7.24 (t, J = 7.5 Hz, 1 H, H₁₀), 7.16 (d, J = 6.0 Hz, 1 H, H₉), 7.08 (d, J = 7.2 Hz, 1 H, H₁₂), 7.02 (t, J = 5.7 Hz, 1 H, H₁₁), 6.95 (d, J = 8.8 Hz, 1 H, H₇), 6.47 (d, J^{P-H} = 7.5 Hz, 1 H, H₈), 3.24-3.01 (m, 2 H, H₁₄), 2.97 (s, 4 H, H₁), 2.65 (t, J = 7.2 Hz, 2 H, H₂), 2.40 (t, J = 7.2 Hz, 2 H, H₄), 2.20 (dt, J^{P-H} = 15.3 Hz, J = 7.8 Hz, 2 H, H₁₃), 2.07 (quin, J = 6.9 Hz, 2 H, H₃)

¹³C NMR (75.44 MHz, CD₂Cl₂): δ 176.47, 172.71, 170.10, 151.70 (d, J^{C-P} = 6.7 Hz), 135.30, 133.87, 129.73, 128.77, 124.85 (d, J^{C-P} = 27.0 Hz), 124.36, 121.69, 120.16 (d, J^{C-P} = 14.5 Hz), 119.39 (d, J^{C-P} = 16.7 Hz), 35.56, 33.23, 30.29, 24.97 (d, J^{C-P} = 8.2 Hz), 22.05 (d, J^{C-P} = 140.3 Hz), 21.93

³¹P NMR (121.44 MHz, CD₂Cl₂): δ 26.90

4.1.2 Synthesis of Hapten 74



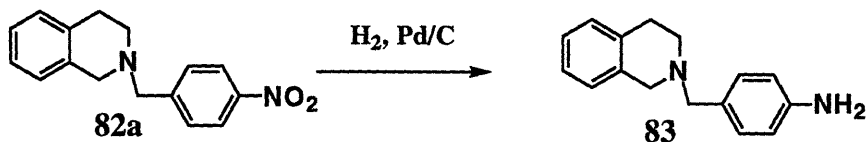
Alkylation of dihydroisoquinoline with *p*-Nitrobenzyl bromide:

To a stirred suspension of 80% NaH (0.5 g, 16.5 mmol) in 20 mL THF was added dihydroisoquinoline (1.9 mL, 15 mmol) dropwise via a syringe and stirred at room temperature for 3 hours. A solution of *p*-nitrobenzyl bromide (3.24g, 15 mmol) in 20 mL of THF was added dropwise and the reaction mixture was stirred overnight at room temperature. The reaction mixture was filtered and concentrated in vacuo. Purification by column chromatography afforded **82a** as a yellow solid (3.76 g, 94%)

Physical Data:

¹H NMR (300 MHz, CDCl₃): δ 8.83, (d, *J* = 8.7 Hz, 2 H), 7.58 (d, *J* = 8.7 Hz, 2 H), 7.20-7.05 (m, 3 H), 7.00-6.95 (m, 1 H), 3.77 (s, 2 H), 3.65 (s, 2 H), 2.92 (t, *J* = 6.0 Hz, 2 H), 2.67 (t, *J* = 6.0 Hz, 2 H).

¹³C NMR (75.44 MHz, CDCl₃): δ 146.48, 134.32, 134.05, 129.37, 128.71, 126.48, 126.30, 125.72, 123.57, 77.44, 77.01, 76.57, 61.83, 56.06, 50.81, 29.06



Reduction of the nitro group of **82a** to amine:

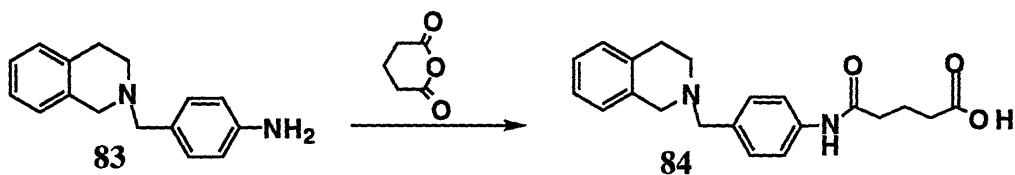
A mixture of nitrobenzyl isoquinoline **82a** (1.67 g, 6.23 mmol), 10% Pd/C (cat.) and hydrazine hydrate (1.0 g, 20 mmol) in 20 mL of isopropyl alcohol was refluxed for 24 hours. After cooling, the solution was decanted, concentrated in vacuo and purified by column chromatography to give aminobenzyl isoquinoline **83** (1.27 g, 86%) as a white solid. It can be recrystallized from acetonitrile for analytical purposes.

Physical Data:

^1H NMR (300 MHz, DMSO): δ 8.27 (s, 1 H), 8.19 (s, 1 H), 7.13 (d, $J = 8.4$ Hz, 2 H), 7.10-7.02 (m, 3 H), 3.52 (s, 2 H), 3.32 (s, 2 H), 2.78 (t, $J = 6.1$ Hz, 2 H), 2.64 (t, $J = 6.1$ Hz, 2 H)

^{13}C NMR (75.44 MHz, DMSO): δ 151.12, 134.96, 134.23, 129.65, 129.08, 128.84, 128.44, 126.33, 125.92, 125.84, 125.41, 112.61, 61.81, 55.36, 50.11, 28.76

IR (film) 2902, 2799, 2352, 1600, 1496, 1462, 1416, 1392, 1366, 1312, 1262, 1236, 1140, 1086, 1056, 1016, 838, 808, 738.



Addition of glutaric acid linker to aminobenzyl isoquinoline 84:

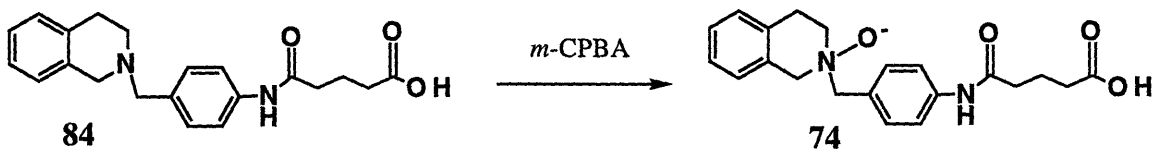
A solution of aminobenzyl isoquinoline **83** (1.0 g, 4.2 mmol) and glutaryl anhydride (0.57 g, 5 mmol) was stirred for 1 hour in EtOAc under air atmosphere. The reaction mixture was concentrated in vacuo and purified by column chromatography (15-50% MeOH in CH₂Cl₂) to yield **84** (1.45 g, 98%) as an off-white solid which can be recrystallized from EtOAc/Hexane.

Physical Data:

¹H NMR (300 MHz, DMSO): δ 9.88 (s, 1 H), 7.41 (d, *J* = 8.4 Hz), 7.25 (d, *J* = 8.4 Hz), 7.12-7.02 (m, 3 H), 7.02-6.95 (m, 1 H), 3.55 (s, 2 H), 3.16 (s, 2 H), 2.78 (t, *J* = 6.1 Hz, 2 H), 2.64 (t, *J* = 6.1 Hz, 2 H), 2.33 (t, *J* = 7.8 Hz, 2 H), 2.26 (t, *J* = 7.2 Hz, 2 H), 1.79 (quin, *J* = 7.4 Hz, 2 H)

¹³C NMR (75.44 MHz, DMSO): δ 173.62, 170.08, 137.63, 134.22, 133.55, 132.23, 128.49, 127.83, 125.76, 125.35, 124.85, 118.41, 60.85, 54.79, 49.57, 34.87, 32.52, 28.10, 19.96

HRMS (M⁺): Calcd 354.4332 Found 354.4335



Oxidation of the glutarylbenzyl isoquinoline **84** to the *N*-oxide:

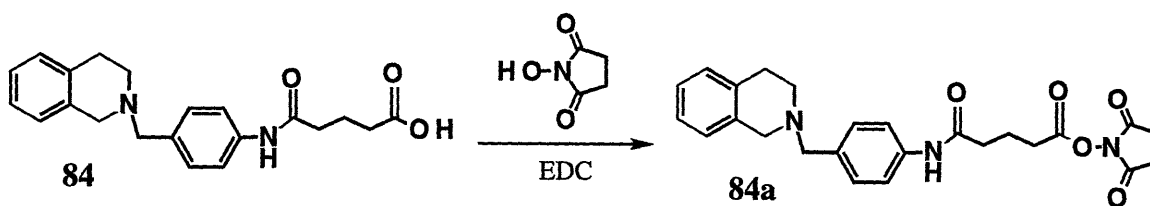
To a stirred solution of **84** (0.446 g, 1.27 mmol) in THF was added 85% *m*-CPBA (0.386 g, 1.9 mmol) over 2 minutes. The reaction was complete within 10 minutes and the precipitated product **74** was isolated via filtration, washed with THF and CH₂Cl₂, and dried to give **74** (0.40 g, 97%) as a white solid.

Physical Data:

¹H NMR (300 MHz, DMSO): δ 10.13 (s, 1H), 7.63 (d, *J* = 8.4 Hz, 2 H), 7.49 (d, *J* = 8.4 Hz, 2 H), 7.23-7.10 (m, 3 H), 6.98 (d, *J* = 8.2 Hz, 2 H), 4.64 (s, 3 H), 4.17 (d, 15.1 Hz, 2 H), 3.70-3.54 (m, 3 H), 3.34-3.18 (m, 3 H), 2.32 (t, *J* = 7.4 Hz, 2 H), 2.23 (t, *J* = 7.4 Hz, 2 H), 1.83-1.69 (m, 2 H)

¹³C NMR (75.44 MHz, DMSO): δ 175.52, 171.30, 140.36, 133.37, 131.49, 129.12, 128.08, 127.08, 126.79, 126.21, 123.75, 118.50, 71.02, 67.02, 64.00, 35.80, 34.53, 25.12, 21.01.

HRMS (M⁺): Calcd 370.4326 Found 368.4323



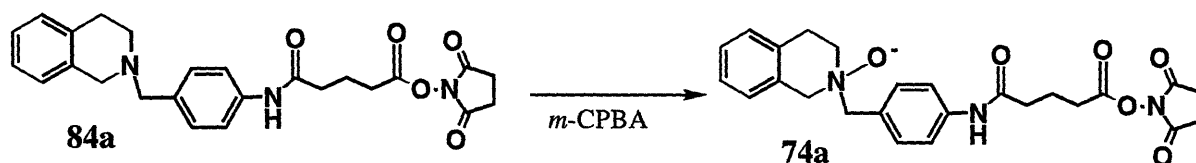
The *N*-hydroxysuccinamide ester of the glutarylamidobenzyl isoquinoline **84**:

To a suspension *N*-hydroxysuccinamide (0.011 g, 0.094 mmol) in a solution of **84** (0.03 g, 0.085 mmol) and DMAP (cat) in 2 mL of dry CH₂Cl₂ was added EDC (0.025 g, 0.13 mmol) and stirred for 18 hours. The mixture was washed water. The organic layer was dried with MgSO₄, and concentrated in vacuo. Purification by column chromatography (5% MeOH in CH₂Cl₂) afforded **84a** (0.03 g, 79%) as a white solid. It can be recrystallized from EtOAc/Et₂O for analytical purposes.

Physical Data:

¹H NMR (300 MHz, CD₂Cl₂): δ 7.96 (s, 1 H), 7.52 (d, *J* = 8.2 Hz, 2 H), 7.34 (d, *J* = 8.2 Hz, 2 H), 7.13-7.05 (m, 3 H), 7.01-6.95 (m, 1 H), 3.65 (s, 2 H), 3.60 (s, 2 H), 2.88 (t, *J* = 5.4 Hz, 2 H), 2.85 (s, 4 H), 2.74 (t, *J* = 5.4 Hz, 2 H), 2.73 (t, *J* = 6.9 Hz, 2 H), 2.46 (t, *J* = 6.9 Hz, 2 H), 2.15 (quin, *J* = 6.9 Hz, 2 H)

¹³C NMR (75.44 MHz, CD₂Cl₂): δ 170.26, 169.99, 168.93, 137.70, 135.19, 134.81, 134.35, 129.97, 128.96, 126.84, 126.44, 125.86, 120.01, 62.35, 56.47, 35.76, 30.36, 29.35, 26.04, 21.28



Oxidation of *N*-hydroxysuccinamide ester of glutarylamido-benzylisoquinoline **84a** to the N-Oxide **74a**:

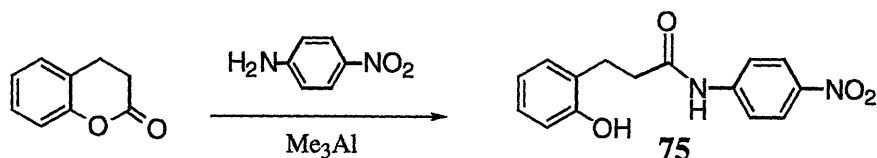
To a stirred solution of **84a** (0.105 g, 0.234 mmol) in 10mL of dry CH₂Cl₂ was added *m*-CPBA (0.053 g, 0.258 mmol). The reaction was complete after 5 minutes. The reaction mixture was concentrated in vacuo and purified by flash column chromatography (5-16% MeOH in CH₂Cl₂) to yield **74a** (0.099 g, 91%) as a white film.

Physical Data:

¹H NMR (300 MHz, CD₃OD): δ 7.67 (d, *J* = 8.4 Hz, 2 H), 7.52 (d, *J* = 8.4 Hz, 2 H), 7.29-7.13 (m, 3 H), 6.93 (d, *J* = 8.0 Hz, 1 H), 4.77-4.52 (m, 3 H), 4.23 (d, *J* = 14.2 Hz, 1 H), 3.72-3.61 (m, 2 H), 3.33-3.29 (m, 1 H), 2.97 (d, *J* = 14.2 Hz, 1 H), 2.78 (s, 4 H), 2.74 (t, *J* = 5.4 Hz, 2 H), 2.49 (t, *J* = 7.1 Hz, 2 H), 2.10-1.98 (m, 2 H)

¹³C NMR (75.44 MHz, CD₃OD): δ 176.42, 173.12, 171.81, 169.96, 141.67, 134.71, 132.09, 130.22, 129.48, 129.16, 128.98, 128.04, 127.86, 125.00, 120.72, 72.95, 65.49, 61.80, 36.13, 33.93, 30.86, 26.48, 25.62, 21.67

4.1.3 Synthesis of the Substrate 75



Trimethylaluminium assisted ring opening of dihydrocoumarin with *p*-nitroaniline:

To a stirred suspension of *p*-nitroaniline (1.03 g, 7.5 mmol) in 25 mL of CH₂Cl₂, was added a 2 M solution of trimethylaluminium in CH₂Cl₂ (3.8 mL, 7.6 mmol) dropwise. The mixture was stirred for 30 minutes until the gas generation was complete and it became a deep red color. To this dihydrocoumarin (0.85 mL, 6.8 mmol) was added dropwise and the reaction was stirred for 24 hours, diluted with 50 mL of 1N HCl and extracted twice with 50 mL of CH₂Cl₂. The extracts were combined, dried with MgSO₄, and concentrated in vacuo. Recrystallization from CH₂Cl₂ afforded substrate **75** as light yellow crystals (1.42 g, 78%).

Physical Data:

¹H NMR (300 MHz, DMSO): δ 10.47 (s, 1 H), 9.32 (s, 1 H), 8.17 (d, *J* = 8.6 Hz, 2 H), 7.89 (d, *J* = 8.6 Hz, 2 H), 7.04 (d, *J* = 7.6 Hz, 2 H), 6.97 (t, *J* = 7.4 Hz, 2 H), 6.75 (d, *J* = 7.6 Hz, 2 H), 6.66 (t, *J* = 7.4 Hz, 2 H), 2.82 (t, *J* = 7.8 Hz, 2 H), 2.63 (t, *J* = 7.8 Hz, 2 H)

¹³C NMR (75.44 MHz, DMSO): δ 175.48, 145.68, 134.97, 134.56, 129.87, 128.46, 127.18, 126.94, 126.62, 122.17, 118.37, 52.42, 28.54

HRMS (M⁺): Calcd 270.2879 Found 270.2877

4.2 Biological Methods

All of the cell culture work including the fusion protocol was performed in a sterile laminar flow hood, using sterile instruments and upon sterilization of hands with ethanol. Cells were incubated in a 37 °C sterile incubator containing 90% humidity and 5% CO₂ (for buffering with carbonate buffer in the cell media). Development of yellow color indicates the depletion of nutrients in the cell cultures (generation of acidic pH by metabolites indicated by phenol red in cell medium) and these cultures should be replenished immediately with the appropriate fresh medium (pre-warmed to 37 °C). Cells should never be left to stand at room temperature for longer than 15 minutes and sterile cell containers should only be opened to the atmosphere under a sterile laminar flow hood. Cell cultures should be monitored at least daily and those that are observed to be infected should be discarded immediately to contain the infection.

All biological solutions were stored in sterile containers and at 4 °C unless otherwise noted. 0.1% Sodium Azide can be added to biological samples to inhibit bacterial growth when it is not expected to interfere with the ensuing assays.

4.2.1 Preparation of Carrier Protein-Hapten Conjugates

Hapten-protein conjugation reactions were performed at room temperature with stirring in 5 mL covered vials. Conjugates were exhaustively dialyzed against 0.2 M sodium phosphate buffer (Kpi, pH 7.2) at 4°C. Exhaustive dialysis is defined as a minimum of 10⁶-fold dilution of the sample buffer.

Protein assays were performed according to the method of Bradford using the Bradford Assay solution (Bio-Rad) diluted 1/4 (v/v) with H₂O. Pure BSA (Bovine Serum Albumin) and KLH (Keyhole Limpocet Hemocyanin) were used for the standard curve. Quantitation of the hapten/protein ratios was determined through

a comparison of the U.V. spectra of the protein-hapten conjugate, unconjugated protein and the free hapten.

4.2.1.1 Carrier Protein-72 and -74 Conjugates

To a solution of 5 mg hapten bearing an activated ester in DMF (0.25 mL) was added carefully 0.25mL of Kpi. This solution was added dropwise to solution of 5 mg carrier protein (BSA or KLH) in 0.5 mL Kpi while swirling. After gentle stirring for 2 h, the solution was transferred into a dialysis tube (Spectra/Por 2, molecular cut-off 14,000) and dialyzed twice against 500 mL of Kpi.

4.2.1.2 Carrier Protein-73 Conjugate

To a solution of 5 mg hapten **73** bearing an activated ester in Kpi (0.5 mL) was added dropwise to solution of 5 mg carrier protein (BSA or KLH) in 0.5mL Kpi while swirling. After gently stirring for 2 hours the solution was transferred into a dialysis tube and dialyzed twice against 500 mL of Kpi.

4.2.2 Immunizations

For soluble conjugates 1 mg of Hapten-protein conjugate was diluted with PBS to a final volume of 2 mL. After transferring this solution into a bottle of RIBI adjuvant (MPM and TDM emulsion) at room temperature it was vortexed vigorously for 2-3 minutes to provide an emulsified antigen solution. For precipitated conjugates, 0.1 mg of hapten-protein conjugate was diluted with PBS to a final volume of 150 μ L and emulsified with 50 μ L of Alum (Pierce Biosciences). 100 μ L of the emulsions was injected subcutaneously to each side on the back of a Balb/c mouse using a 1 mL syringe with a 25G 5/8 needle. Fourteen days after the primary injection a secondary injection was performed according to above procedure. Twenty-one days after the first injection, the mouse was bled and the

titer of the serum was estimated by ELISA (section 4.2.3). Intravenous injection was performed about five weeks after the primary injection using an 29 G 1/2 gauge needle and was given through a tail vein. The mouse was first warmed to dilate its blood vessels by shining a heat lamp directly into the open cage (from a distance of about 1 foot) for 3-5 minutes. The mouse was then removed, placed in a mouse restraint, and one of the four blood vessels running laterally through the tail was injected with a solution of 100 µg hapten-protein conjugate in 0.1 mL sterile PBS. Three days after the last injection the mouse was sacrificed by CO₂ asphyxiation and the spleen harvested to prepare hybridoma cells.

4.2.3 Enzyme Linked ImmunoSorbent Assay (ELISA)

An ELISA was performed to identify positive hybridoma clones producing IgG molecules which specifically bind to the hapten. The standard ELISA protocol requires the following buffers:

<u>Buffer</u>	<u>Components</u>
Coating Buffer	0.05 M NaCO ₃ (pH 9.0)
Washing Buffer	PBS: 0.8 g NaCl, 0.2 g KCl, 0.2 g KH ₂ PO ₄ , 1.15 g Na ₂ HPO ₄ in 1 L dd H ₂ O
Blocking Buffer	PBS containing 10 µg/ mL of protein (BSA or Fib)
PBS-Tween	PBS containing tween 20 (1:1000 dilution)
Substrate Solution	0.1 M Sodium citrate (pH 5.0) containing 1,2-phenylenediamine (4 mg/10 mL) and 30% hydrogen peroxide (1:1000 dilution).

Each well of a 96-well polyvinyl assay plate (ELISA plate) was coated with 100 µL of the appropriate protein-hapten conjugate (2 µg/mL) in Coating Buffer and incubated at 4 °C overnight or at room temperature for 2 hours. The solutions were discarded by gentle tapping, each well was filled with 200 µL of blocking buffer, and

the plates were allowed to stand at room temperature for 1 hour. The plate was rinsed with PBS Tween followed by three rinses with distilled water (Washing Protocol). The hybridoma supernatant from each well of the 96-well cell culture plates was added to the ELISA plates and incubated for 1 hour, the supernatant was removed, and the plates were washed according to the washing protocol. Goat anti-mouse IgG-HRP conjugate, diluted in washing buffer (1:1000 dilution), was added to each well (100 μ L/well) and the plates were allowed to stand at room temperature for 1 hour. The plates were washed again according to the washing protocol. Finally, each well was treated with 100 μ L of a solution of 1,2-phenylenediamine (0.4 mg/mL) in 0.1 M sodium citrate (pH 5.0) containing 0.1 % hydrogen peroxide. The yellow color was allowed to develop for approximately 5 minutes, and the reaction was stopped upon addition of 20 μ L of 1.0 M H₂SO₄. Positive clones were identified by measuring the absorbance at 450 nm using a microtiter plate reader or more simply by visual identification through comparison with the negative controls.

Titration of antibodies in animal serum was carried out as follows. The protein-hapten coated ELISA plate was prepared as described above, and to each well was added 100 μ L of PBS. The serum was diluted 200-fold in PBS, and 100 μ L was added to the first well (A1) of the plate. The resulting solution was serially diluted 2-fold from well A1 to well A8 (from 1:400 to 1:51,200 dilution), and the plate was incubated for 1 hour. The ELISA procedure was then applied as described above, and the absorbance at 450 nm was measured. A plot of the log of the serum dilution vs. absorbance provided a sigmoidal curve, and the titer was defined as the serum dilution at which the absorbance became comparable to that of the background.

4.2.4 Preparation of media

All tissue culture work was carried out using Dulbecco's modified Eagle's medium with glucose (DME, Sigma). The following stock solutions of supplements (sterile filtered) were prepared in a sterile laminar flow hood.

<u>Supplement</u>	<u>Components</u>
O.P.	1.5 g oxaloacetic acid, 0.5 g pyruvic acid, 100 mL dd H ₂ O, pH 7.4
Glutamine	200 mM in dd H ₂ O
Gentamicin	50 mg/mL (Sigma)
8-Azaguanine	6.6 x 10 ⁻³ M (Sigma) in DME

All supplement quantities are per 1L of DME medium.

a) Myeloma Growth Medium (MG-medium):

- 10% Fetal Bovine Serum (FBS)
- 10 mL O.P.
- 20 mL Glutamine
- 3 mL 8-Azaguanine
- 10 mL ITS+ (Collaborative Research)
- 2 mL Gentamicin

b) Serum Free Medium (SF-medium):

- 150 mg Endothelial Cell Growth Supplement (ECGS, Collaborative Research)
- 2 mL Gentamicin

c) Selection Medium (HAT-medium):

- 20% FBS
- 10 mL O.P.
- 20 mL Glutamine
- 10 mL Nonessential amino acids (Sigma)
- 10 mL Hybridoma Enhancing Supplement (HES, Sigma)
- 20 mL Hybridoma Cloning Supplement (HCS, Boehringer)
- 10 mL ITS+
- 2 mL Gentamicin
- 2 vials HAT 50x (Sigma)

d) Recovery Medium (HT-medium):

- 20% FBS
- 10 mL O.P.
- 20 mL Glutamine
- 10 mL Nonessential amino acids (Sigma)
- 10 mL Hybridoma Enhancing Supplement (HES, Sigma)
- 20 mL Hybridoma Cloning Supplement (HCS, Boehringer)
- 10 mL ITS+
- 2 mL Gentamicin
- 2 vials HAT 50x (Sigma)

e) Hybridoma Expansion Medium (HE-medium):

- 20% FBS
- 10 mL O.P.
- 20 mL Glutamine
- 10 mL Nonessential amino acids (Sigma)
- 10 mL Hybridoma Enhancing Supplement (HES, Sigma)
- 20 mL Hybridoma Cloning Supplement (HCS, Boehringer)
- 10 mL ITS+
- 2 mL Gentamicin
- MITO+ (Collaborative Research)

4.2.5 Preparation of Myeloma cells

A vial with frozen X63Ag8.653 myeloma cells was removed from liquid nitrogen and immediately thawed at 37 °C in a water bath. The cells were transferred into a 15 mL centrifuge tube containing 10 mL of prewarmed MG-medium. After the pelleting of the cells by centrifugation for 5 minutes (400 x G on a bench-top centrifuge) the supernatant was removed by aspiration and discarded. The cell-pellet was loosened and resuspended in 10 mL of MG-medium. Again, the cells were centrifuged and the supernatant discarded. The pellet was loosened by gentle tapping, suspended in 1 mL of MG-medium and transferred into a T-75 flask containing 20 mL of MG-medium. The cells should be grown at a cell density between 0.2 and 1×10^6 cells/ mL to obtain maximum viability (greater than 95%).

4.2.6 Determination of Cell Viability

Cell densities were determined by tryphan-blue staining as follows: To a 20 μL aliquot of a thoroughly suspended cell sample in a small glass test tube was added 20 μL of tryphan-blue stain and the resulting cell suspension was thoroughly mixed. The cells were slowly pipetted into the sample groove of a clean hemacytometer until the observation window was completely filled. The hemacytometer was placed on an inverted phase microscope and the living cells (absence of blue stain in the interior of the cells) in the four counting grids were counted, divided by four and multiplied by 1×10^4 (the volume of a counting grid). This number was then multiplied by two, to account for the tryphan-blue dilution, to afford the number of cells/ mL.

4.2.7 Fusion

1. An immunized mouse was sacrificed and the fur in the abdominal area was washed with 95% ethanol. The chest cavity was then cut-open with sterile instruments and the spleen was removed
2. The spleen was placed in a sterile 50 mL conical tube containing 25 mL of prewarmed (37 °C) SF-medium.
3. In a sterile laminar-flow hood, the spleen and the media were transferred to a 35 mm tissue culture dish. The spleen was washed by transferring into a fresh tissue culture dish containing 20 mL of SF-medium. Holes were poked in the spleen with an 18 1/2 gauge needle and medium was injected to wash out the splenocytes. The spleen was gently teased between two sterile glass slides to provide a splenocyte suspension (approximately 1×10^8 cells).
4. The cells were transferred into a 50 mL sterile centrifuge tube carefully leaving fatty tissue behind, and centrifuged for 5 minutes at 1100 rpm.

5. While the cells were being centrifuged, Geys hemolytic medium was made up: 14.5 mL of sterile water was mixed with 4.0 mL of Geys solution A, 1.0 mL of Geys solution B and 0.5 mL of Geys solution C.*
6. The supernatant was removed by aspiration. The pellet was loosened and re-suspended in Geys hemolytic medium and left to stand for exactly 5 minutes.
7. While the cells were being treated with Geys hemolytic medium, 2×10^7 myeloma cells were transferred into a conical tube. These were then centrifuged simultaneously with the hemolyzed spleen cells (1100 rpm, 5 min).
8. After aspiration of the supernatants, the pellets were loosened and re-suspended in 20 mL of SF-medium. The spleen and myeloma cells were combined and centrifuged (1100 rpm, 5 min).
9. The supernatant was discarded, the pellet was loosened, and 1 mL of pre-warmed (37 °C) polyethylene glycol (PEG 1500, Boehringer-Mannheim) was added with gentle swirling over a period of 1 minute at room temperature.
10. Following the complete addition, the 50 mL tube was sealed and the fusion mixture was immersed in a 37 °C bath and swirled for 90 seconds.
11. Fusion was ended by the addition of the fusion media to the mixture with gentle swirling according to the following schedule: 1 mL over a period of 1 minute, then 3 mL over 1 minute, and finally 20 mL over 1 minute. The centrifuge bottle was then filled to a final volume of 40 mL with fusion media and allowed to stand for 10 minutes at room temperature.
12. The mixture was centrifuged for 15 minutes at 1100 rpm, the supernatant was removed via aspiration, and the pellet was loosened and then resuspended in 100 mL of HAT-medium.
13. Cells were dispensed into ten 96-well sterile plates (100 μ L per well) and left to stand at 37 °C in a CO₂ incubator for 7 days. After 7 days, each well was supplemented with 100 μ L of HT-medium

14. After the clones became visible under a microscope (after 14 days) ELISA was performed to identify positive colonies for subcloning (section 4.2.3).

*Geys Solution A:	35.0 g	NH ₄ Cl
	1.85 g	KCl
	1.50 g	Na ₂ HPO ₄ x 12H ₂ O
	0.119 g	KH ₂ PO ₄
	5.0 g	Glucose
	0.05 g	Phenol red
	25.0 g	Gelatine (Difco)
	1000 mL	dd H ₂ O

Geys Solution B:	4.2 g	MgCl ₂ x 6H ₂ O
	1.4 g	MgSO ₄ x 7H ₂ O
	3.4 g	CaCl ₂
	100 mL	ddH ₂ O

Geys Solution C:	5.6 g	NaHCO ₃
	100 mL	ddH ₂ O

4.2.8 Limiting Dilution (Subcloning)

Confluent and ELISA positive wells were subcloned according to the following procedure: The cells were counted and 5000 viable cells were diluted into 1 mL of HE-medium. 100 µl of the dilution were transferred into a tissue culture dish containing 10 mL of HE-medium (50 cells/mL). 2 mL of this dilution were transferred into a second tissue culture dish containing 8 mL of HE-medium (10 cells/mL). 2 mL of the resulting dilution were transferred into a third tissue culture dish containing 6 mL of HE-medium (1 cell/0.4 mL). The most dilute suspension was dispensed (100 µl/well) into the first six rows of a 96-well plate (0.25 cell/well). The second dilution was put (100 µl/well) into the next four rows (1 cell/well), while the most concentrated dilution was dispensed (100 µl/well) into the remaining two rows (5 cells/well). After seven days, each well was supplemented with 100 µl of HE-medium. Typically, after 14 days ELISA could be performed. Above procedure was repeated until all wells containing a colony were positive by ELISA (proof of monoclonality).

4.2.9 Cryogenic Storage of Cell Lines

Each monoclonal cell line was frozen according to the following protocol. A healthy cell line (viability > 95%) was grown in 10 mL of HE-medium in a T-15 tissue culture flask to a final density of 1×10^6 cells/mL. The cells were transferred into a 10 mL centrifuge tube, and centrifuged for 5 minutes at 1100 rpm. The supernatant was removed by aspiration and the pellet was re-suspended in 1 mL of pre-warmed freezing solution (8% DMSO, 92% FBS). The resulting suspension was then aliquoted between four freezing vials (250 μ L/vial) and placed in ice for 1 hour. The vials were then placed in a styrofoam container leaving the outermost rows empty to insure gradual cooling and were placed in a -78 °C freezer. Cell lines can be transferred to a liquid nitrogen storage container for long-term storage no sooner than 1 week after the initial freezing.

4.2.10 Ascites Production From Monoclonal Hybridomas

In order to generate large quantities of monoclonal antibodies, cell lines were propagated *in vivo* in pristane primed mice. Balb/c mice (retired breeders) were intraperitoneally injected with pristane (0.5 mL per mouse) at least 10 days prior to the injection of hybridoma cell lines. Each monoclonal hybridoma cell line was individually prepared for injection into a mouse by growing the healthy cell line (viability > 95%) in 10 mL of HE-medium in a T-15 tissue culture flask to a final density of 1×10^6 cells/mL. A volume containing 1.5×10^6 cells were transferred into a 10 mL conical tube and centrifuged for 5 minutes at 1100 rpm. The supernatant was removed by aspiration, the pellet was resuspended in 0.5 mL of sterile PBS, and the suspension was injected intraperitoneally into a pristane primed mouse. Only one monoclonal hybridoma cell line was injected per mouse. Within one to two weeks, abdominal swelling was generally observed in the injected mice. Each mouse was "tapped" for the ascites fluid by draining the swelled

abdominal area into a sterile tube using an 18-gauge needle. It is important that only the tip of the needle is inserted and penetration of underlying organs is avoided. Mice were tapped 1-3 times (depending on their health) prior to being sacrificed.

4.2.11 Purification of Monoclonal Antibodies

Monoclonal antibodies were purified in three steps from the ascites fluid according to the following protocol. Freshly collected ascites fluid was centrifuged at 3000 rpm for 20 minutes at 4 °C to pellet red blood cells. The supernatant was collected and an equal volume of saturated ammonium sulfate was added dropwise with stirring at 4 °C to selectively precipitate the antibodies (with some other large molecular weight proteins). The samples were allowed to stand overnight at 4 °C and then were centrifuged at 8000 rpm for 20 minutes. The supernatant was discarded and the precipitates were solubilized in and exhaustively dialyzed against 50 mM Tris•HCl (pH 7.8) at 4 °C. Dialyzed samples were centrifuged at 20,000 rpm for 20 minutes and then filtered through a 0.22 µm low protein binding syringe filter (Millipore). Each antibody solution was individually loaded onto a DEAE-Sephacel anion-exchange column (XK26) attached to a Pharmacia FPLC at 4 °C. A salt gradient (from 0 mM to 500 mM NaCl in 50 mM Tris•HCl, pH 7.8) served to elute partially purified antibodies. The elution program was as follows: 0-45 mL (0 mM NaCl), 45-46 mL (50 mM NaCl), 46-85 mL (50 mM NaCl), 85-170 mL (150 mM NaCl), 165-166 mL (500 mM NaCl), 166-205 mL (500 mM NaCl), 205-206 mL (0 mM NaCl), 206-260 mL (0 mM NaCl) at a rate of 2 mL/min, collecting 10 mL fractions. Antibody containing fractions were collected (typically between fraction 16 and 22), concentrated using AMICON filtration apparatus (YM-100 membranes, 10 psi pressure) to a final volume of approximately 10 mL, and exhaustively dialyzed against 20 mM Kpi (pH 7.2) at 4 °C in dialysis tubes.

Samples were filtered through a 0.22 μm syringe filter and loaded onto a protein G-Sepharose affinity column (HR 16/5) attached to a Pharmacia FPLC at 4 $^{\circ}\text{C}$. A low pH buffer (100 mM glycine $\cdot\text{HCl}$, pH 2.7) was used to elute pure antibody (>95%) from the affinity column (equilibrated with 20 mM Kpi at pH 7.2). Antibody containing fractions were immediately neutralized with 1 M Tris $\cdot\text{HCl}$ (pH 9) and buffered with 1 M Kpi (pH 7.2). The elution program was as follows: 0-100 mL (0 mM glycine), 100-101 mL (100 mM glycine), 101-160 mL (100 mM glycine), 160-161 mL (0 mM glycine), 161-220 mL (0 mM glycine) at a rate of 2 mL/min, collecting 6 mL fractions. Antibody concentrations were determined using the absorbance at 280 nm and an extinction coefficient of 1.35. Each antibody solution was concentrated to a working concentration of 6 mg/mL in PIPES-buffer (10 mM, 80 μM NaCl, 0.1% NaN_3 , pH 6.8) using AMICON Centriprep 100 concentrators for buffer exchange and concentration.

4.2.12 Assays for Catalysis

Preliminary assays for catalysis were performed at pH 6.8 (50 mM PIPES, 80 μM NaCl) and at pH 9.0 (50 mM CHES, 80 μM NaCl). Each assay contained 10% DMSO as organic co-solvent. A 200 μL reaction mixture contained the following: 1 mM amide **75**, 10 μM Antibody, 50 μM 4-phenylazophenol as Internal Standard Calibrant (ISTD). Typically reaction mixtures were made from a 10 fold concentrated stock solution (10 mM **75**, 0.5 mM ISTD in DMSO). Stock solutions with appropriate dilutions were made in the beginning of the catalytic assays and were stored frozen at 4 $^{\circ}\text{C}$. The same stock solutions were used throughout all of the assays for consistency. Reactions were initiated with the addition of the appropriate volume of concentrated antibody solution (6 mg/mL) to a pre-mixture of **75**, ISTD and buffer (and inhibitor where appropriate). Reactions were assayed at room temperature over 3 days.

The reactions were followed at 382 nm (absorption maxima for *p*-nitroaniline) in a RAININ UV-D spectrophotometer (an absorption peak area of 3120 was calibrated to correspond to 1 μ M *p*-nitroaniline release with a 20 μ L sample volume). The reaction components were separated using a Waters Nova-Pak C₈ column (150 mm length x 3.9 mm i.d.) attached to a Rainin HPLC system. 45% AcN, 0.1% trifluoroacetic acid in *dd*H₂O was used as an isocratic eluent at 1.7 mL/min flow rate. The elution times of the observed species is as follows: *p*-nitroaniline 1.33 min., amide **75** 1.92 min., 4-phenylazophenol 2.55 min. Typically spectra were recorded for 4 minutes. Integration of the peaks were performed using the dedicated Rainin Dynamax computer program run in Apple Macintosh computers.

Assays for the bi-molecular reactions were done similar to the above except a 35% AcN, 0.1% trifluoroacetic acid in *dd*H₂O isocratic eluent was used at 2.0 mL flow rate. The elution times of the observed species was as follows: *p*-nitroaniline 1.62 min., amide **87** 2.03 min., 4-phenylazophenol 5.71 min. Typically spectra were recorded for 7 minutes. Generally 40 μ L reaction volumes were assayed over 6 days with 10 μ L sample volumes. Reactions contained 10% DMSO and 5% AcN as organic co-solvents. Amide **77** stock solutions were made at 20x concentration including 0.5 mM ISTD in a 1:1 DMSO/AcN mixture. 20x concentrated phenol solutions were made in DMSO. All stock solutions were made at the beginning of the assays and used through-out for consistency. Stock solutions were stored frozen at 4 °C. Reactions were initiated upon addition of the appropriate volume of the antibody solution (6 mg/mL) to a pre-mixture of **77**, Phenol, ISTD and buffer (also inhibitors where appropriate).

All measurements were done in triplicate. Kinetic plots were determined using KaleidaGraph program (SYNERGY Software) for Apple Macintosh computers.

Biographical Note

The author, Oguz Ersoy, was born in Istanbul, Turkey on February 23, 1968 to parents Dr. Ülkü Ersoy (mother) and Suphi Ersoy (father). He was raised in the same city and graduated from Istanbul Robert College high-school in 1986. To his good fortune, in March 14, 1978, his brother Burak Ersoy was born. After attending the medical school of Marmara University, Istanbul in 1986-87, the author enrolled in Bates College, where he studied under the tutelage of professors Joseph G. Pellicia (biology) and David B. Ledlie (chemistry). In the summer of 1988, the author worked as an undergraduate research fellow at California Institute of Technology with Dr. Kai Zinn. In 1990, he graduated cum laude from Bates College, B.S. biology and chemistry, with honors in chemistry. He was also awarded memberships to Phi Beta Kappa and Phi Lambda Upsilon honorary societies, as well as receiving the Merck Index Award. In September 1990, he enrolled in MIT, and soon after began conducting research under the supervision of Professor Satoru Masamune on catalytic antibodies. Upon the completion of his Sc.D., the author will travel to Stockholm, Sweden to work as a research scientist at the Karolinska Institute.

References

- ¹Thomas, J. M.; Zamaraev, K. I. eds. *Perspectives in Catalysis* **1992**, Blackwell Scientific Publications, Oxford.
- ²Ko, S.Y.; Lee, A.W.M.; Masamune, S.; Reed, L.A.; Sharpless, K.B.; Walker, F.J. *Science*, **1983**, *220*, 949.
- ³Ojima, I. ed. *Catalytic Asymmetric Synthesis* **1993**, VCH Publishers, New York.
- ⁴a) Pauling, L. *Chem. Eng. News*, **1946**, *24*, 1375. b) Pauling, L. *Am. Sci.*, **1948**, *36*, 51.
- ⁵Jencks, W.P. *Catalysis in Chemistry and Enzymology*, **1969**, McGraw Hill, New York, p.288.
- ⁶a) Raso, V.; Stollar, B.D. *J. Am. Chem. Soc.*, **1973**, *95*, 162; b) *ibid. Biochemistry*, **1975**, *14*, 584; c) *ibid.* 591.
- ⁷Kohler, G.; Milstein, C. *Nature*, **1975**, *256*, 495.
- ⁸Lerner, R.A. *Adv. Immunol.* **1984**, *36*, 1.
- ⁹Bartlett, P.A. and Marlowe, C.K. *Biochemistry* **1983**, *22*, 4618.
- ¹⁰Tramontano, A.; Janda, K.D.; Lerner, R.A. *Proc. Natl. Acad. Sci., USA* **1986**, *83*, 6736.
- ¹¹Tramontano, A.; Janda, K.D.; Lerner, R.A. *Science*, **1986**, *234*, 1566.
- ¹²Pollack, S.J.; Jacobs, J.W.; Schultz, P.G. *Science*, **1986**, *234*, 1570.
- ¹³for example see: Jacobs, J.W.; Schultz, P.G.; Sugasawara, R.; Powell, M. *J. Am. Chem. Soc.*, **1987**, *109*, 2174; Napper, A.D.; Benkovic, S.J.; Tramontano, A.; Lerner, R.A. *Science*, **1987**, *237*, 1041; Benkovic, S.J.; Napper, A.D.; Lerner, R.A. *Proc. Natl. Acad. Sci., USA* **1988**, *85*, 5355; Janda, K.D.; Schloeder, D.; Benkovic, S.J.; Lerner, R.A. *Science*, **1988**, *241*, 1188; Janda, K.D.; Lerner, R.A.; Tramontano, A. *J. Am. Chem. Soc.*, **1988**, *110*, 4835.
- ¹⁴a) Hilvert, D.; Carpenter, S.H.; Nared, K.D.; Auditor, M-T M. *Proc. Natl. Acad. Sci., USA* **1988**, *85*, 4953; b) Hilvert, D.; Nared, K.D. *J. Am. Chem. Soc.*, **1988**, *110*, 5593; c) Jackson, D.Y.; Jacobs, J.W.; Sugasawara, R.; Reich, S.H.; Bartlett, P.A.; Schultz, P.G. *J. Am. Chem. Soc.*, **1988**, *110*, 4841.
- ¹⁵Shokat, K.M.; Leumann, C.L.; Sugasawara, R.; Schultz, P.G. *Nature*, **1989**, *338*, 269.
- ¹⁶Sheriff, S.; Silverton, E.W.; Padlan, E.A.; Cohen, G.H.; Smith-Gill, S.J.; Finzel, B.C.; Davies, D.R. *Proc. Natl. Acad. Sci., USA* **1987**, *84*, 8075.
- ¹⁷Lerner, R.A.; Benkovic, S.J. *BioEssays*, **1988**, *9*, 107.
- ¹⁸Ersoy, O.; Williams, S.F.; Masamune, S. *unpublished results*.
- ¹⁹a) Lerner, R.A.; Benkovic, S.J.; Schultz, P.G. *Science* **1991**, *252*, 659. b) *Acc. Chem. Res.* **1993**, vol. 8.
- ²⁰Iwabuchi, Y.; Miyashita, H.; Tanimura, R.; Kinoshita, K.; Kikuchi, M.; Fujii, I. *J. Am. Chem. Soc.* **1994**, *116*, 771.
- ²¹Napper, A.D.; Benkovic, S.J.; Tramontano, A.; Lerner, R.A. *Science* **1987**, *237*, 1041.
- ²²Benkovic, S. J.; Napper, A. D.; Lerner, R. A. *Proc. Natl. Acad. Sci. USA* **1988**, *85*, 5355.
- ²³Ikeda, S.; Weinhouse, M. I.; Janda, K. D.; Lerner, R. A.; Danishefsky, S. J. *J. Am. Chem. Soc.* **1991**, *113*, 7763.
- ²⁴Janda, K. D.; Benkovic, S. J.; Lerner, R. A. *Science* **1989**, *244*, 437.
- ²⁵Janda, K.D., Ashley, J.A., Jones, T.M., McLeod, D.A., Schloeder, D.M. and Weinhouse, M.I. *J. Am. Chem. Soc.* **1990**, *112*, 8886.
- ²⁶Wirsching, P.; Ashley, J. A.; Benkovic, S. J.; Janda, K. D.; Lerner, R. A. *Science* **1991**, *252*, 680.
- ²⁷Landry, D. W.; Zhao, K.; Yang, G. X.-Q.; Glickman, M.; Georgiadis, T. M. *Science* **1993**, *259*, 1899.
- ²⁸Kurokawa, T.; Iwasa, S.; Kakinuma, A. *Bio/Technology* **1989**, *7*, 1163.
- ²⁹Miyashita, H.; Karaki, Y.; Kikuchi, M.; Fujii, I. *Proc. Natl. Acad. Sci. USA* **1993**, *90*, 5337.
- ³⁰Campbell, D.A.; Gong, B.; Kochersperger, L.M.; Yonkovich, S.; Gallop, M.A.; Schultz, P.G. *J. Am. Chem. Soc.* **1994**, *116*, 2165.
- ³¹Janda, K. D.; Schloeder, D.; Benkovic, S. J.; Lerner, R. A. *Science* **1988**, *241*, 1188.
- ³²Chen, Y.-C. J.; Danon, T.; Sastry, L.; Mubaraki, M.; Janda, K. D.; Lerner, R. A. *J. Am. Chem. Soc.* **1993**, *115*, 357.
- ³³Gibbs, R.A., Taylor, S. and Benkovic, S.J. *Science* **1992**, *258*, 803-805.

- ³⁴a) Liotta, L.J.; Benkovic, P.A.; Miller, G.A.; Benkovic, S.J. *J. Am. Chem. Soc.* **1993**, *115*, 350. b) Liotta, L.J.; Gibbs, R.A.; Taylor, S.D.; Benkovic, P.A.; Benkovic, S.J. *J. Am. Chem. Soc.* **1995**, *117*, 4729.
- ³⁵Martin, M.T.; Angeles, T.S.; Sugawara, R.; Aman, N.I.; Napper, A.D.; Darsley, M.J.; Sanchez, R.I.; Booth, P.; Titmas, R.C. *J. Am. Chem. Soc.* **1994**, *116*, 6508.
- ³⁶(a) Janda, K. D.; Weinhouse, M. I.; Schloeder, D. M.; Lerner, R. A.; Benkovic, S. J. *J. Am. Chem. Soc.* **1990**, *112*, 1274.
- ³⁷Janda, K. D.; Weinhouse, M. I.; Danon, T.; Pacelli, K. A.; Schloeder, D. M. *Ibid.* **1991**, *113*, 5427.
- ³⁸A significant amount of the actual experimental work that is discussed within this section has been performed by the author in the second and third years of his tenure as a graduate student. As a detailed discussion of this work has already been presented in the Ph.D. dissertation of Dr. Hiroaki Suga (MIT Dept. of Chemistry, 1994) as well as published (see ref. 49) only a brief summary will be offered here.
- ³⁹Suga, H.; Ersoy, O.; Tsumuraya, T.; Lee, J.; Sinskey, A.J., Masamune, S. *J. Am. Chem. Soc.*, **1994**, *116*, 487.
- ⁴⁰Suga, H.; Ersoy, O., Masamune, S. *unpublished results*.
- ⁴¹Iverson, B. L.; Lerner, R. A. *Science* **1989**, *243*, 1184.
- ⁴²Blackburn, G.M.; Deng, S.-X. *Biochem. Soc. Trans.* **1994**, *21*, 1102.
- ⁴³Sell, S. *Basic Immunology*, **1987**, Elsevier, New York, p. 199-234.
- ⁴⁴Francis, R. Jr. *Ann. Intern. Med.* **1953**, *39*, 203.
- ⁴⁵a) Fazekas de St. Groth S.; Webster, R. G. *J. Exp. Med.* **1966**, *124*, 347. b) Levin, H. A.; Herman, J.; Levine, H.; Schlossman, S. F. *J. Immunol.* **1972**, *108*, 538.
- ⁴⁶Deutsch S.; Bussard, A. E. *Eur. J. Immunol.* **1972**, *2*, 374.
- ⁴⁷Fish, S.; Zenowich, E.; Fleming, M.; Manser, T. *J. Exp. Med.* **1989**, *170*, 1191.
- ⁴⁸Manser, T, Wysocki, L. J.; Margolies, M. N.; Gefter, M. L. *Immunol. Rev.* **1987**, *96*, 141.
- ⁴⁹a) Suga, H.; Ersoy, O.; Williams, S.F.; Tsumuraya, T.; Margolies, M.N.; Sinskey, A.J., Masamune, S. *J. Am. Chem. Soc.*, **1994**, *116*, 6025. b) Suga, H.; Ersoy, O.; Williams, S.F.; Tsumuraya, T.; Margolies, M.N.; Sinskey, A.J., Masamune, S. *J. Am. Chem. Soc.*, **1994**, *116*, 8432. c) Tsumuraya, T.; Suga, H.; Meguro, S.; Tsukanawa, A.; Masamune, S. *J. Am. Chem. Soc.*, **1995**, *117*, 11390.
- ⁵⁰Page, M.I.; Williams, A. Eds. *Enzyme Mechanisms The Royal Society of Chemistry*, London, **1987**
- ⁵¹Benkovic, S. J.; Adams, J. A.; Borders Jr., C. L.; Janda, K. D.; Lerner, R. A. *Science* **1990**, *250*, 1135.
- ⁵²Janda, K.D., Ashley, J.A., Jones, T.M., McLeod, D.A., Schloeder, D.M., Weinhouse, M.I., Lerner, R.A., Gibbs, R.A., Benkovic, P.A., Hilhorst, R. and Benkovic, S.J. *J. Am. Chem. Soc.* **1991**, *113*, 291.
- ⁵³Gibbs, R. A.; Benkovic, P. A.; Janda, K. D.; Lerner, R. A.; Benkovic, S. J. *J. Am. Chem. Soc.* **1992**, *114*, 3528.
- ⁵⁴a) Stewart, J.D.; Krebs, J.F.; Siuzdak, G.; Berdis, A.J.; Smithrud, D.B.; Benkovic, S.J. *Proc. Natl. Acad. Sci. USA*, **1994**, *91*, 7404. b) Stewart, J.D.; Roberts, V.A.; Thomas, N.R.; Getzoff, E.D.; Benkovic, S.J. *Biochemistry* **1994**, *33*, 1994.
- ⁵⁵Siuzdak, G.; Krebs, J.F.; Benkovic, S.J.; Dyson, H.J. *J. Am. Chem. Soc.* **1994**, *116*, 7937.
- ⁵⁶Martin, M. T.; Napper, A. D.; Schultz, P. G.; Ress, A. R. *Biochemistry* **1991**, *30*, 9757.
- ⁵⁷Guo, J.; Wei, H.; Scanlan, T.S. *J. Am. Chem. Soc.* **1994**, *116*, 6062.
- ⁵⁸Zhou, G.W.; Guo, J; Wei, H.; Fletterick, R.J.; Scanlan, T.S. *Science*, **1994**, *265*, 1059.
- ⁵⁹Guo, J; Wei, H.; Zhou, G.W.; Fletterick, R.J.; Scanlan, T.S. *Proc. Natl. Acad. Sci. USA*, **1995**, *92*, 1694.
- ⁶⁰a) Baldwin, E.; Schultz, P.G. *Science* **1989**, *245*, 1104. b) Jackson, D.Y., Prudent; J.R., Baldwin, E.P.; Schultz, P.G. *Proc. Natl. Acad. Sci. USA* **1991**, *88*, 58. c) Wade, W.S.; Koh, J.S.; Han, N.; Hoekstra, D.M.; Lerner, R.A. *J. Am. Chem. Soc.* **1993**, *115*, 4449. d) Crowder, M.W.; Stewart, J.D.; Roberts, V.A.; Bender, C.J.; Tevelrakh, E.; Peisach, J.; Getzoff, E.D.; Gaffney, B.J.; Benkovic, S.J. *J. Am. Chem. Soc.* **1995**, *117*, 5627.

⁶¹This work was done in collaboration with Mr. Roman Fleck, and the relevant parts of this work, esp. the syntheses of hapten **73** and substrate **77** will be reported in the dissertation thesis of this author.

⁶²Huval, C.; Masamune, S. *unpublished results*

⁶³Mikolajczyk, M.; Grzejszczak, G.; Midura, W.; Zatorski, A. *Synthesis* **1976**, 396.

⁶⁴This background rate is in accordance with a previously determined background rate for a similar *p*-nitroanilide substrate, see: Janda, K. D.; Schloeder, D.; Benkovic, S. J.; Lerner, R. A. *Science* **1988**, *241*, 1188.

⁶⁵a) Tawfik, D.S.; Green, B.S.; Chap, R.; Sela, R.; Eshhar, Z. *Proc. Natl. Acad. Sci. USA* **1993**, *90*, 373.

b) MacBeath, G.; Hilvert, D. *J. Am. Chem. Soc.* **1994**, *116*, 6101.

⁶⁶Schmidhammer, H.; Brossi, A. *J. Org. Chem.* **1983**, *48*, 1469.